FUNCTIONAL CHARACTERIZATION OF SCN5A, THE CARDIAC SODIUM CHANNEL GENE ASSOCIATED WITH CARDIAC ARRHYTHMIAS AND SUDDEN DEATH

LING WU

Bachelor of Medicine in Psychiatry and Mental Health

Hunan Medical University, China

July, 1991

Master of Medicine in Psychiatry and Mental Health

Hunan Medical University, China

June, 1997

Submitted in partial fulfillment of requirements for the degree

DOCTOR OF PHILOSOPHY IN REGULATORY BIOLOGY

at the

CLEVELAND STATE UNIVERSITY

May, 2008

This dissertation has been approved for

the Department of Biological, Geological, and Environmental Sciences and for the

College of Graduate Studies of

Cleveland State University

by

_____Date_____
Dr. Qing Wang, Dept of Molecular Cardiology/CCF
Major Advisor

_____Date_____
Dr. Christine Moravec, Dept of Cardiovascular Medicine/CCF
Advisory Committee Member

_____Date_____
Dr. Jeffrey Dean, BGES/CSU
Advisory Committee Member

_____Date_____
Dr. Philip Howe, Dept of Cancer Biology/CCF
Advisory Committee Member

_____Date_____
Dr. Crystal Weyman, BGES/CSU
Advisory Committee Member

_____Date_____
Dr. Xiaoxia Li, Dept of Immunology/CCF
Internal Examiner

_____Date_____
Dr. David Van Wagoner, Dept of Molecular Cardiology/CCF
External Examiner

ACKNOWLEGEMENTS

I would like to take this opportunity to thank everyone who made this possible for me. Especially to my major advisor, Dr. Qing Wang, for his guidance, time, patience, encouragement, and financial support.

Particularly, I would like to express my appreciation to my committee members, Dr. Christine Moravec, Dr. David Van Wagoner, Dr. Philip Howe, Dr. Jeffrey Dean and Dr. Crystal Weyman for their valuble advices, suggestions and encouragements for this dissertation. Also, I am thankful to Dr. Xiaoxia Li and Dr. David Van Wagoner for reading my dissertation and giving me great suggestions.

Many thanks to all the members in Wang lab for their kind help in various ways. Special thanks to Dr. Sandro Yong and Mrs.Ying Ni, who gave advice and assistance in the EP studies and powerpoint slide preparations. Dr. Teng Zhang, Dr. Shi Yoo and Dr. Chun Fan helped me with the functional studies involved in the project.

I also thank Dr. Sudhiranjan Gupta and Biswajit Das in Dr. Subha Sen's lab for showing me how to isolate cardiomyocytes. Dr. Anita H. Corbett in Emory University School of Medicine generously provided the MOG1 expression plasmid.

DEDICATION

This work is dedicated to my parents, to my husband, to my daughter Alice, and to my son Christopher

FUNCTIONAL CHARACTERIZATION OF SCN5A, THE CARDIAC SODIUM CHANNEL GENE ASSOCIATED WITH CARDIAC ARRHYTHMIAS AND SUDDEN DEATH

LING WU

ABSTRACT

The cardiac sodium channel α subunit $Na_v1.5$ (encoded by the SCN5A gene) plays an important role in the generation and propagation of electrical signals in the heart, and can cause cardiac arrhythmias, heart failure and sudden death when mutated or dysregulated. However, the precise composition of the multi-protein complex for the sodium channel has not been completely defined. The molecular mechanisms by which $Na_v1.5$ mutations cause cardiac arrhythmias have not yet been well-studied *in vivo*. It remains to be explored whether $Na_v1.5$ is expressed in other tissues and plays novel roles in other tissues or organs. This dissertation addresses these aspects of $Na_v1.5$ regulation.

I found that MOG1, a small protein that is highly conserved from yeast to humans, is a central component of the channel complex and distinctly modulates the physiological function of $Na_v1.5$. A yeast two-hybrid screen identified MOG1 as a new protein that interacts with the cytoplasmic loop II (between transmembrane domain DII and III) of $Na_v1.5$. The interaction was further demonstrated by both *in vitro* GST pull-down and *in vivo* co-immunoprecipitation assays. Co-expression of MOG1 with $Na_v1.5$ in HEK293 cells increased sodium current densities, whereas two siRNAs that knocked down

expression of MOG1 decreased current densities. In neonatal myocytes, over-expression of MOG1 increased current densities nearly two-fold, and MOG1 siRNAs down-regulated the sodium currents. Immunostaining revealed that in the heart, MOG1 was expressed in both atrial and ventricular tissues and was highly localized in the intercalated discs. These results suggest that MOG1 may be a critical regulator of sodium channel function in the heart and reveal a new function for MOG1. Furthermore, I showed that MOG1 increased sodium current density by increasing cell membrane localization of $Na_v1.5$. This study further demonstrates the functional diversity of $Na_v1.5$-binding proteins, which may be important for the function of $Na_v1.5$ under different cellular conditions.

The second major project I worked on was identification by microarray analysis of genes differentially expressed in transgenic mice with cardiac expression of LQTS mutation N1325S of SCN5A. I identified 33 genes in five different functional groups that showed differential expression. *STAT1*, which encodes a transcription factor involved in apoptosis and interferon response, showed the most significant difference of expression between TG-NS and control mice (a nearly 10-fold increase in expression, $P = 4 \times 10^{-6}$). The results were further confirmed by quantitative real-time PCR and Western blot analyses. Accordingly, many interferon response genes also showed differential expression in TG-NS hearts. This study represents the first microarray analysis for LQTS and implicates *STAT1* in the pathogenesis and progression of LQTS and heart failure developed in the transgenic mice.

The third project focused on the distribution of $Na_V1.5$ protein in the mouse brain which was investigated using immunohistochemistry. Immuno-staining with a $Na_V1.5$-

specific antibody revealed that $Na_V1.5$ protein was localized in certain distinct regions of brain including the cerebral cortex, thalamus, hypothalamus, basal ganglia, cerebellum and brainstem. Notably, I found that $Na_V1.5$ protein co-localized with neurofilaments and clustered at a high density in the neuronal processes, mainly axons. These results suggest that $Na_V1.5$ protein may play a role in the physiology of the central nervous system (generation and propagation of electrical signals by axons).

These studies on $Na_v1.5$ provide new insights into the regulation of the function of $Na_v1.5$, and shed light on the possible pathogenetic mechanism of cardiac arrhythmias at the molecular level.

TABLE CONTENTS

LIST OF FIGURES

Figure

LIST OF TABLES

Table

LIST OF ABBREVIATIONS

APD	Action Potential Duration
AF	Atrial Fibrillation
AS	Atrial Standstill
BS	Brugada Syndromes
DCM	Dilated Cardiomyopathy
EAD	Early Afterdepolarization
ECG	Electrocardiogram
ER	Endoplasmic reticulum
FHF1B	Fibroblast Growth Factor Homologous Factor 1B
Gsα	G protein Stimulatory α-subunit
IVF	Idiopathic Ventricular Fibrillation
LQTs	Long QT Syndromes
MOG1	Multicopy Suppressor of gsp1 Mutants
PCCD	Progressive Cardiac Conduction Defect
PKA	Protein Kinase A
PKC	Protein Kinase C
RT-PCR	Real-Time Polymerase Chain Reaction
SGK	Serum and Glucocorticoid-inducible Kinase
SIDS	Sudden Infant Death Syndrome
SSS	Sick Sinus Syndrome
STAT1	Signal Transducer and Activator of Transcription 1

TTXs	Tetrodotoxin-sensitive
TTXr	Tetrodotoxin-resistant
VF	Ventricular Fibrillation

CHAPTER I

GENERAL INTRODUCTION

1.1. Sodium channel $Na_v1.5$ and its functions

1.1.1. Sodium channel gene family

Voltage-gated sodium channels are transmembrane proteins that are critical to the generation and rapid propagation of the electrical signals (action potentials) in excitable membranes of cardiomyocytes, neurons, and other cells. To date at least twelve different sodium channel α-subunit genes have been cloned and they include *SCN1A* (brain, chromosome 2q23-q24), *SCN2A* (brain, 2q22-q23), *SCN3A* (brain and dorsal root ganglion or DRG, 2q24-q31), *SCN4A* (skeletal muscle, 17q23.1-q25.3), *SCN5A* (heart, 3p21), *SCN6A* (uterus and heart, 2q21-q23), *SCN7A* (glial cells, DRG, 2q21-23), *SCN8A* (brain, DRG and spinal cord, 12q13), *SCN9A* (DRG, brain and spinal cord, 2q24), *SCN10A* (DRG, 3p22-24), *SCN11A* (DRG, 3p21-24), and *SCN12A* (central nervous system, DRG, non-neural tissues, 3p23-p21.3) (George et al. 1992; Jeong et al. 2000; Novakovic et al. 2001; Ogata et al. 2000; Wang et al. 1996). The sodium channels are

related to the founder member, the voltage-gated sodium channel from the electric eel electroplax, and also related to each other by sequence homology and a conserved structure consisting of four transmembrane domains, each of which is composed of six transmembrane segments (Balser et al. 1999; Catterall et al. 2000; Wang et al. 1996; Wang et al. 1995a). Dysfunction of sodium channels causes multiple human diseases. Mutations in the cardiac sodium channel gene *SCN5A* cause cardiac arrhythmias and sudden death associated with long QT syndrome (LQTS), idiopathic ventricular fibrillation and Brugada syndrome, and cardiac conduction disease (Chen et al. 1998; Dumaine et al. 1996; Schott et al. 1999; Tan et al. 2001; Wan et al 2001; Wang et al. 2000; Wang et al . 2001; Wang et al. 1995a). Mutations in the skeletal muscle sodium channel gene *SCN4A* cause hyperkalemic periodic paralysis and paramyotonia congenital (Ptacek et al. 1992; Ptacek et al. 1991). Mutations in the brain sodium channel gene *SCN1A, SCN2A and SCN3A* cause generalized epilepsy with febrile seizures type 2 (Escayg et al. 2000).

Based on the channel sensitivity to blockade by TTX on the connecting segment between S5 and S6, the tetrodotoxin (TTX) binding site, sodium channels are classified into three types: TTX-sensitive sodium channels (TTXs; TTX, IC_{50}=1-5 nM), TTX-resistant Na channels (TTXr; 0.2-1 μM TTX), and TTX-insensitive Na channels (TTXi; 30-100 μM TTX) (Donahue et al. 2000, Fozzard et al. 1996). The $Na_v1.5$ channel encoded by *SCN5A* gene is TTX-resistant (Gellens et al. 1992). TTXr Na channels generate currents that are slower, but recover from inactivation much faster than those from TTXs channels (Elliott et al. 1993), suggesting a possible role of TTXr sodium channels in sustained firing of neurons or as pace-makers.

1.1.2. Cardiac sodium channel $Na_v1.5$

The human cardiac sodium channel $Na_v1.5$ belongs to the voltage-gated sodium channel family, and is encoded by the *SCN5A* gene. This gene is located on chromosome 3p21 and contains 27 introns and 28 exons (Gellens et al. 1992). The human SCN5A gene has two alternatively spliced variants, $Na_v1.5c$ and $Na_v1.5d$. $Na_v1.5c$ contains 2,015 amino acids without glutamine at position 1077 compared to wild type $Na_v1.5$ with 2,016 amino acids, while $Na_v1.5d$ has a 40 amino acid deletion in the intracellular loop II between domain II and domain III (Gellens et al. 1992, Makielski JC et al. 2003, Camacho et al. 2006). The cardiac sodium channel $Na_v1.5$ was initially cloned from the human cardiac cDNA library. $Na_v1.5$ is mainly expressed in the heart, although it is also expressed in brain, DRG and skeletal muscle at a much lower level (Gellens et al. 1992, Hartmann et al. 1999, Plummer et al. 1999). $Na_v1.5$ is highly homologous to $Na_v1.8$ (82%) and $Na_v1.9$ (72%), which are mainly expressed in the peripheral nervous system (Plummer et al. 1999, Kerr et al. 2004) on the amino acid level.

$Na_v1.5$ is the pore-forming α subunit of the cardiac sodium channel. It consists of four homologous domains (I-IV) with each domain composed of six transmembrane α-helices (Fig. 1.1). There are at least four different β-subunits, β1, β2 β3 and β4, that are associated with the α subunit. The β1 subunit has been detected in skeletal muscle, heart and brain tissues (Makita et al. 1994), whereas the β3 subunit has been identified in the brain, kidney, skeletal muscle and heart (Morgan et al. 2000, Stevens et al. 2001). The β2 and β4 subunits are also expressed in the heart, but at significantly lower levels than those in the brain (Maier et al. 2004; Eubanks et al. 1997, Malhotra et al., 2001, Yu et al., 2003). The structure of β1 is most similar to that of the β3 subunit with a noncovalent link to the

α subunit (Isom et al., 1992, Morgan et al., 2000, Qu et al., 2001). The β2 and β4 subunits are more similar to each other with an unpaired cysteine that interacts with the α subunit by a disulfide bond (Hartshorne et al., 1984, Yu et al., 2003). The β1 and β2 subunits are similar to cell adhesion molecules in their extracellular immunoglobulin-like motifs (Isom et al.1996), which is consistent with their function for regulating the targeting and localization of the sodium channel to the cell membrane (Novakovic et al. 2001).

1.1.3. Functional characterization of cardiac sodium channel $Na_v1.5$

The major functions of $Na_v1.5$ are to generate the cardiac action potential and to maintain rapid conduction of electrical signals through cardiac tissues. This voltage–gated sodium channel exists in three main transitional states: closed, open (activated) and inactivated. These channel states control sodium ion permeability through the channel into the cardiac cell. Sodium channel acticvation allows sodium ion influx into the cell and inactivation blocks entry of inward sodium ions. Inactivation is mediated by the inactivation gate, a cytoplasmic link between domain III and domain IV where the triad IFM (Ile 1488, Phe 1489, Met 1490) serves as a hydrophobic 'latch' that limits or restricts sodium ion pass through the pore (West et al. 1992). When the cell membrane senses a voltage change (i.e., depolarization), the voltage sensor (the S4 segment) moves outward (towards external face). Following this change, the four transmembrane domains (I-IV) undergo several conformational changes whereby the overall channel conformation is in the open state. The sodium ions enter the cells rapidly, which initiates the cardiac action potential. Several milliseconds later, the inactivation

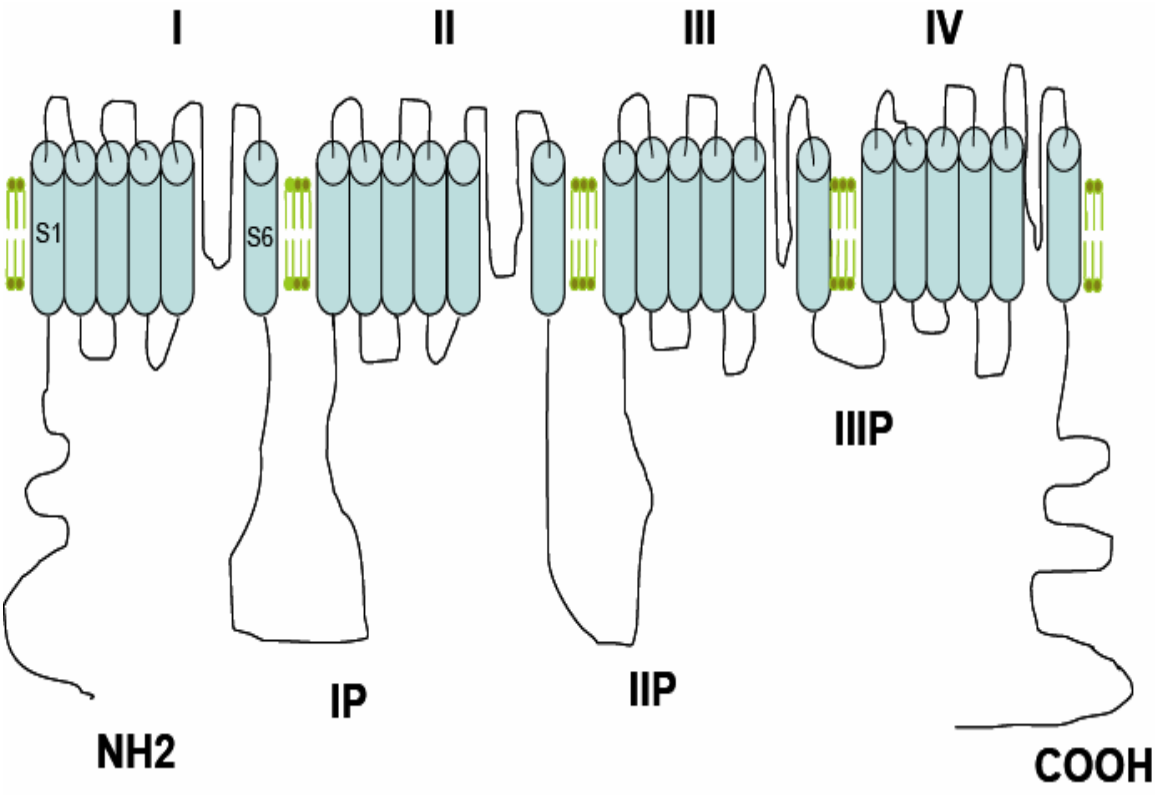

Fig. 1.1. The structure of $Na_v1.5$. Sodium channel $Na_v1.5$ consists of four transmembrane domains (I-IV) and five cytoplasmic domains. Each transmembrane domain contains six alpha-helix segments (S1-S6). Cytoplasmic domains are composed of the N-terminus, loops I, II, III and C-terminus.

gate closes and blocks movement of sodium ions across the cell membrane. The sodium channel is then converted to the inactivated state. The recovery of the sodium channel to reopen is voltage-dependent. Highly polarized (-80 to 90 mV) cell membrane can be depolarized rapidly by stimuli due to more sodium channels reopening. While partially depolarized cells with potentials close to threshold -70 mV causes a much slower upstroke because of the inactivation of some channels. The recovery of channels from inactivation is also time-dependent. Sodium channels typically activate within 200-300 μs and inactivate completely within 2-5 ms.

1.1.3. 1. $Na_v1.5$ and the cardiac action potential

The cardiac action potential refers to changes in voltage that travel along the membrane of the cardiac cell. These changes are composed of 5 phases (0-4) which collectively make up the cardiac action potential. The sodium channel makes a contribution in two phases of the action potential, the upstroke of rapid depolarization or phase 0 and the plateau phase or phase 2 (Fig. 1.2). Phase 3 is the repolarization phase. Phase 4 is the resting phase with a membrane potential of approx -90 mV in ventricular myocardium, which is sustained until the cell is stimulated by an external stimulus. During phase 4, most sodium channels are in the closed state, the activation gate is in the closed state and the inactivation gate is in an open state. Upon the external stimulus, the membrane potential of the cell achieves a threshold voltage (about -70 mV) and initiates the rapid depolarization phase (Phase 0) by the activation of the sodium channels. When the cell is depolarized, the channel is changed from a closed state to the open state. In this open conformation, both the activation and inactivation gates are shifted to their open

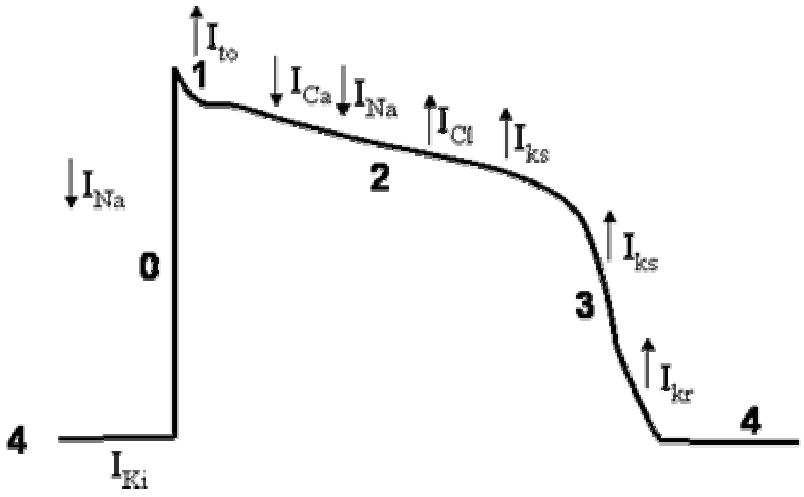

Fig. 1.2. A schematic view of an idealized action potential for ventricular myocytes. The action potential has 5 phases (numbered 0-4). Phase 4 is the resting membrane potential, in which the cell is not stimulated, mainly maintained by the movement of K^+. Phase 0 is the rapid depolarization phase due to the rapid influx of Na^+. Phase 1 occurs with the inactivation of the fast Na^+ channels and efflux of K^+. Phase 2 is the "plateau" phase sustained by a balance between inward movement of Ca^{2+} and outward movement of K^+. Phase 3 is the repolarization phase due to the outward I_K caused by the opening of the slow delayed rectifier (I_{Ks}) K^+ channels, and the rapid delayed rectifier K^+ channels (I_{Kr}).

state. Sodium ions permeate across the channel pore. This is quickly followed by inactivation of the channels (Phase 1) and the opening of the transient outward K^+ channel. Delayed sodium channel inactivation can cause late sodium currents and prolong action potential duration (APD). Phase 2 of the action potential represents the "plateau" phase maintained by the influx of Ca^{2+} ions through L-type calcium channels, the influx of sodium ions through sodium channel and Na/Ca exchanger and the efflux of K^+ ions through the slow delayed rectifier potassium channels, I_{Ks}. During Phase 3, the slow delayed rectifier (I_{Ks}) and rapid delayed rectifier (I_{Kr}) K^+ channels remain open and the L-type Ca^{2+} channels are inactivated. After membrane repolarization, the sodium channels convert back to their resting or closed state.

The cardiac electrical impulse originates from the sinoatrial node pacemaker cells that depolarize spontaneously. The impulse is conducted to and through the atria to the atrioventricular junction, and then propagates to ventricles via the right/left bundle branches and Purkinje fibers. Voltage-gated sodium channels, mainly $Na_v1.5$, play a key role for impulse propagation and conduction.

Sodium ionic currents can be measured under voltage clamp at the whole cell membrane level, referred to as whole cell patch clamp, a broadly used method to measure membrane currents from isolated cells. A typical laboratory setup is shown in Fig. 1.3.

1.1.3.2. $Na_v1.5$ and the excitation-contraction coupling (ECC) process

After the cell depolarizes, L-type voltage-dependent calcium channels on the cell surface open and allow calcium ions to enter the cell. This small amount of calcium entry stimulates calcium-release channels named ryanodine receptors (RYR2) and triggers a

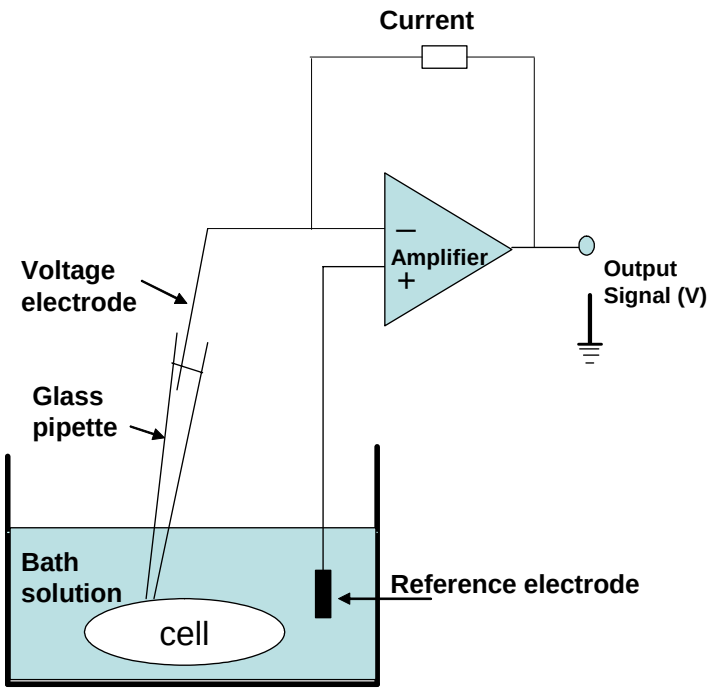

Fig. 1.3 Schematic diagram for a typical electrophysiological laboratory set-up.
The set-up represents a technique for studying ionic currents at the cellular level. A glass pipette is pressed gently on the cell membrane to form a seal. When suction is applied to the pipette the membrane breaks and the cytoplasm and pipette solution start to equilibrate. Cells are voltage-clamped and currents are recorded with the help of hardware (computer and amplifier) and software (pClamp9.0).

subsequent release of a larger amount of calcium ions stored in the sarcoplasmic reticulum (SR). The free calcium ions bind to troponin-C (TN-C), one of the triple regulatory complexes attached to the thin filaments, inducing a conformational change and relieving inhibition on the actin-myosin crossbridge by troponin I. These changes result in a movement between the myosin heads and the actin and cause muscle contraction. This physiological process that converts an electrical stimulus to a mechanical response has been named excitation-contraction coupling (Sandow, 1952). Recent work has shown that late sodium currents generated by the mutant sodium channel N1325S of $Na_v1.5$ may lead to intracellular calcium overload (Yong et al. 2007). Irregularities in Ca^{2+} transients caused by the altered sodium currents may affect cardiac cell contractility.

1.2. Cardiac diseases associated with the *SCN5A* gene

Mutations in the cardiac sodium channel gene *SCN5A* have been linked to the pathogenesis of several serious cardiac diseases. Appendix A summarizes the $Na_v1.5$ mutations associated with cardiac diseases. The relationship between $Na_v1.5$ mutations and the physiological functions associated with the corresponding cardiac diseases is described as follows.

1.2.1. The Long QT Syndrome (LQTS)

The long QT syndrome (LQTS) is characterized by prolongation of the QT interval and T wave abnormalities on electrocardiograms (ECG) and it is associated symptoms including syncope and sudden death caused by a specific ventricular

arrhythmia, *torsade de pointes* (Schwartz et al. 1975; Wang et al. 1997). Two major clinical forms of LQTS have been described based on genetic transmission patterns: autosomal dominant LQTS (Romano-Ward syndrome) with normal hearing (Ward et al. 1964; Romano et al. 1965) and the much rarer autosomal recessive LQTS (Jervell-Lange-Nielsen syndrome) that is associated with congenital neural deafness (Jervell et al. 1957). LQTS can also be sporadic and acquired (Towbin et al. 2001). Although most clinical symptoms are "triggered" by strong emotional outpouring, exercise and sudden awakening from sleep, syncope and sudden death can also occur during sleep or at rest (Keating et al. 2001).

1.2.1.1. Genetics of long QT syndrome (LQTS)

During the past decade, nine LQT genes have been discovered. *KCNQ1 (LQT1,* mapped to chromosome 11p15.5*)* (Wang et al. 1996, Keating et al. 1991), *KCNH2 (LQT2,* on chromosome 7q35-36*)* (Curran et al. 1995, Jiang, 1994), *KCNE1 or MinK (LQT5,* on chromosome 21q22*)* (Splawski et al. 1997, Schulze-Bahr et al. 1997), *KCNE2 or MiRP1 (LQT6,* on chromosome 21q22 *)* (Abbott et al. 1999), *KCNJ2 (LQT7,* on chromosome 17q23*)* (Tristani-Firouzi et al. 2002, Plaster er al. 2001) all encode potassium channel subunits. *SCN5A (LQT3,* on chromosome 3p21-24*)* gene has been shown as the chromosome 3-linked LQT gene (3p24-p21), and encodes the cardiac sodium channel protein (Wang et al. 1995a, Jiang, 1994). The LQT8 gene is *CACNA1C* mapped to chromosome 12p13, which encodes the alpha 1c subunit of voltage-gated cardiac L Type calcium channel (Splawski et al. 2004, Jacobs et al. 2006). The first non ion channel gene to be linked to the LQTS (LQT4, on chromosome 4q25-27) is *ANK2*, a gene

encoding ankyrin-B, a member of a family of versatile membrane adapters (Mohler et al. 2003, Schott et al. 1995). Recent research work reported *CAV3*, a gene encoding caveolin-3, an ion channel-associated protein, as a novel LQTS gene (LQT9, on chromosome 3p25) (Vatta et al. 2006). Heterozygous mutations in all these genes cause autosomal dominant LQTS (Romano-Ward syndrome). Among LQTS patients, 40-45% have *KCNQ1* mutations, 40-45% have *KCNH2* mutations, and 5-8% have mutations in *SCN5A*. Less than 1% of clinical cases are reported to have rare LQTS forms, which include LQT4, LQT5, LQT6, LQT7, LQT8, and LQT9 (Zareba W 2006, Vatta et al. 2006). Homozygous mutations in *KvLQT1* and *KCNE1* result in autosomal recessive LQT (Jervell-Lange-Nielsen syndrome) (Splawski et al. 1997; Neyroud et al. 1997).

1.2.1.2. *SCN5A* mutations and LQT3

Long QT syndrome type 3 (LQT3) results from gain-of-function mutations in the cardiac sodium channel $Na_v1.5$. A late persistent inward current is a common electrophysiological property of mutations in $Na_v1.5$ leading to LQTS. This late sodium current results in a gain of sodium current during the plateau of the action potential, and thus results in a longer plateau phase of the cardiac action potential and a prolongation of the Q-T interval. (Bennett et al. 1995, Clancy et al. 1999). To date, there are at least forty-seven mutations reported to be associated with LQT3 (Appedix A). These mutations include thirty-eight missense mutations, six deletion mutations, one splice mutation and two insertion mutations. Among them, 15 mutations are located in Domain IV. The most studied of these mutations are *$Na_v1.5$*-ΔKPQ, *$Na_v1.5$*-N1325S, *$Na_v1.5$*-R1644H, *$Na_v1.5$*-D1790G and *$Na_v1.5$*-I1768V. *$Na_v1.5$*-ΔKPQ, *$Na_v1.5$*-N1325S and

$Na_v1.5$-R1644H mutations cause persistent late inward sodium currents and exhibit prolonged APD, which are due to dispersed reopenings or long-lasting bursts (Dumaine et al. 1996). In contrast, both *$Na_v1.5$*-D1790G and *$Na_v1.5$*-I1768V do not enhance sustained inward currents (An et al. 1998, Rivolta et al. 2002). Mutant channels with *$Na_v1.5$*-D1790G cause the prolonged APD by increasing $[Ca^{2+}]_i$ transient at slow heart rates (Wehrens et al. 2000), and *$Na_v1.5$*-I1768V induces prolonged APD by enhancing recovery from inactivation and changing the steady-state inactivation kinetics (Rivolta et al. 2002).

1.2.1.3. Mouse models for LQT3

Several SCN5A mutations have been characterized in either transgenic overexpression or knock-in mice. Three mouse models for LQT3 have been established: SCN5A-ΔKPQ knock-in, SCN5A-1795insD knock-in and SCN5A-N1325S transgenic overexpression models (Nuyens et al. 2001, Remme et al. 2006, Tian et al. 2004).

Wang et al. identified the ΔKPQ mutation first in two unrelated LQT3 families (Wang et al. 1995), and later found the same mutation in two other unrelated families (Wang et al. 1995b). The ΔKPQ mutation is the first *SCN5A* mutation identified in humans and is located in the highly conserved portion of the cytoplasmic III-IV linker, the putative channel inactivation gate. The stability of inactivation of the cardiac sodium channel during prolonged depolarization was reported to be decreased in mutant channels with the ΔKPQ mutation, which resulted in prolongation of APD and facilitated the development of arrhythmogenic early afterdepolarizations (EADs) (Bennett et al. 1995). This SCN5A-delKPQ mutation was further overexpressed in mice (Nuyens et al. 2001).

Homozygous embryos ($SCN5A^{\Delta/\Delta}$) died at embryonic day 10.5 when SCN5A becomes important for cardiac excitability. Mice heterozygous for knock-in ΔKPQ ($SCN5A^{\Delta/+}$) exhibited the typical LQT3 features including prolonged action potential and QT intervals, low resting heart rate, early afterdepolarization, ventricular arrhythmias and sudden death (Nuyens et al. 2001). Increased late inward sodium currents during the plateau phase of action potential were blocked by mexiletine, a sodium channel blocker. Ventricular tachyarrhythmias and ventricular extrasystoles were the results of prolonged action potential duration and EAD in $SCN5A^{\Delta/+}$ mice (Nuyens et al. 2001).

The second mouse model for a LQTS mutation is the SCN5A 1795insD/+ mouse. This mutation results from an insertion of an aspartic acid in the C-terminus of SCN5A. This mutation was identified in a Dutch family with a high incidence of LQT3 and Brugada syndrome (Bezzina et al.1999). Expression of 1795insD mutation in *Xenopus oocytes* and HEK293 cells reduced sodium current amplitude, changed channel kinetics characterized by a positive shift of the activation curve, a negative shift of the inactivation curve, disruption of fast inactivation and delayed recovery of sodium channel from inactivation (Bezzina et al.1999, Marieke et al. 2000). This mutation also enhances channel bursting, leading to a persistent component of noninactivating current (Clancy et al. 2002). Heterozygous mice expressing 1795insD, $SCN5A^{1795insD/+}$, exhibited bradycardia, increased PQ interval, prolonged QRS duration and QT interval compared with wild-type mice on ECG (Remme et al. 2006). Epicardial mapping in Langendorff-perfused hearts displayed conduction delay in the right ventricle of $SCN5A^{1795insD/+}$ mice (Remme et al. 2006). Whole cell patch clamp revealed reduction in peak sodium current

density, prolongation of the action potential and a delayed time course of current decay in $SCN5A^{1795insD/+}$ cardiomyocytes (Remme et al. 2006).

The $Na_v1.5$ N1325S mutation is another well-studied LQT mutation, which involves a substitution of an asparagine residue by a serine at position 1325 in the intracellular region between domains DIII S4 and DIII S5. Expression of this mutation in *Xenopus oocytes* and HEK293 cells produced persistent late currents and prolonged APD which can be inhibited by mexiletine and tetrodotoxin (Dumaine et al.1996; Wang et al.1997). Tian et al. in our laboratory developed a LQT3 mouse model by transgenic overexpression of $Na_v1.5$ N1325S mutation in the mouse heart using a murine, cardiac specific α-myosin heavy chain promoter. The LQT3 phenotypes including prolonged QT interval, syncope, ventricular tachycardia, ventricular fibrillation, and sudden death were observed in the transgenic mice. Prolonged APD due to the late persistent sodium current, EAD and a slow recovery from inactivation of I_{Na} were detected in transgenic ventricular myocytes (Tian et al. 2004).

1.2.2. Brugada syndrome

Brugada syndrome is one of the commonly recognized forms of idiopathic ventricular fibrillation (IVF). IVF refers to ventricular fibrillation occurring without underlying structural heart disease, metabolic abnormalities or QT interval prolongation on ECG (Jalife 2000; Viskin et al. 1990). Two commonly recognized forms of IVF include: (1) IVF with normal ECG; (2) Brugada syndrome with characteristic ECG features of right bundle branch block (RBBB) and persistent ST segment elevation (STE) in leads V1 to V3 (Viskin et al 1998).

Brugada syndrome has been estimated to be responsible for 18-30% of all sudden deaths and at least 20% of patient death with a normal heart structure (Antzelevitch et al. 2005). Brugada syndrome can be caused by *SCN5A* mutations (Chen et al 1998). *SCN5A* mutations associated with Brugada syndrome act by a loss-of-function mechanism.

The *SCN5A* mutations in patients with Brugada syndrome result in different electrophysiological abnormalities compared with those known to cause LQTS or conduction system disease. Mutations in the coding region of *SCN5A* in three IVF families were identified in 1998 and those patients have typical ST segment elevation and RBBB ECG pattern (Chen et al.1998). Later a novel *SCN5A* mutation (S1710L) was identified in IVF patients without STE and RBBB on ECG (Akai et al.2000). Research revealed more than one hundred *SCN5A* mutations linked to Brugada syndrome and these mutations are located throughout the *SCN5A* gene (Appendix A). Most of them are exonic mutations including seventy-two missense mutations, four deletions, four frameshifts and one insertion. There are seven mutations in introns affecting RNA splicing. The physiological effects of SCN5A mutations for Brugada syndrome are more complicated than those for LQTS because heterologously expressed sodium channel mutants displayed a broad variety of functional properties (Akai et al. 2000). For example, shifts in the voltage-dependence of activation and inactivation are not always consistent with loss of function. R1512W and S1710L shift the steady-state inactivation curve to more hyperpolarizing potentials (Rook et al. 1999, Akai et al. 2000), and A1924T causes a hyperpolarizing shift of the activation curve (Rook et al. 1999). In contrast, the first mutation T1620M gave a depolarizing shift of steady-state inactivation

curve when expressed in *Xenopus oocytes* (Chen et al.1998, Baroudi et al. 2000), but no effects on inactivation curve when expressed in mammalian tsA201 cells (Baroudi et al. 2000). Most missense and splice-donor mutations lead to a faster recovery from inactivation (Chen et al. 1998, Herbert et al. 2006), while frameshift mutations inactivate the channel, causing a non-functional channel (Chen et al.1998).

1.2.3. Progressive cardiac conduction defect

Loss-of-function mutations in *SCN5A* were also identified in patients with progressive cardiac conduction defects (PCCD), also known as Lev-Lenegre disease (Probst et al. 1999). The progressive cardiac conduction defect is one of the most common cardiac conduction disturbances characterized by progressive alteration of cardiac conduction through the His-Purkinje system with prolonged QRS complexes (Probst et al. 1999). Patients may suffer from syncope or sudden death due to complete atria-ventricular block. This disease affects the conductive tissue associated with myocardial rearrangement and fibrosis (Royer et al. 2005). Affected conduction parameters are P wave, PR and QRS interval duration which increases with age (Probst et al. 2003 and 2006, Royer et al. 2005). Ten mutations in *SCN5A* have been identified in patients with the cardiac conduction defect (Appendix A). These mutations include seven exonic mutations, one frameshift and two splicing mutations. The first *SCN5A* mutation related to PCCD was found in the highly conserved +2 donor splicing site of *SCN5A* intron 22 in a French family. The T→C substitution mutation results in abnormal transcriptional products with the deletion of exon 22, which encodes the voltage-sensitive S4 segment in domain III and results in a non-functional channel (Schott et al.1999,

Probst et al. 2003). Surprisingly, three missense and one splicing *SCN5A* mutations were reported to cause Brugada syndrome and isolated cardiac conduction defect as well (Kyndt et al. 2001, Smits et al. 2005, Rossenbacker 2004 and 2005). Recently, it was found that the severity of symptoms increase with age in PCCD patients with *SCN5A* mutation W1421X (LQT3). An *SCN5A* polymorphism R1193Q was reported to complement the clinical manifestations of the cardiac conduction defect caused by nonsense SCN5A mutation W1421X (Niu et al. 2006). Therefore, the mechanism for PCCD seems complex.

1.2.4. Sudden infant death syndrome (SIDS)

Sudden infant death syndrome (SIDS) is defined as sudden and unanticipated death of an infant younger than one year (Plant et al. 2006). The death is unexplained after a thorough investigation, including a complete autopsy and a review of the clinical history. SIDS is one of the leading causes of infant mortality during the first year of life in developed countries (Tester et al. 2005). The pathogenesis of SIDS is multifactorial, and involves abnormalities in respiratory, cardiac, endocrine and potential neurological functions (Makielski 2006). Prolongation of the QT interval was first detected in 39% of the siblings and 11 (26%) of parents of infants with SIDS (Maron et al. 1976). SIDS was previously considered as a form of LQT3 in infants (Moric et al. 2003). Mutation screening for all known LQTS genes in SIDS identified a *SCN5A* mutation A1330P, which increased channel availability and induced faster recovery from inactivation (Wedekind et al. 2001). Another mutation screen of seven LQTS genes found that 9.5%

of SIDS patients carried LQTS gene variants, which included four *SCN5A* mutations (del AL 586-587, R680H, T1304M, F1486L) and 5 rare genetic variants (S216L, R1193Q, V1951L, F2004L, P2006A) (Arnestad et al. 2007). All of these variants showed defects in the voltage-dependent of inactivation (Wang et al. 2007). Expression of S1103Y in HEK293 cells under different pH demonstrated that acidosis was involved in SIDS, which is consistent with clinical observations (Plant et al. 2006). Prenatal findings and postpartum electrocardiograms strongly suggested that sinus bradycardia was related to severe prolongation of the QTc in infants with SIDS (Schwartz et al. 2000, Beinder et al. 2000). In addition, recent research work showed that mutations in caveolin-3 are also linked to SIDS, and cause LQT3-like phenotype with an increased late sodium current (Cronk, 2007).

1.2.5. Sinus node dysfunction

Sinus node dysfunction (SND) is also called sick sinus syndrome which is accompanied by symptoms such as dizziness or syncope. This syndrome is caused by a malfunction of the sinus node. The sinus node cell is characterized by initiation of the automatic depolarization. Calcium channels ($I_{ca,T}$, $I_{ca,L}$) make the major contribution for the action potential upstroke of nodal cells in the center of nodal tissue. In contrast, sodium channels play a major role in pacemaking in the periphery of sinus node (Kodama et al. 1997). Mutations in the cardiac sodium channel gene *SCN5A* were found to cause sinus node dysfunction. Mutational screening in ten pediatric patients with sick sinus syndrome from seven families identified six mutations (T220I, P1298L, G1408R, delF1617, R1623X, and R1632H). Electrophysiological studies by expression of these

mutations (T220I, P1298L, delF1617 and R1632H) in tsA201 cells identified a loss of channel function, including a reduced peak sodium current density, hyperpolarizing shifts in the voltage dependence of steady-state channel availability, and slow recovery from inactivation (Benson et al. 2003). The nonsense mutation (R1623X) produced nonfunctional channels and missense mutation G1408R was demonstrated to silence the sodium channel function (Benson et al. 2003; Kyndt et al. 2001). These results suggest that *SCN5A* mutations reduce myocardial excitability in patients with sinus node dysfunction.

1.2.6. Atrial dysfunction

Mutations in SCN5A have been linked to atrial dysfunction, including atrial standstill and atrial fibrillation. Atrial standstill is a rare arrhythmogenic condition characterized by the absence of electrical and mechanical activity in the atria. Genetic analysis for a patient with Brugada syndrome accompanied by atrial standstill revealed a missense mutation (R367H) in *SCN5A*. The mutant sodium channel was nonfunctional when expressed heterologously in *Xenopus* oocytes (Takehara et al. 2004). *SCN5A* mutation L212P is another mutation associated with a severe clinical phenotype in atrial standstill (Makita et al. 2005). The heterologously expressed L212P mutant channel in tsA-201 cells exhibited a hyperpolarization shift of steady-state inactivation and delayed recovery from inactivation. Coinherited atrial-specific gap junction connexin 40 (Cx40) SNPs with *SCN5A* mutation L212P may enhance the severity of symptoms by disrupting the spatial distribution of Cx40 and thus influence atrial conduction and excitability (Makita et al. 2005). Therefore, *SCN5A* mutations contribute to the development of atrial

standstill by reducing sodium channel availability and slowing cardiac impulse conduction.

Atrial fibrillation (AF) is another atrial dysfunction associated with *SCN5A* mutations. A common loss-of-function H558R polymorphism in *SCN5A*, which is presented in one-third of the population, was reported to be more common in AF patients than in controls (Chen et al. 2007). In a dog model of chronic atrial fibrillation, the sodium current density decreased with slowing of recovery kinetics in atrial cells (Yagi et al. 2002). *SCN5A* mutations were also identified in patients with both dilated cardiomyopathy and atrial fibrillation (Olson et al. 2005).

1.2.7. Heart failure

Heart failure is a condition in which the heart is unable to pump a sufficient amount of blood to meet the needs of the body, which may result from any abnormality of cardiac structure or function. In a dog model of heart failure induced by sequential coronary microembolization, the expression of $Na_v1.5$ protein was reduced about 30% and sodium current density was decreased significantly (Zicha et al. 2004). Mutations in SCN5A have been shown to increase the risk for dilated cardiomyopathy and heart failure with atrial fibrillation (Olson et al. 2005).

1.3. Regulation of $Na_v1.5$

The mechanisms that underlie modulation of sodium channel functions have been complex and vary according to the sodium channels studied. Research work over last several years identified a few $Na_v1.5$ regulatory proteins (Fig. 1.4). They include

auxiliary β subunits, C-terminal interacting proteins including fibroblast growth factor homologous factor1B (FHF1B), calmodulin, ubiquitin-protein ligase Nedd4 and syntrophin/dystrophin complex, cytoplasmic loop I interacting protein 14-3-3, and cytoplasmic loop II interacting protein ankyrin G. The $Na_v1.5$ channel can also be modulated by phosphorylation (Fyn, protein kinase A, protein kinase C, glucocorticoid–inducible kinases SGK1 and SGK3) and dephosphorylation (protein tyrosin phosphatase H1). I will discuss these $Na_v1.5$ interacting proteins in detail below.

1.3.1. Regulation by auxiliary β subunits

The regulation of $Na_v1.5$ channels by β subunits has been extensively studied. At least four different β-subunits, β1, β2, β3, and β4, have been identified in the heart with different expression levels. Co-expression of SCN1B (encoding β1) with $Na_v1.5$ induced acceleration in the recovery from inactivation in the heart (Nuss *et al.* 1995). Co-expression of SCN5A with either SCN3b (β3) or SCN1b (β1) in *Xenopus* oocytes increased $Na_v1.5$ expression on plasma membrane by threefold (Fahmi et al., 2001), and induced acceleration in the recovery from inactivation in heart (Nuss *et al.* 1995, Baroudi *et al.* 2000). However, SCN3b and SCN1b have different effects on the kinetics of $Na_v1.5$, with β3 causing a significant depolarizing shift in steady-state inactivation, whereas β1 induced faster recovery from inactivation compared to β3 subunit (Fahmi et al. 2001). The β2 subunit was shown to cause a hyperpolarizing shift in $Na_v1.5$ gating (Johnson et al. 2006). Recent study showed that a mutation (L179F) in the β4 subunit

increased the late sodium currents, the similar effect to the LQT3 mutation, ΔKPQ (Medeiros-Domingo et al. 2007).

1.3.2. Regulation by protein kinases/phosphatases

The cardiac sodium channel has been reported to be subjected to phosphorylation and de-phosphorylation by kinases or phosphatases. cAMP-dependent protein kinase A (PKA) and G protein stimulatory α–subunit (Gsα) modulate $Na_v1.5$ upon β-adrenergic stimulation. Activation of protein kinase A increased sodium currents derived from cardiac sodium channels (Schreibmayer et al.1994, Frohnwieser et al.1997). The underlying mechanism may be related to an increased number of sodium channels on the plasma membrane. Preincubation with two cell surface protein recycling interrupters, chloroquine and monensin, prevented the PKA-mediated increase of sodium currents on cell membrane (Zhou et al. 2000). Further studies showed that PKA mediated modulation of the trafficking of sodium channels by phosphorylation of residues in the cytoplasmic I-II interdomain loop (Ser526 and Ser529 of $Na_v1.5$) (Murphy et al. 1996, Zhou et al. 2000). In addition, the presence of putative ER 'retention' signals in the I-II interdomain loop of the human cardiac sodium channel is also necessary for PKA–mediated enhancement of sodium currents (Zhou et al. 2000 and 2002). Matsuda et al. reported that the N-terminus of the native Gsα was able to modulate the function of the cardiac sodium channel directly, i.e., independent of PKA (Matsuda et al. 1992). Lu et al. further found that the mechanism was an increase of the number of sodium channels

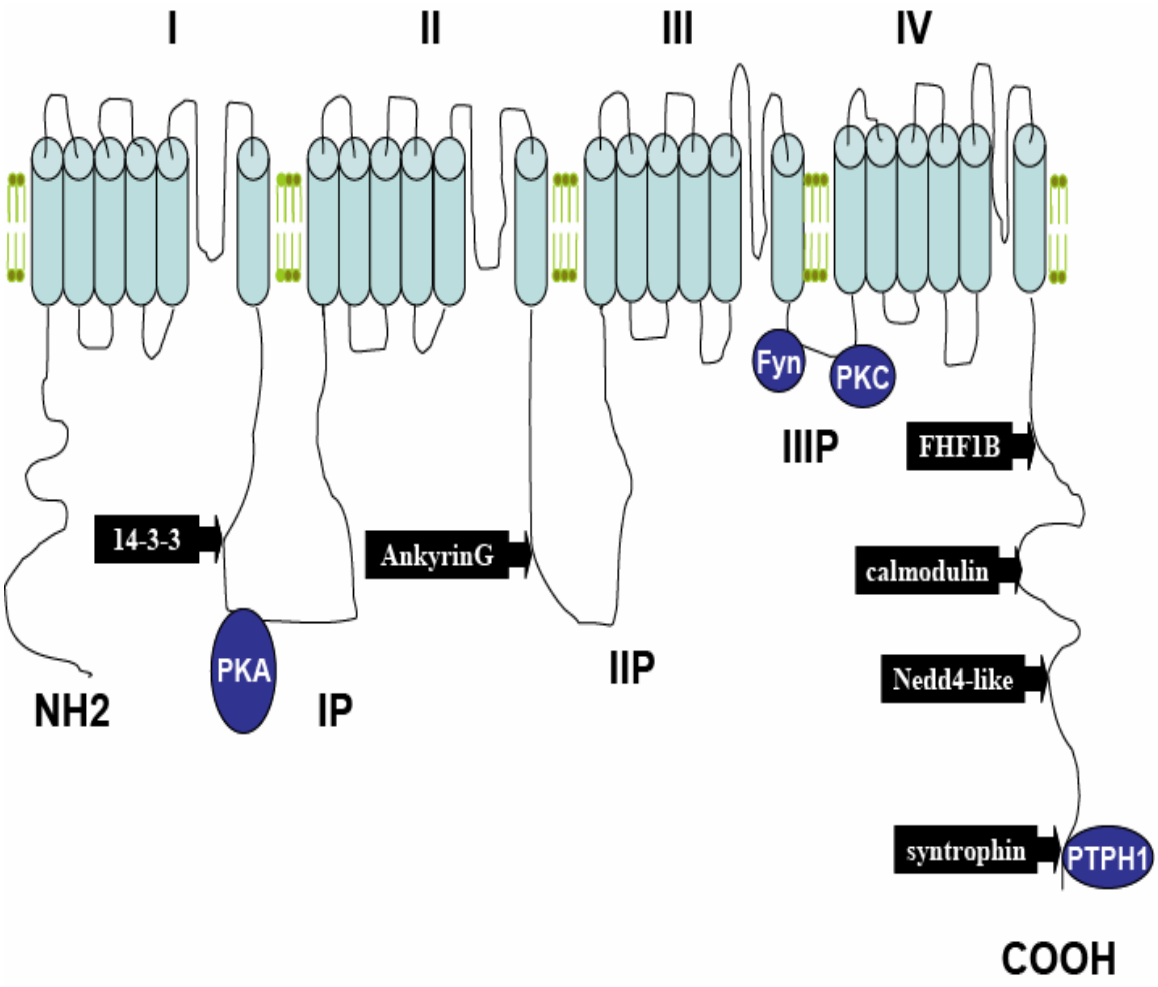

Fig. 1.4. Schematic representation of $Na_v1.5$ and its associating proteins. Ten proteins that have been reported to be associated with $Na_v1.5$ are represented schematically. These proteins include FHF1B, calmodulin, Nedd-4-like and syntrophin that interact with the C-terminus of Nav1.5, ankyrin interacting with the cytoplasmic loop II between transmembrane domains II and III, and the 14-3-3 protein interacting with the loop I of Nav1.5. Four kinases/phosphatases, PKA and PTPH1 that interact with the cytoplamic loop I and C-terminus respectively. PKC and Fyn interact with loop III. Beta subunits have not been shown here. This Figure was modified from Abriel et al. *Trends Cardiovasc Med* 2005;15:35–40).

on cell surface (Lu et al. 1999). In contrast, activation of α-adrenergic stimulating protein kinase C (PKC) resulted in the reduction of sodium currents through phosphorylation of serine 1503 (Serine 1505 in rat) of the cardiac sodium channel (Qu et al. 1996, Tateyama et al. 2003). Phosphorylation of this serine residue by PKC was further demonstrated to suppress the sustained sodium channel current (I_{sus}) caused by disease-linked mutations (Tateyama et al. 2003). Another tyrosine kinase Fyn has been shown to induce a depolarizing shift of steady-state inactivation and to accelerate the recovery from inactivation of $Na_v1.5$ channels when heterologously coexpressed in HEK293 cells with $Na_v1.5$ (Ahern et al. 2005).

Coexpression of the protein tyrosine phosphatase H1 (PTPH1) in HEK293 cells shifted the steady-state inactivation curve towards more hyperpolarized potentials, the function that is mediated by the interaction with PDZ-domain binding motif of $Na_v1.5$ (Jespersen et al. 2006). Therefore, the function of the cardiac sodium channel is regulated by phosphorylation and dephophorylation.

1.3.3. The 14-3-3 protein interacts with the cytoplasmic I-II linker of $Na_v1.5$

The 14-3-3 protein is a highly conserved cytosolic protein expressed broadly in various organisms and tissues. It plays an important role in cell signaling, cell growth, division, adhesion, differentiation, apoptosis, and ion-channel regulation. The 14-3-3 protein was recently found to interact with cytoplasmic loop I between DI and DII of $Na_v1.5$ (Allouis et al. 2006). Coexpression of 14-3-3 and $Na_v1.5$ in COS-7 cells shifted

the steady-state inactivation curve toward hyperpolarizing potentials and slowed the recovery from inactivation.

1.3.4. A protein that interacts with the cytoplasmic II-III linker of $Na_v1.5$: ankyrinG

Ankyrins are intracellular adaptor proteins that link diverse proteins to plasma membrane and endoplasmic reticulum. Ankyrin-G and ankyrin B have been shown to modulate the functions of the pore-forming α-subunit of sodium channel. Lemaillet et al. demonstrated that ankyrin-G interacts with $Na_v1.5$ and this interaction involved a 9-amino acid motif in the cytoplasmic loop II conserved through vertebrate sodium channels (Lemaillet et al. 2003). Further studies revealed that a Brugada syndrome mutation in $Na_v1.5$ (E1053K) is located in the binding site for ankyrinG. This mutation prevented the localization of the cardiac sodium channel to membrane in cardiomyocytes (Mohler et al. 2004).

1.3.5. Proteins that interact with the C-terminal domain of $Na_v1.5$: FHF1B, calmodulin, Nedd4-like and syntrophin/dystrophin

The C-terminal domain of $Na_v1.5$ contains 243 amino acid residues that are important for interactions with several proteins including fibroblast growth factor homologous factor 1B (FHF1B), calmodulin (CaM), Nedd4-like ubiquitin-protein ligase,

and syntrophin/dystrophin (Liu et al. 2003, Tan et al. 2002, Abriel et al 2000, Ou et al 2003).

1.3.5.1. Fibroblast growth factor homologous factor 1B (FHF1B)

Fibroblast growth factor homologous factor 1B (FHF1B) belongs to a subset of the fibroblast growth factor (FGF) family, one of the largest families of polypeptide growth factors. Recent research showed that the C-terminus of both $Na_v1.5$ and $Na_v1.9$ interacted with the N-terminus of FHF1B (Liu et al., 2001, 2003). Coexpression of FHF1B with $Na_v1.5$ shifted the inactivation curve to hyperpolarized potentials, but the detailed role of FHF1B in $Na_v1.5$ function and regulation is unknown (Liu et al., 2003).

1.3.5.2. Calmodulin

Calmodulin (CaM) is a calcium binding protein that serves as a Ca^{2+} sensor through which increased calcium levels are translated into cellular responses by conformational changes of calmodulin (Nelson et al., 1998). The interaction of CaM with the IQ motif at the C-terminus of $Na_v1.5$ (I1908-R1918) is controversial with four studies reporting positive binding (Deschenes et al., 2002, Kim et al., 2004, Tan et al, 2002, Young et al. 2005) and one report of negative binding (Herzog et al. 2003). Data presented by Tan et al suggested that CaM increased slow inactivation of $Na_v1.5$ significantly by performing studies in tsA201 cells (Tan et al 2002). However,

Deschenes et al. did not detect effects of CaM on $Na_v1.5$ by co-expression of CaM and $Na_v1.5$ in HEK293 cells (Deschenes et al. 2002). Recent studies showed that CaM induced a hyperpolarizing shift in the voltage dependence of activation with CaM and $Na_v1.5$ overexpressed in CHO cells (Young et al. 2005). The explanation for these discrepancies might be due to the endogenous expression of different β-subunits among studied cells. On the other hand, Wingo et al. proposed a different Ca^{2+} model for functional modulation of $Na_v1.5$ by which Ca^{2+} regulates the function of $Na_v1.5$ by direct binding to the EF-hand motif in the C-terminal domain of $Na_v1.5$ independent of CaM. Another study reported that the binding of CaM to the $Na_v1.5$ C-terminal domain modulated the interaction between the C-terminal domain and the inactivation gate (III-IV linker) of $Na_v1.5$ (Kim et al., 2004), and presented data against the direct binding between Ca^{2+} and the C-terminal domain of $Na_v1.5$. The mechanism for the regulation of $Na_v1.5$ by Ca^{2+}-dependent CaM thus remains to be further explored.

1.3.5.3. Nedd4 and SGKs

The ubiquitin-protein ligase Nedd4-2 was shown to interact directly with the PY motif (xPPxY) of $Na_v1.5$ (van Bemmelen et al., 2004), and may be involved in regulation of membrane turnover of $Na_v1.5$ by ubiquitination. Co-expression of the ubiquitin-protein ligase Nedd4 in *Xenopus oocytes* decreased the peak sodium current in wild type $Na_v1.5$, but not the channel with mutated PY, suggesting that Nedd4 down-regulated cardiac channel abundance by direct interaction with the PY domain at the C-terminus (Abriel et al. 2000). In a detailed study, human Nedd4-2 (homolog to *Xenopus oocytes*

Nedd4) decreased the expression of $Na_v1.5$ on cell membrane by ubiquitination (van Bemmelen et al., 2004). Further studies revealed that the effects of Nedd4 on $Na_v1.5$ could be related to the serum and glucocorticoid–inducible kinases SGK1 and SGK3. Coexpression of wild type SGK1 and constitutively active ^{S422D}SGK1 in *Xenopus* oocytes reversed the suppression of the endogeneous Nedd4 by phosphorylation, and thus modulated channel abundance in the plasma membrane and enhanced the peak sodium current. In contrast, coexpression of SGK3 may have influence on the gating properties of $Na_v1.5$ directly, not by inactivation of Nedd4 (Boehmer et al. 2003). In addition, phosphorylation of Nedd4-2 induced the degradation of SGK (Zhou et al., 2005). The degradation and internalization of $Na_v1.5$ on cell membrane deserved further studies.

1.3.5.4. Syntrophin/dystrophin

Syntrophins are a family of intracellular adaptors contained in the large dystrophin-associated protein complexes (Ou et al. 2003). Syntrophin β2 has been shown to be involved in regulation of $Na_v1.5$ mechanosensitivity and channel kinetics through interaction between the PDZ domain of syntrophin β2 and the C-terminus of $Na_v1.5$ (Ou et al. 2003). The increased peak inward sodium current was detected in response to bath perfusion, which was used to assess the mechanosensitivity of the sodium channel, whereas the perfusion-induced increase in sodium currents was abolished by the introduction of a PDZ binding domain containing peptide (Ou et al. 2003). Co-transfection of $Na_v1.5$ and syntrophin β2 reduced the availability of sodium channel and changed channel activation and inactivation kinetics (Ou et al. 2003). A recent study

suggested that dystrophin together with syntrophin are part of a multiple protein complex that modulated the expression level and function of $Na_v1.5$ (Gavillet et al. 2006).

1.4. Rationale and objectives

$Na_v1.5$ is a key protein invovled in generation and propagation of the cardiac action potential. $Na_v1.5$ mutations were demonstrated to cause lethal arrhythmias including LQTS, Brugada syndrome and PCCD. However, many questions remained to be answered. First, when this thesis project first began, the only known protein that could modulate the function of $Na_v1.5$ was the β1-subunit. Are there other proteins that can interact with and regulate the function of $Na_v1.5$? Does $Na_v1.5$ function in a large protein complex? Second, the molecular mechanisms by which $Na_v1.5$ mutations cause LQTS were not well-defined *in vivo*. Do LQTS mutations cause re-modeling of gene expression in the heart? Third, is $Na_v1.5$ expressed in other tissues and does it play a role in other tissues or organs? To address these questions, I initiated three studies. Thus, this thesis covers three interesting areas on $Na_v1.5$. Chapter II concerns the regulation of $Na_v1.5$ function. I have identified a new regulatory protein, MOG1, that modulates the function of $Na_v1.5$. In Chapter 3, I tested the hypothesis that LQTS mutations cause remodeling of gene expression in the heart. Genes whose expression is significantly altered by transgenic overexpression of one LQTS mutation in the mouse heart have been identified. Studies on $Na_v1.5$ are also expanded into non-cardiac tissues in searching for novel roles it may play. Thus, in Chapter 4, I investigated the localization of $Na_v1.5$ in the mouse brain to explore the possible novel roles $Na_v1.5$ may play in the brain. These studies on $Na_v1.5$ are expected to help us understand how the function of $Na_v1.5$ is regulated, how

$Na_v1.5$ mutations cause life-threatening cardiac diseases and provide insights into the pathogenetic molecular mechanism of cardiac arrhythmias. They will also shed light on the new functions that $Na_v1.5$ may play.

CHAPTER II.

IDENTIFICATION OF A NOVEL PROTEIN THAT INTERACTS WITH AND REGULATES THE FUNCTION OF CARDIAC SODIUM CHANNEL $NA_V1.5$: MOG1 INCREASES SODIUM CURRENTS[1]

2.1 ABSTRACT

The cardiac sodium channel α subunit $Na_v1.5$ plays an important role in the generation and propagation of electrical signals in the heart, and can cause cardiac arrhythmias, heart failure and sudden death when mutated or deregulated. However, the precise composition of the multi-protein complex for the channel has not been completely defined. Here we report that the physiological function of $Na_v1.5$ is regulated by MOG1, a small protein highly conserved from yeast to humans. Although MOG1 has been implicated in nuclear trafficking of proteins, its localization in cytoplasm and potential interaction with a yeast membrane-associated sensor Sln1p suggest that the *in vivo* physiological roles of MOG1 need to be further defined. Yeast two-hybrid screening with the $Na_v1.5$ identified MOG1 as an interactor. The interaction was confirmed by *in*

[1]Most of the data in this chapter are in press as Wu L et al. (2008) *Journal of Biological Chemistry* 283:6968-78. However this chapter has been rewritten for the purpose of this dissertation.

vitro GST pull-down and *in vivo* co-immunoprecipitation assays. Co-expression of MOG1 with $Na_v1.5$ in HEK293 cells increased sodium current densities, whereas knock-down of the expression of MOG1 by siRNA in HEK293 cells with stable expression of $Na_v1.5$ revealed a significant reduction of the amplitude or complete abolition of sodium currents. The results were replicated in neonatal mouse ventricular myocytes. Immunostaining studies revealed that in the heart, MOG1 was expressed in both atrial and ventricular tissues with predominant localization at the intercalated discs. These results indicate that MOG1 is a critical regulator of sodium channel function in the heart and reveal a new function for MOG1. This study further demonstrates the functional diversity of $Na_v1.5$-binding proteins, which serve important functions for $Na_v1.5$ under different cellular conditions.

2.2 INTRODUCTION

The *SCN5A* gene encodes $Na_v1.5$, the α-subunit of the cardiac sodium channel which plays an important role in generating the cardiac action potential and mediating the rapid conduction of electrical impulses through cardiac tissues. Mutations in the cardiac sodium channel have been identified in several important human diseases including long QT syndrome, Brugada syndrome, idiopathic ventricular fibrillation, cardiac conduction defects, and dilated cardiomyopathy associated with atrial fibrillation (Wang et al. 1995, Chen et al. 1998, Schott et al. 1999, Tan et al. 2001, Olson et al. 2005).

Due to its critical importance in cardiac physiology and human disease, studies to define the regulatory proteins and other components of $Na_v1.5$ associated complex have been of great interest. The major component of the sodium channel complex is the pore-

forming α-subunit that consists of four homologous domains (DI, DII, DIII, and DIV), each of which contains six transmembrane segments (S1-S6) (Gellens et al. 1992, Wang et al. 1996). The channel complex contains other subunits, including at least four β-subunits identified thus far. Co-expression of the β1-subunit with $Na_v1.5$ caused a small but significant acceleration of the recovery from inactivation as well as an increase in current density which may be due to an increased targeting efficiency of the mature channel to the cell membrane (Nuss et al. 1995, Qu et al. 1995). The β3 subunit caused a depolarizing shift in steady-state inactivation and a slower recovery from inactivation than the β1-subunit (Fahmi et al. 2001). The β2 subunit was shown to cause a hyperpolarizing shift in $Na_v1.5$ gating (Johnson et al. 2006). A mutation in the β4 subunit was reported to increase the late sodium current associated with long QT syndrome (Medeiros-Domingo et al. 2007).

In addition to the β subunits, other accessory proteins have been identified for $Na_v1.5$. Their interactions have been shown to form a multi-protein complex (Abriel et al., 2005). Lemaillet et al. demonstrated that a 9-amino acid motif in the cytoplasmic loop II conserved through vertebrate sodium channels is responsible for binding to ankyrin G and the localization of sodium channel to cell membrane (Lemaillet et al. 2003). The C-terminus of $Na_v1.5$ contains 244 amino acid residues that have been shown to be important for interactions with proteins such as FHF1B (fibroblast growth factor homologous factor 1B), calmodulin (CaM), Nedd4-like ubiquitin-protein ligases, syntrophin, Fyn, and protein tyrosine phosphatase (PTPH1) (Abriel H et al. 2005, Jespersen T et al. 2006). In a recent study, 14-3-3 was found to interact with the cytoplasmic loop I between DI and DII and its dimerization was needed for regulation of

sodium currents (Allouis M et al. 2006). Despite the diversity in accessory proteins, the composition of the cardiac sodium channel complex remains poorly understood. It is reasonable to expect that many more proteins are involved in the dynamic networks of protein-protein interactions with $Na_v1.5$ and underscores the significance of multi-protein complexes that are critical for normal cardiac function.

Finding new $Na_v1.5$-associated proteins in myocyte ionic homeostasis was expected to provide an explanation for the disruption of cardiac conduction system that leads to arrhythmias and sudden death. To identify new proteins associated with the cardiac sodium channel complex, we performed a yeast two-hybrid screen with separate intracellular domains of $Na_v1.5$ as baits. When the cytoplasmic loop II between DII and DIII was used as the bait, a candidate $Na_v1.5$-interacting protein, MOG1, was identified.

MOG1 was initially identified as a suppressor that was able to rescue the temperature-sensitive defect of *S. cerevisiae* Ran, a protein involved in nucleocytoplasmic transport, microtubule and nuclear assembly, and the spatial and temporal organization of the eukaryotic cell (Oki et al. 1998, Quimby et al. 2003). *In vitro* studies showed that MOG1 can bind to Ran-GTP (Oki et al. 1998), and release GTP (Steggerda et al. 2000), but its *in vivo* function is not clear. MOG1 has been shown to be a highly conserved protein from yeast to humans (Marfatia et al. 2001). Human *MOG1* gene contains 5 exons and 4 introns and encodes a protein of 187 amino acids with a calculated molecular weight of 20 kDa (Marfatia et al. 2001). The highest expression of MOG1 was detected in the heart by Northern blot analysis (Marfatia et al. 2001), However, the exact physiological function of MOG1 remains to be studied. Our finding

that MOG1 interacts with $Na_v1.5$ suggests that MOG1 may play a role in cardiac physiology.

We further demonstrated the interaction between MOG1 and $Na_v1.5$ by both *in vitro* GST-pull-down and *in vivo* co-immunoprecipitation assays. We examined the physiological role of MOG1 by co-expression of MOG1 and $Na_v1.5$ in HEK293 cells and neonatal cardiomyocytes. Our results indicate that MOG1 is a co-factor for $Na_v1.5$ and modulates the appropriate expression and function of $Na_v1.5$.

2.3 MATERIALS AND METHODS

Construction of Plasmids and Antibodies

The human *MOG1* gene was cloned into vector pET28a at the *EcoR* I and *Sal* I sites (pET28a-MOG1) as previously described (Marfatia et al., 2001). The *MOG1* insert was released from pET28a-MOG1 and subcloned into pcDNA3.1C (Invitrogen) at the *BamH* I and *Not* I sites or into pCMV10, yielding mammalian expression constructs for His-tagged MOG1 (pcDNA3.1C-MOG1) and Flag-tagged MOG1 (pCMV10-MOG1), respectively.

Human cardiac sodium channel gene *SCN5A* was cloned into vector pcDNA3 (pcDNA3-$Na_v1.5$) as described (Wan et al., 2000, Wan et al., 2001), and used for establishing a stable HEK293 cell line with constant expression of $Na_v1.5$, (hereafter referred to as "HEK293/$Na_v1.5$"; a generous gift from Dr. Glenn E. Kirsch). The cytoplasmic loop II (LII) between transmembrane domains DII and DIII of $Na_v1.5$ was amplified by PCR using oligos containing *Xho* I and *EcoR* I restriction sites (Forward: 5'-AGAATTCAGCTCCTTC AGTGCAGA-3', Reverse: 5'-TCTCGAGTTAGTGGT

AGCAGGTCTT-3') and cloned into vector pGEX4T-1-GST-tag (Novagen) (pGEX4T-1-GST-Na_v1.5-LII) for expression and purification of GST-Na_v1.5-LII fusion protein. The cytoplasmic loop I (LI) between DI and DII of Na_v1.5 was amplified and cloned using an identical approach to generate pGEX4T-1-GST-Na_v1.5-LI for expression and purification of GST-Na_v1.5-LI fusion protein. Primers used to amplify the Na_v1.5-LI are 5'-AGTTCAGGATCCGAGGAGCAAAA-3' and 5'-CTTACAGCGGCCGCTTACTTCA CTCCCT-3'. Na_v1.5-LII was also sub-cloned into pcDNA3.1A to express His-tagged Na_v1.5-LII (pcDNA3.1A-Na_v1.5-LII) in mammalian cells.

Two anti-MOG1 antibodies were developed by Genemed Synthesis, Inc. The first MOG1 antibody (#2738) was developed with a MOG1-specific peptide, C-QPPPDNRSSLGPENL at the N-terminal section, and the immunogen for the second antibody (#3350) was a peptide, C-NQQVAKDVTLHQALLRLPQYQTDL at the C-terminal section. The rabbit polyclonal anti-Na_v1.5 antibody was developed as described in chapter IV.

Yeast Two-Hybrid Screen

Yeast two-hybrid analysis was performed with a pre-made MATCHMAKER, human heart cDNA library constructed in *S. cerevisiae* host strain, Y187 (ClonTech Laboratories, Inc.). pACT2-derived constructs generate fusion proteins with the GAL4 activation domain (GAL4 AD) fused to a library of other proteins. The baits for library screening were five different segments of Na_v1.5 fused to GAL4-DNA binding domain (GAL4 BD) in the pAS2 vector. As Na_v1.5 is a membrane protein, the yeast two-hybrid screen with the entire Na_v1.5 protein is unlikely to be fruitful because the protein may not

enter the yeast nuclei. Thus, we selected five cytoplasmic segments of $Na_v1.5$ as baits. These include the N-terminal domain (amino acids 1 to 123), cytoplasmic loop I between DI and DII ($Na_v1.5$-LI, amino acids 437 to 711), cytoplasmic loop II between DII and DIII ($Na_v1.5$-LII, amino acids 940 to 1200), the inactivation gate between DIII and DIV (amino acids 1471 to 1523), and the C-terminal domain (amino acids 1773 to 2016). A bait plasmid was transfected into yeast strain Y187 with a library of human heart cDNAs fused to GAL4-AD. Positive colonies were identified as instructed by the manufacturer (ClonTech Laboratories, Inc.). Approximately 10^7 primary transformants were screened for each of the baits. DNA was isolated from each positive clone and used to transform *E. coli* HB101 (Leu^-) to isolate only pACT2 derivative plasmids. The cDNA insert from each positive pACT2 derivative clone was amplified by PCR and sequenced by the BigDye Terminator v1.1 Cycle Sequencing kit and an ABI PRISM 3100 Genetic Analyzer. The DNA sequences were then characterized by Blast analysis against the NCBI database to determine the identity of the potential $Na_v1.5$-interacting proteins.

GST Pull-down Assays

Construct pGEX4T-1-GST, pGEX4T-1-GST-$Na_v1.5$-LI, or pGEX4T-1-GST-$Na_v1.5$-LII was transformed into *E. coli* BL21 to express the GST, GST-$Na_v1.5$-LI, and GST-$Na_v1.5$-LII proteins. The GST and GST-fusion proteins were then affinity-purified using glutathione sepharose 4B beads according to the manufacturer's protocol (Amersham Pharmacia Biotech). The proteins were eluted with 0.01 M glutathione/100 mM Tris-HCl, pH 7.5, and dialyzed in dialysis buffer (20 mM Tris-HCl, pH 7.5, 50 mM NaCl, 0.1 mM EDTA, 20% glycerol, and 0.5 mM DTT).

The [^{35}S]-labeled MOG1 protein was prepared using a TNT Quick Coupled Transcription/Translation system (Promega). Briefly, 1 μg of plasmid DNA was mixed with TNT Quick Master mix and [^{35}S]-methionine, and incubated for 90 minutes at 30°C. The [^{35}S]-labeled MOG1 protein was mixed with GST, GST-Na_v1.5-LI, or GST-Na_v1.5-LII immobilized on glutathione sephrose 4B beads in binding buffer (1 mM DTT, 0.5 mM PMSF, 1 mM EDTA, 20 mM Tris-HCl, 150 mM NaCl, 0.1% Triton X-100), and incubated for 2-3 hours at 4°C. After binding, the beads were washed with binding buffer, and bound proteins were eluted with 1X SDS loading buffer, separated on a 12% SDS-polyacrylamide gel, dried, and visualized by exposing to X-ray film at -80°C for 12 hours.

Co-Immunoprecipitation (co-IP) Analysis

HEK293/Na_v1.5 cells were maintained in Dulbecco's minimum essential medium (DMEM) supplemented with 10% heat inactivated fetal bovine serum (Invitrogen) and transfected with 10 μg of pcDNA3.1C-MOG1 DNA for the expression of His-tagged MOG1 with Lipofectamine 2000 (Invitrogen). Transfection was carried out with 80% confluent cells in a 10 cm plate. Harvested HEK293 cells/cardiomyocytes were lysed in the TNEN buffer (50 mM Tris/HCl, pH 7.5, 150 mM NaCl, 2.0 mM EDTA, 1.0% Nonidet P40, protease inhibitor cocktail (Roche Molecular Biochemicals Complete Solution) for 24 to 48 hours after transfection. 500 μg of total cell extracts was mixed with a rabbit polyclonal anti-Na_v1.5 antibody (Wu et al., 2002) and incubated on a rotator for 3 hours at 4°C. Protein A/G sepharose 4B beads (Sigma-Aldrich) were added and incubation was continued for another 2 hours. The bound proteins were eluted by boiling the samples for 5 minutes in 1X SDS loading buffer, separated by SDS-PAGE, and

transferred onto a nitrocellulose membrane. The membrane was probed with an anti-His antibody (Sigma-Aldrich) recognizing His-MOG1 fusion protein, and the protein signal was visualized by enhanced chemiluminescence according to the manufacturer's instructions (Amersham Biosciences). For reverse co-IP, a rabbit polyclonal anti-MOG1 antibody was used for immunoprecipitation and the anti-$Na_v1.5$ antibody was used for Western blot analysis. Similar co-IP studies were performed to study the interaction between the cytoplasmic loop II of $Na_v1.5$ and MOG1 by co-expressing His-tagged $Na_v1.5$-LII and Flag-tagged MOG1 in HEK293 cells and with an anti-His antibody and an anti-Flag antibody.

For co-immunoprecipitation analysis of MOG1 and $Na_v1.5$ in cardiac cells, total protein lysates were isolated from adult mouse hearts. Mice were sacrificed and the hearts were excised, washed in Hanks buffer, cut into pieces, add lysed in the lysis buffer (20 mM Tris-HCl, pH7.4, 1 mM EDTA, 150 mM NaCl, 1% NP-40, cocktail of protease inhibitors). The lysates were sonicated on ice (Sonicator 3000, Misonic Inc, NY), incubated on ice for 30 min, and then microcentrifuged at 4^0C for 10 min. The supernatant was collected and its concentration was measured using the BioRad Protein Assay dye. The lysates were pre-cleared on protein A/G beads at 4 °C for 40 min prior to co-IP studies. Protein A/G beads (40 µl) were incubated with 2 µg of the anti-$Na_v1.5$ (or anti-MOG1) (1:500 dilution in PBST) and 500 µg of cell lysates with gentle rocking for 2 h at 4 °C. After washing five times with washing buffer (PBS buffer, protease inhibitors, and 0.5% Triton X-100), the immunoprecipitates were subjected to SDS-PAGE and immunoblot analysis using the anti-MOG1 antibody (or anti-$Na_v1.5$). Cell lysates incubated with protein A/G beads alone were used as a negative control. Co-IP of lysates

with normal IgG was also used as a negative control in each experiment. Studies were repeated at least three times.

Isolation of Mouse Cardiomyocytes

For isolation of neonatal mouse cardiomyocytes, 10-15 mouse hearts were collected from 3-day-old CBA/B6 mouse neonates. The ventricles were excised and myocytes were isolated using the Neonal Rat/Mouse Cardiomyocyte Isolation kit from CELLUTRON Life Technology. The cells were plated on uncoated 100 mm plates to reduce the contamination of cardiac fibroblasts. Myocytes were then cultured in the NS medium (CELLUTRON Life Technology) supplemented with 10% FBS. Isolation of adult cardiomyocytes was performed as previously described by us (Tian et al., 2004, Yong et al., 2006, Yong et al., 2007). The heart was isolated from a mouse (6-8 months) and mounted on a Langendorff apparatus for retrograde perfusion in calcium-containing buffer (in mM): 118, $CaCl_2$; 2.5 $MgCl_2$; NaCl; 4.8, KCl; 2, 1.2 KH_2PO_4; 11, glucose; 13.8, $NaHCO_3$; 4.9, pyruvic acid; pH 7.2–7.4, with 95% O_2:5% CO_2; at 37 °C. The calcium free buffer was then replaced and 0.5 mg/ml collagenase was added for digestion (Type II, Worthington). After 30 minutes of digestion, cells were collected for further studies.

Immunohistochemistry

Immunostaining was performed on adult cardiomyocytes or frozen heart sections (6 μm) with polyclonal anti-$Na_v1.5$ and anti-MOG1 antibodies. Briefly, a freshly excised mouse heart was embedded in Tissue-TEK O.C.D. Compound (Ted Pella, Inc.CA) and frozen in

liquid nitrogen. The frozen sections were pretreated with hydrogen peroxide. The cardiomyocytes were pretreated with 2% Triton-X100. The pretreated section or the cardiomyocytes were then blocked in blocking buffer (5% bovine serum albumin and 0.3% Triton X-100 in 1x PBS) for 2 hr, and then incubated with the primary antibody (1:250 dilution) at 4°C for 24 hours. The sections were then incubated with a secondary antibody mixture containing the FITC-conjugated and Texas Red-conjugated secondary antibodies at room temperature for 2 hours. The immunostained slides were mounted with anti-fading media, and visualized under a confocal microscope.

RNA Interference Analysis

MOG1-specific siRNAs were synthesized by Dharmacon RNA Technologies. Two siRNAs were targeted to mouse MOG1 and their sequences were: siRNA1, 5'-GAGCCUGAGUAACUUUGAAdTdT-3' and siRNA2, 5'-UAACUAGUUUGACU CUUCAdTdT-3'. Blast analysis against the NCBI database suggests that the two siRNAs are specific to MOG1 and do not match any other genes in the mouse genome. The control scrambled siRNA sequences were selected by GenScrip. The sequences for scrambler siRNAs were 5'-UCAUGCCAUUCUUAGUAAU dTdT-3' for siRNA1, and 5'-CGAUAGU TTCTUGUCTGGAdTdT-3' for siRNA2. The siRNAs were labeled with fluorescein at the 5'-end. The siRNAs were transfected into cells by oligofectamine (Invitrogen). Cells were incubated for another 48 hours for expression and functional studies.

Quantitative Real-Time (RT)-PCR Analysis

Total RNA was isolated from siRNA-treated cells using TRIzol reagent (Invitrogen). Reverse transcription was performed using the SuperScript Choice System (Invitrogen). Quantitative RT-PCR was performed with SYBR Green (Applied Biosystems) with an ABI Prism 7900HT Sequence Detection System. 18S rRNA was used as an internal control. The relative mRNA expression level of MOG1 was indirectly shown as CT values (threshold cycle or the fractional cycle number at which the amount of amplified target reaches a fixed threshold). The CT values were then normalized by the RT program as previously described (Tan et al. 2002). Briefly, the target PCR CT value subtracts 18S PCR CT value to yield the ΔCT value, and this value is then adjusted to the mean ΔCT value of untreated cells, generating the ΔΔCT value. The relative mRNA expression level for each sample was then calculated using the following equation: relative mRNA expression = $2^{-\Delta\Delta CT}$ (Tan et al. 2002).

Electrophysiological Analysis

HEK293/$Na_v1.5$ cells or neonatal cardiomyocytes were transfected with pcDNA3.1C-MOG1 using Lipofectamine 2000 (Invitrogen) and electrophysiological recordings were performed as described previously (Tian et al., 2004, Yong et al., 2007). Vector pIRE-GFP DNA expressing green fluorescent GFP protein (0.25 μg) was co-transfected together with pcDNA3.1C-MOG1 to serve as an indicator (Wan et al., 2001, Wu et al. 2002). Only GFP-positive cells were selected for recording sodium currents. Cells with successful transfection of siRNAs were also identified by the green color as the siRNAs were labeled with fluorescence at the 5'-end. Pipettes were fabricated from boroscillate glass (FHC, Inc.) and electrode resistance ranged from 2-3 MΩ when filled

with pipette solution with the following composition (in mM): NaCl, 20; CsCl, 130; HEPES, 10; EGTA, 10; pH 7.2 with CsOH. Voltage command pulses were generated using the Multipatch 700B amplifier (Axon Instruments) under the control of a desktop computer with pCLAMP software (9.0, Axon Instruments). Currents were filtered at 5 kHz (-3 dB, 4-pole Bessel filter) following series resistance compensation. The holding potential for all pulse protocols was -100 mV and experiments were performed at room temperature (22°C). For HEK293 cells, the composition of the bath solution was (in mM): NaCl, 70; CsCl, 80; KCl, 5.4; $CaCl_2$, 2; $MgCl_2$, 1; HEPES, 10; glucose, 10; pH 7.3 with CsOH. For neonatal cells, the NaCl concentration was reduced to 20 mM and CsCl was increased to 120 mM for better voltage control. To reduce contaminating Ca^{2+} and K^+ (transient outward) currents, 2 mM $CdCl_2$ and 2 mM 4-AP, respectively, were added to the bath.

Western blot analysis

To determine the expression level of the $Na_v1.5$ protein in the membrane fraction, total protein lysates were extracted from HEK293/$Na_v1.5$ cells transiently transfected with pcDNA3.1C-MOG1 or empty vector pcDNA3.1C as control using the lysis buffer (1% Triton-100, 150 mM NaCl, 50 mM Tris-HCl, pH7.5, 1 mM EDTA, a protease inhibitor cocktail). Membrane fractions were isolated by centrifugation at 40,000 rpm followed by another centrifugation at 14,000 rpm. The final pellet contains the membrane protein fraction and the supernatant contains the cytosolic protein fraction. Equal amounts of protein extracts were separated on SDS-PAGE. Western blot analysis was performed as described previously (22). A rabbit polyclonal anti–$Na_v1.5$ was diluted

in 1:500 in 0.3% BSA in PBST, and used in Western blot analysis. The signal was detected using enhanced chemiluminescence (ECL kit, Amersham Biosciences, Buckinghamshire,UK). An anti-KCNQ1 antibody (Santa Cruz Biotechnology) was used as a loading control at 1:500 dilution in PBST.

Statistical Analysis

Data are represented as mean values ± SEM. Statistical analysis was performed using an ANOVA and two-tailed Student's t-test to compare means. Significance was set at the indicated P values.

2.4 RESULTS

MOG1 was identified as a candidate protein that interacts with $Na_v1.5$ by a yeast two-hybrid screen

To identify proteins that interact with $Na_v1.5$, we carried out a yeast two-hybrid screen. We screened a human cardiac pre-transformed MATCHMAKER cDNA library (ClonTech, Inc.). Five cytoplasmic segments of $Na_v1.5$ were used as baits for the screening and these include the N-terminus, loop I (between DI-DII), loop II (between DII–DIII), loop III (between DIII–DIV), and C-terminus. The $Na_v1.5$ C-terminus-GAL4-BD fusion protein alone activated transcription of reporter genes, thus no further screening was performed with this bait. No positive clones were obtained with the N-terminal domain and cytoplasmic loop I baits. There were 223 positive clones obtained with the cytoplasmic loop II bait, and 29 positive clones with the loop III bait (Appendix B). One positive clone from the screening was found to encode the portion of MOG1

(GenBank Accession# AF265206, amino acids 65 to 186), and was independently identified twice from the library screening.

Interaction between MOG1 and $Na_v1.5$ as shown by GST pull-down

To further evaluate the interaction between MOG1 and $Na_v1.5$, we carried out a GST pull-down assay. The cytoplasmic loop II of $Na_v1.5$ (amino acids 940 to 1200) was fused to GST (GST-$Na_v1.5$-LII), expressed in *E. coli*, and purified. Radioactively-labeled MOG1 protein was prepared by *in vitro* transcription followed by translation using ^{35}S-methionine and this appeared as a single band of 28 kDa (Fig. 2.1A, lane 1). The GST-$Na_v1.5$-LII fusion protein successfully pulled down ^{35}S-MOG1 in the assay (Fig. 1A, lane 2), whereas two negative controls, GST alone (Fig. 2.1A, lane 4) and the GST-$Na_v1.5$ cytoplasmic loop I fusion protein (GST-$Na_v1.5$-LI, Fig. 2.1A, and lane 3) failed to interact with ^{35}S-MOG1. These results suggest that MOG1 interacts with the cytoplasmic loop II of $Na_v1.5$ *in vitro*.

Interaction between MOG1 and $Na_v1.5$ as shown by co-immunoprecipitation

HEK293/$Na_v1.5$ was transfected with pcDNA3.1C-His-MOG1. Cell extracts were immunoprecipitated using an antibody against MOG1 (Fig. 2.2A, lane 3) or with control rabbit pre-serum IgG (Fig. 2.2A, lane 2). The bound proteins were then detected by Western blot analysis with an anti-$Na_v1.5$ antibody. The anti-MOG1 antibody, but not the control IgG, precipitated a 250 kDa $Na_v1.5$ protein. Reciprocal co-immunoprecipitation was also performed. The anti-$Na_v1.5$ antibody was used for immunoprecipitation, and the anti-MOG1 antibody was used for Western blot analysis.

MOG1 protein was successfully precipitated by the anti-$Na_v1.5$ antibody, but not by the rabbit pre-serum control (Fig. 2.2B). The interaction between $Na_v1.5$ and MOG1 was also evaluated in cardiomyocytes. $Na_v1.5$ was immunoprecipitated by an anti-MOG1 antibody (Fig. 2.2E) and MOG1 was precipitated by an anti-$Na_v1.5$ antibody (Fig. 2.2F). These results support the interaction between MOG1 and $Na_v1.5$.

The interaction between MOG1 and $Na_v1.5$ was further confirmed in mouse cardiac cells. Total protein extracts were prepared from mouse hearts. Both MOG1 and $Na_v1.5$ proteins are abundantly expressed in cardiac cells, and can be easily detected by Western blot analysis (lanes 1 in Fig. 2*E* and lane 1 in Fig 2*F*). Two protein bands were detected for MOG1, which may represent the two MOG1 isoforms derived from alternatively spliced transcripts as reported previously by Marfatia et al (Marfatia et al 2001). Mouse cardiac protein extracts were precipitated either with a polyclonal antibody against MOG1 (Fig. 2*E*, lane 2) or with control IgG (Fig. 2*E*, lane 3). The bound proteins were then detected by immunoblot analysis with an anti-$Na_v1.5$ antibody. The MOG1 antibody easily precipitated a $Na_v1.5$ protein (Fig. 2*E*, lane 2). Similar experiments revealed that the anti $Na_v1.5$ antibody could precipitate MOG1 proteins from mouse cardiac cell extracts (Fig. 2*E*, lane 2). These results indicate that MOG1 interacts with $Na_v1.5$ *in vivo* in cardiac cells.

As MOG1 was pulled out from the yeast two-hybrid library using $Na_v1.5$-LII, we next determined whether the loop II interacts with MOG1 using the co-immunoprecipitation assay. HEK293 cells were transiently co-transfected with

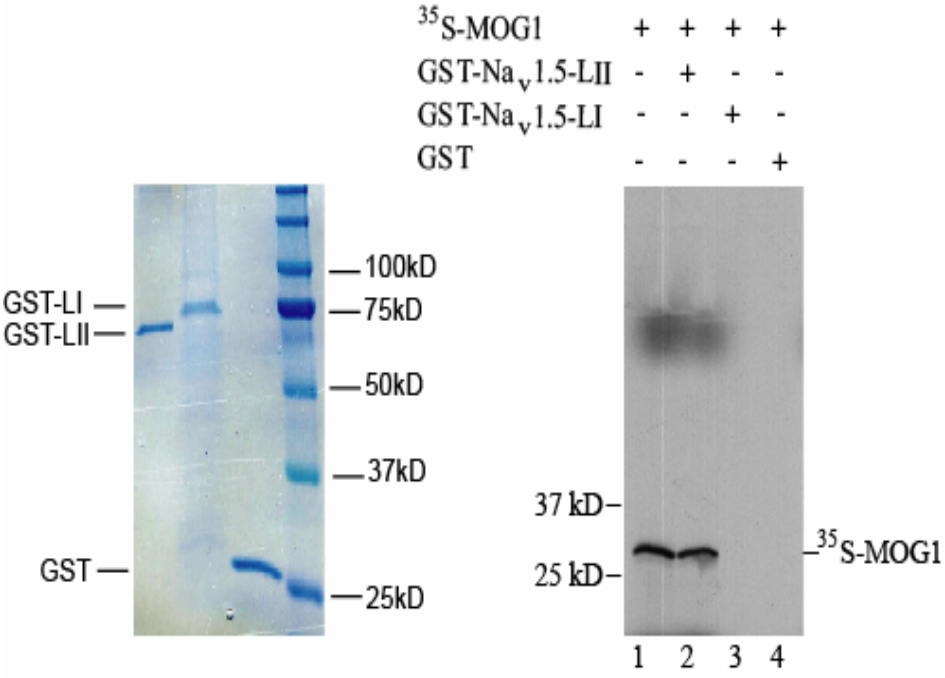

Fig. 2.1. GST pull-down assay for the interaction between $Na_v1.5$ and MOG1. A). Coommassie staining for purified GST and GST fusion proteins. B). *In vitro*-translated ^{35}S-MOG1 bound strongly to $Na_v1.5$ cytoplasmic loop II fused to GST (GST-Nav1.5-LII; lane 2), but not to cytoplasmic loop I fused to GST (GST-$Na_v1.5$-LI; lane 3) or GST alone (lane 4). Lane 1, one-tenth of the input (^{35}S-MOG1).

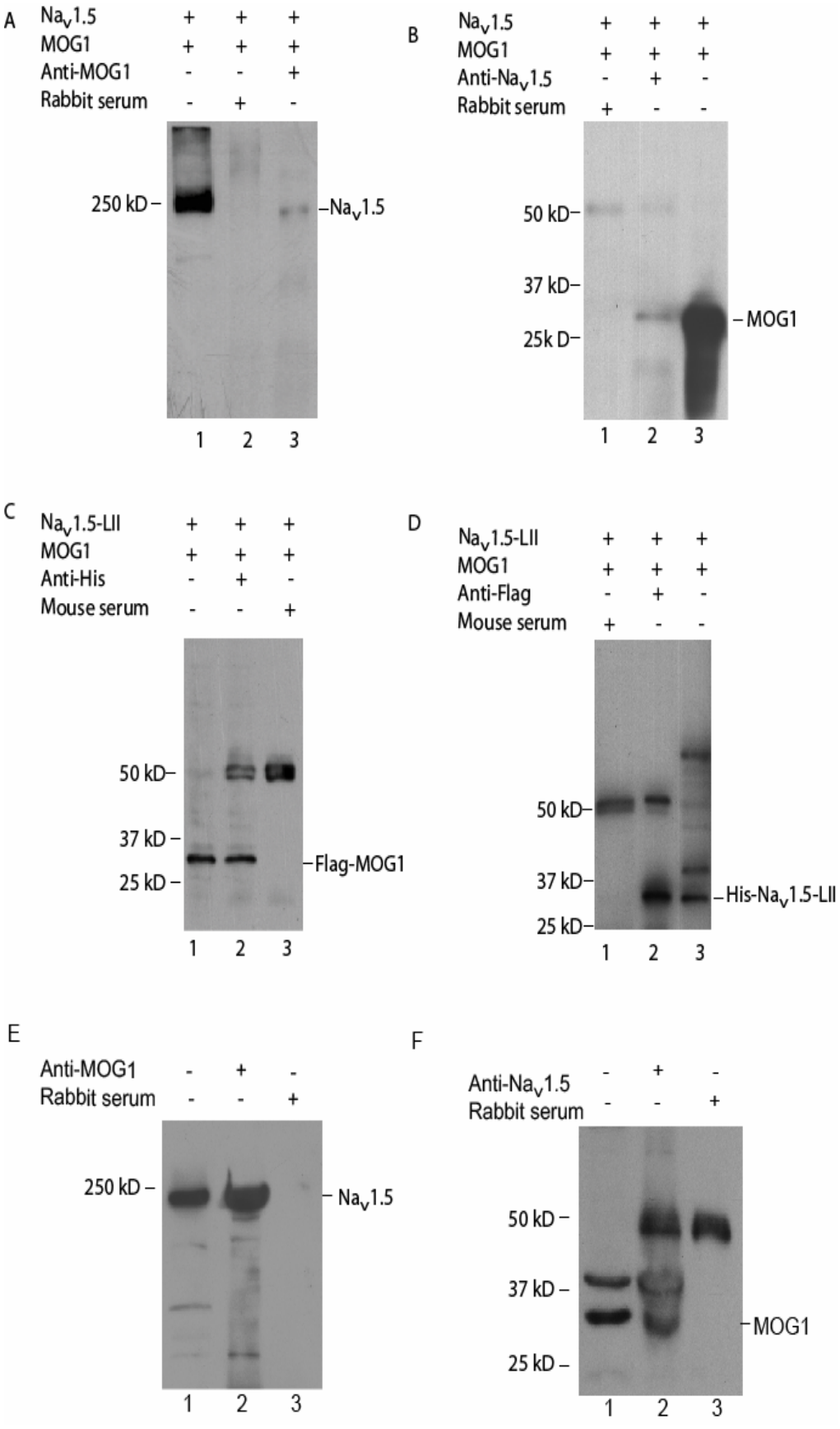
A
Na$_v$1.5 + + +
MOG1 + + +
Anti-MOG1 - - +
Rabbit serum - + -
250 kD
Na$_v$1.5
1 2 3
B
Na$_v$1.5 + + +
MOG1 + + +
Anti-Na$_v$1.5 - + -
Rabbit serum + - -
50 kD
37 kD
25k D
MOG1
1 2 3
C
Na$_v$1.5-LII + + +
MOG1 + + +
Anti-His - + -
Mouse serum - - +
50 kD
37 kD
25 kD
Flag-MOG1
1 2 3
D
Na$_v$1.5-LII + + +
MOG1 + + +
Anti-Flag - + -
Mouse serum + - -
50 kD
37 kD
25 kD
His-Na$_v$1.5-LII
1 2 3
E
Anti-MOG1 - + -
Rabbit serum - - +
250 kD
Na$_v$1.5
1 2 3
F
Anti-Na$_v$1.5 - + -
Rabbit serum - - +
50 kD
37 kD
25 kD
MOG1
1 2 3

Fig. 2.2. Co-immunoprecipitation assay for the interaction between $Na_v1.5$ and MOG1. A, Whole cell lysates prepared from HEK293/$Na_v1.5$ cells transiently transfected with a pCMV-10-MOG1 construct were immunoprecipitated with an anti-MOG1 antibody (lane 3) or pre-serum (lane 2) and analyzed by Western blotting with a polyclonal anti-$Na_v1.5$ antibody. The anti-MOG1 antibody successfully precipitated $Na_v1.5$. Lane1, one-tenth of the input (cell extracts). B, Reciprocal co-immunoprecipitation with an anti-$Na_v1.5$ antibody for immunoprecipitation and the anti-MOG1 antibody for Western blotting. Lane 3, one-tenth of the input (cell extracts). C, Interaction between His-tagged loop II of $Na_v1.5$ and Flag-tagged MOG1 co-transfected into HEK293 cells. An anti-His antibody successfully precipitated Flag-tagged MOG1 (lane 2), but the control mouse serum failed to precipitate Flag-tagged MOG1. Lane 1, 1/50 of the input (cell extracts). D, Reciprocal co-immunoprecipitation for C. Lane 1, control mouse serum failed to precipitate His-tagged $Na_v1.5$-LII; lane 2, an anti-Flag antibody successfully precipitated His-tagged $Na_v1.5$-LII; lane 3, 1/50 of the input (cell extracts). E. Protein lysates extracted from mice cardiac cells were immunoprecipitated with an anti-MOG1 antibody (lane2) and control serum (lane3). Lane 1, one-fifth of input. Signals were detected with an anti-$Na_v1.5$ antibody. F. Reciprocal co-immunoprecipitation with an anti-$Na_v1.5$ antibody for immunoprecipitation and the anti-MOG1 antibody for Western blotting. Lane 1, one-fifth of input. Lane 2, immunoprecipitation with anti-$Na_v1.5$. Lane 3, immunoprecipitation with control serum.

LII (pcDNA3.1A-Na_v1.5-LII). Cell extracts were immunoprecipitated using a monoclonal antibody against His or with control IgG. The bound proteins were then detected by Western blot analysis with a monoclonal anti-Flag antibody. The anti-His antibody, but not the control IgG, precipitated Flag-tagged MOG1 (Fig. 2.2C). A co-immunoprecipitation assay was performed using an anti-Flag antibody for immunoprecipitation. Na_v1.5-LII fusion protein was successfully precipitated by the anti-Flag antibody, but not by control mouse serum IgG (Fig. 2.2D). These coimmunoprecipitation results indicate that the association of MOG1 to Na_v1.5 is mediated by the cytoplasmic loop II of Na_v1.5.

MOG1 increases sodium current density in a mammalian expression system

We wished to determine whether the interaction of MOG1 with Na_v1.5 modified channel function. For this purpose, we expressed MOG1 in HEK293/Na_v1.5 cells and measured whole-cell sodium currents. As shown in Fig. 2.3A and 2.3B, the sodium current density (expressed as peak current normalized to cell capacitance, pA/pF) across the range of test potentials was significantly increased in cells co-expressed with MOG1. The maximum current density normally measured at -30 mV for vector cells was shifted to -35 mV and increased by 61 pA/pF when co-expressed with MOG1. This is despite the fact that co-expression with MOG1 did not alter cell capacitance (16.6 ± 4.1 pF, n = 5 versus 18.6 ± 1.9 pF, n = 9). Steady-state activation and inactivation gating properties were evaluated using the pulse protocols shown in the insets (Fig. 2.3C). The data for channel activation are the mean normalized conductance plotted against the test potential. MOG1 shifted the voltage dependence of activation to more negative potentials by 4 mV

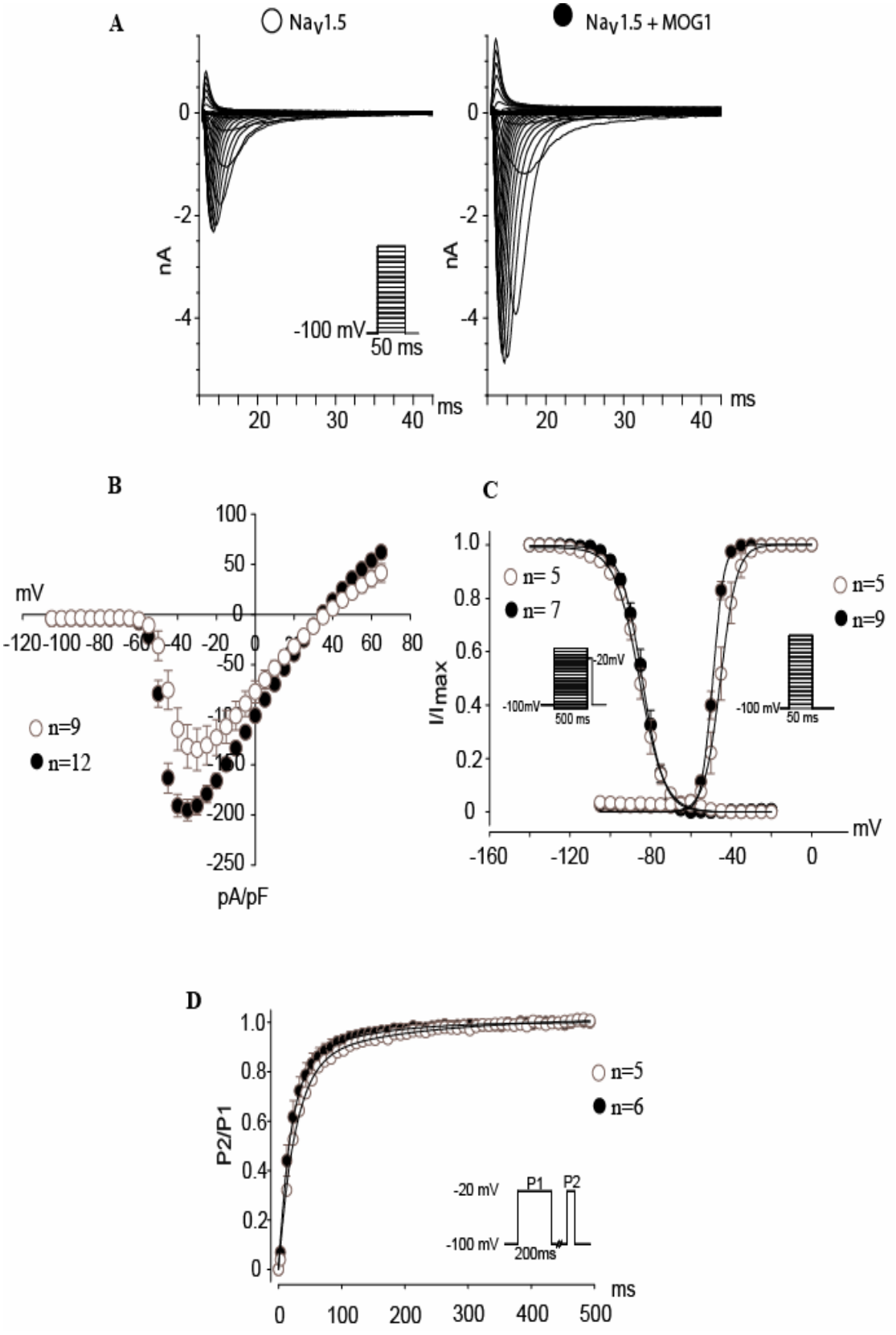
A
Na$_V$1.5
Na$_V$1.5 + MOG1
nA
ms
-100 mV
50 ms
B
mV
pA/pF
n=9
n=12
C
I/Imax
n= 5
n= 7
n=5
n=9
-20mV
-100mV
500 ms
-100 mV
50 ms
mV
D
P2/P1
n=5
n=6
-20 mV
P1
P2
-100 mV
200ms
ms

Fig. 2.3. Over-expression of MOG1 in HEK293/$Na_v1.5$ cells increased sodium current density. A, Raw traces for sodium currents with (right) and without (left) over-expression of MOG1 that were elicited with the current protocol depicted in the inset. B, For activation, cells were held at -100 mV and depolarized in 5 mV increments. The current-voltage relationship for both cell groups is summarized with current amplitudes normalized to cell capacitance (pA/pF, abscissa). Both steady-state activation and inactivation were determined by fitting the peak currents with a Boltzman distribution: $I/I_{max} = 1/(1+e((-V-V_{1/2})/s))$, where I is the current at test potential V, I_{max} is the maximum current, $V_{1/2}$ is the potential giving the half-maximum current; see Text for fitting parameters. C, Steady-state activation (right) and inactivation curves (left). Steady-state activation was plotted over the indicated voltage range and expressed as the current at the test potential over the maximum current (I/I_{max}, abscissa). A two-pulse protocol was used to estimate the membrane potential dependence of inactivation. Cells were stepped to conditioning potentials for 500 ms as shown on the abscissa before depolarization to -20 mV (50 ms step) and peak sodium current from the test potential was normalized to peak sodium current in the absence of a conditioning step. D, Recovery from inactivation was assessed for both cell groups utilizing a two-pulse protocol and the fractional current (P2/P1) was plotted against inter-pulse duration between P1 and P2. The fraction of channels that had recovered following various time intervals was calculated by dividing the peak current measured during a test pulse to -20 mV. The average data were fitted with a bi-exponential function: $I/I_{max} = A_{1x}(1-e(-t/\tau_1))+A_{2x}(1-e(-t/\tau_2))$. In cells over-expressing MOG1, no effects in the inactivation kinetics were observed but a hyperpolarizing 4 mV shift was detected in channel activation.

($V_{1/2act}$ = -49.1 ± 0.1 mV, n = 5 versus -45.1 ± 0.2 mV, n = 9, P<0.05). A two-pulse protocol was used to estimate the membrane potential dependence of inactivation. Cells were stepped to conditioning potentials for 500 ms as shown on the abscissa before depolarization to -20 mV (50 ms step) and the peak current from the test potential was normalized to peak sodium current in the absence of a conditioning step. Cells expressing MOG1 showed no difference in the inactivation kinetics of $Na_v1.5$ (Fig. 2.3C; $V_{1/2inact}$ = -84.1 ± 0.1 mV, n = 5 versus -85.5 ± 0.1 mV, n = 7, P = NS). Similarly, recovery from inactivation was not changed (Fig. 3D; $t_{1/2}$ (τ_1) = 4.2 ± 0.2 ms, n = 5 versus 3.8 ± 0.1 ms, n = 6, P = NS) as this was assessed using a two-pulse protocol and the fractional current (P2/P1) was plotted against inter-pulse duration between P1 and P2. These results show that MOG1 regulates the function of $Na_v1.5$ by increasing sodium current density and by modulating channel activation kinetics with a small hyperpolarizing shift.

Knockdown of MOG1 Expression Reduced Sodium Current Density in a Mammalian Expression System

Two MOG1-specific siRNAs were transfected into HEK293/$Na_v1.5$ cells with expression of MOG1. As shown in Fig. 2.4, Western blot analysis revealed that the siRNAs were effective in knocking down MOG1 expression by around 80% compared to cells treated with scramble siRNAs (18S rRNA was used as an internal control in these experiments). The knockdown of MOG1 expression was further confirmed with quantitative RT-PCR analysis (data not shown). Sodium current density was reduced by

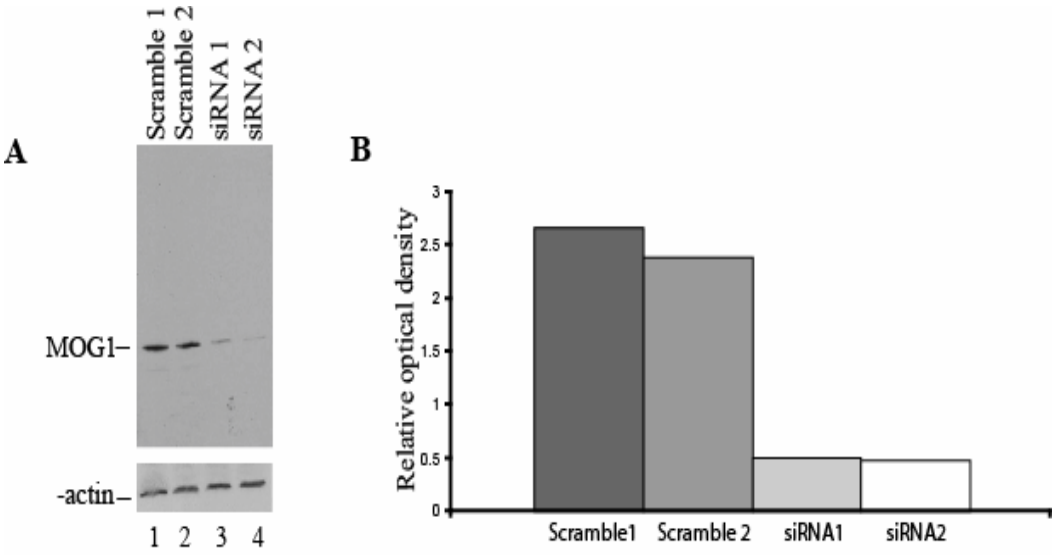

Fig. 2.4. Effects of siRNAs on expression of MOG1. A, Knockdown of MOG1 expression was determined by Western blot analysis (β-actin as loading control). B, The image from Western blot analysis was quantified and plotted. Two siRNAs and corresponding scrambles were tested. siRNA1 and siRNA2 knocked down expression of MOG1 by 4.2-fold and 3.9-fold, respectively.

nearly 2-fold in siRNA-transfected HEK293/$Na_v1.5$ cells (Fig. 2.5A, 2.5B) with no alterations in the activation and inactivation kinetics (Fig. 2.5C, 2.5D). Cell capacitances were no different between cell groups, 15.7 ± 1.3 pF (MOG1- siRNA) and 18.2 ± 1.4 pF (scramble), *P* = NS. The kinetic parameters are as follows for MOG-siRNA versus scramble: $V_{1/2act}$ = -46.3 ± 0.4 mV, n = 6 versus -49.3 ± 0.2 mV, n = 5, *P* = NS; $V_{1/2inact}$ = -83.4 ± 0.2 mV, n = 6 versus -81.7 ± 0.2 mV, n = 5, *P* = NS; and $t_{1/2}$ (τ_1) = 7.1 ± 0.2 ms, n = 6 versus 7.6 ± 0.3 ms, n = 5, *P* = NS. Therefore, reducing the endogenous expression of MOG1 decreases sodium currents and suggests that MOG1 is required for the full activity of cardiac sodium channels.

MOG1 and Sodium Current Density in Neonatal Cardiomyocytes

To determine the role of MOG1 in native cardiomyocytes, we studied the effects of MOG1 on the function of $Na_v1.5$ in neonatal mouse cardiomyocytes as in HEK293/$Na_v1.5$ cells. When MOG1 was over-expressed in 3-day neonatal myocytes, sodium current density was increased by two-fold compared to control vector-transfected myocytes with no apparent changes in cell capacitances (Fig. 2.6). Sodium currents were elicited using a single pulse from -100 to -20 mV. Knockdown of MOG1 expression with siRNAs in neonatal cells nearly eliminated the sodium currents (Fig. 2.7), while no effects on the current were detected following transfection with siRNA scrambles 1 and 2. These results show that in native cardiomyocytes, MOG1 exhibits a similar and significant regulatory role on cardiac sodium channels as in HEK293 cells.

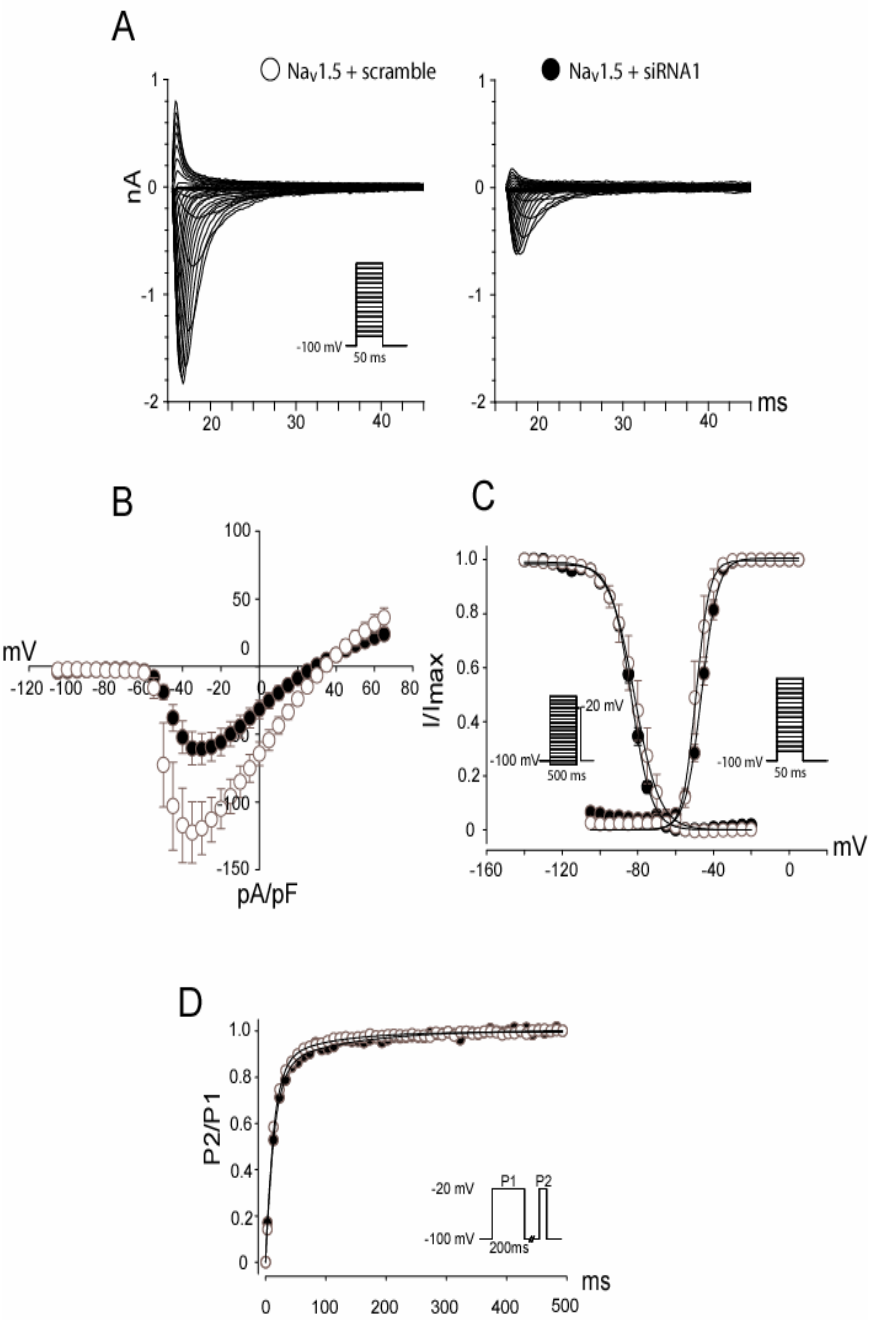

Fig. 2.5. Knockdown of MOG1 expression by siRNAs in HEK293/Na_v1.5 cells decreased sodium current density. A, Raw traces of sodium currents in cells transfected with a scramble (left) and a MOG1-specific siRNA1 (right). B, Effects of MOG1-specific siRNA1 and control scramble siRNA on the current-voltage relationship of Na_v1.5. Identical results were obtained for siRNA2 (data not shown). C, D, The effect of MOG1-specific siRNA1 on steady-state activation, inactivation, and recovery from inactivation, respectively, was evaluated. The sodium currents were recorded and analyzed as described in the Legend of Fig. 3.

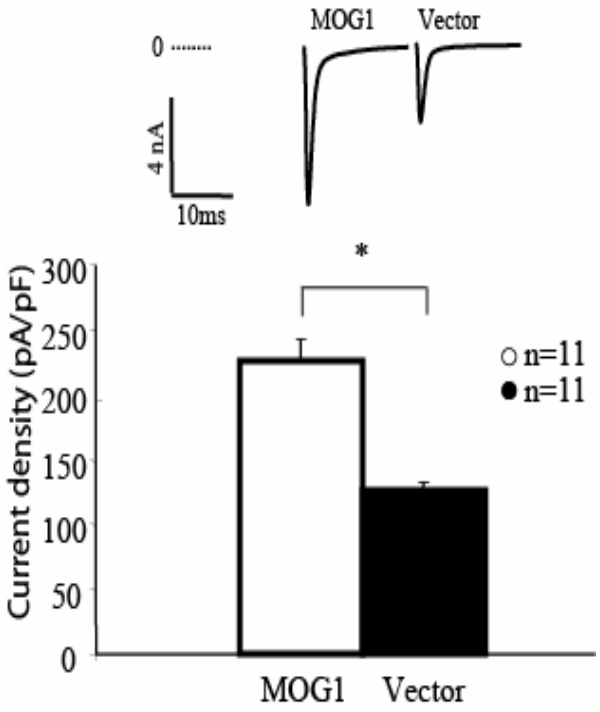

Fig. 2.6. MOG1 over-expression increases sodium current densities in neonatal cardiomyocytes. Maximum currents were elicited using a single pulse from -100 to -20 mV and peak currents were expressed as current densities (pA/pF) and averaged for the cell group. Cell capacitances (C_m) = 32.2 ± 4.7 pF (+ MOG1), 29.3 ± 2.8 pF (-MOG1). "*" indicates P=1.5x10^{-5}.

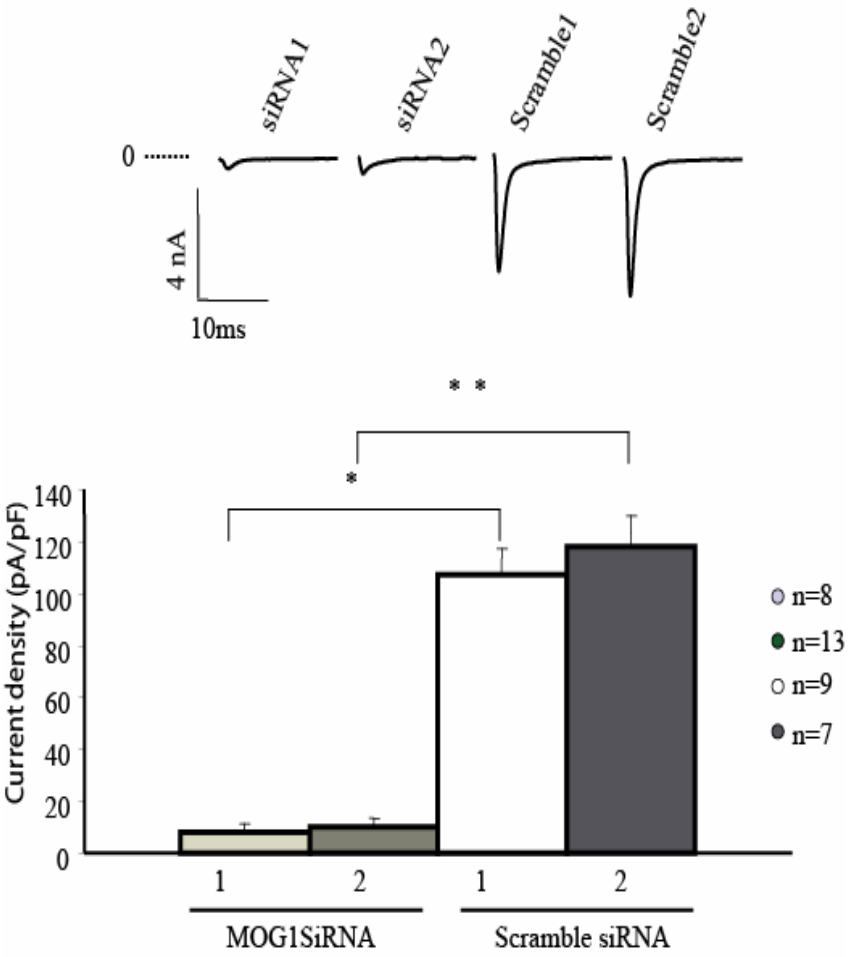

Fig. 2.7. Effects of MOG1 siRNAs on sodium current densities in neonatal cardiomyocytes. Maximum currents were elicited using a single pulse from -100 to -20 mV and peak currents were expressed as current densities (pA/pF) and averaged for the cell group. C_m = 27.3 ± 3.1 pF (siRNA1), 30.4 ± 4.0 pF (siRNA2), 29.3 ± 3.1 pF (scramble 1), 32.3 ± 2.2 pF (scramble 2). "*" indicates P=2.2x10^{-6}, whereas "**" indicates P=2.5x10^{-5}.

Strong expression of MOG1 at intercalated discs in cardiomyocytes and heart tissues

The expression patterns of MOG1 in the heart was studied using immunostaining with two independent anti-MOG1 antibodies. Peptide competition experiment was used to evaluate the specifity of antibody. Immunofluorescent signal was significantly eliminated when the MOG1 antibody (with MOG1 antibody #2728) was pre-absorbed with the antigen peptide (Fig. 2.8A and 2.8B). As shown in Fig. 2.8C, MOG1 was widely expressed in both atrial and ventricular muscles (with MOG1 antibody #2728) and, interestingly, this expression was highly localized in the intercalated discs. Similar results were obtained with the second anti-MOG1 antibody (#3350; data not shown). Immunostaining with a connexin 43 antibody made it possible to easily distinguish the AV node from atrial and ventricular tissues (Fig. 2.8D). Similar to connexin 43, expression of MOG1 protein was high in atrial and ventricular tissues but low in AV nodal tissues. Immunostaining studies were also performed in isolated mouse ventricular myocytes and the results show that MOG1 expression was also particularly strong in the intercalated discs. More importantly, the expression pattern of MOG1 was shown to overlap with that of $Na_v1.5$ in intercalated discs (Fig. 2.8E).

MOG1 Increases Cell Surface Expression of $Na_v1.5$.

To investigate the potential mechanism by which MOG1 increases the sodium channel density, Western blot analysis was performed with the membrane fraction and cytoplasmic fraction of protein extracts isolated from HEK293/$Na_v1.5$ cells transiently transfected with MOG1 or empty vector (control). As shown in Fig 2.9A, $Na_v1.5$

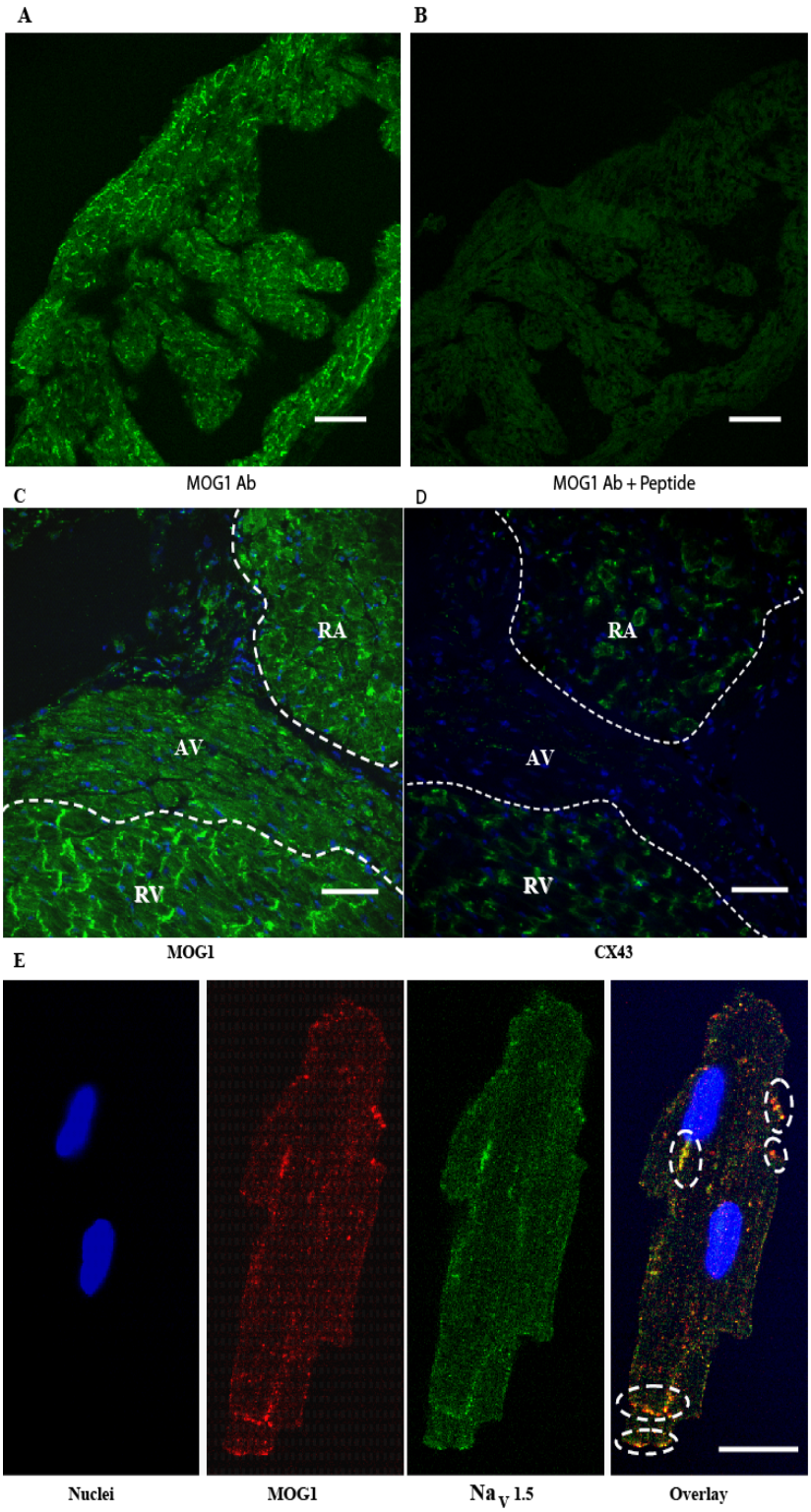
A
B
MOG1 Ab
MOG1 Ab + Peptide
C
D
RA
AV
RV
RA
AV
RV
MOG1
CX43
E
Nuclei
MOG1
$Na_V 1.5$
Overlay

Fig. 2.8. Expression profile of MOG1 protein in heart tissues and isolated ventricular myocytes. MOG1 antibody specificity was examined in two adjacent tissue slides (A and B). Atrial muscle was immunostained by an anti-MOG1 antibody (A) or the MOG1 antibody preincubated with the peptide immunogen (B). scale bar=100 μm. C, Strong expression of MOG1 in right atrium (RA) and right ventricle (RV) with relatively lower expression in the distal common bundle or atrio-ventricular node (AV). D, Immunostaining showing expression profile of connexin 43 (CX43). Scale bar=100 μm E, Co-localization of MOG1 and $Na_v1.5$ at intercalated discs in a cardiomyocyte. Adult ventricular myocytes were isolated and double-stained with polyclonal anti-MOG1 (red) and anti-$Na_v1.5$ (green) antibodies. Nuclei were stained with DAPI (blue). Right panel indicates the overlay of MOG1 and $Na_v1.5$ images. Scale bar=10μm.

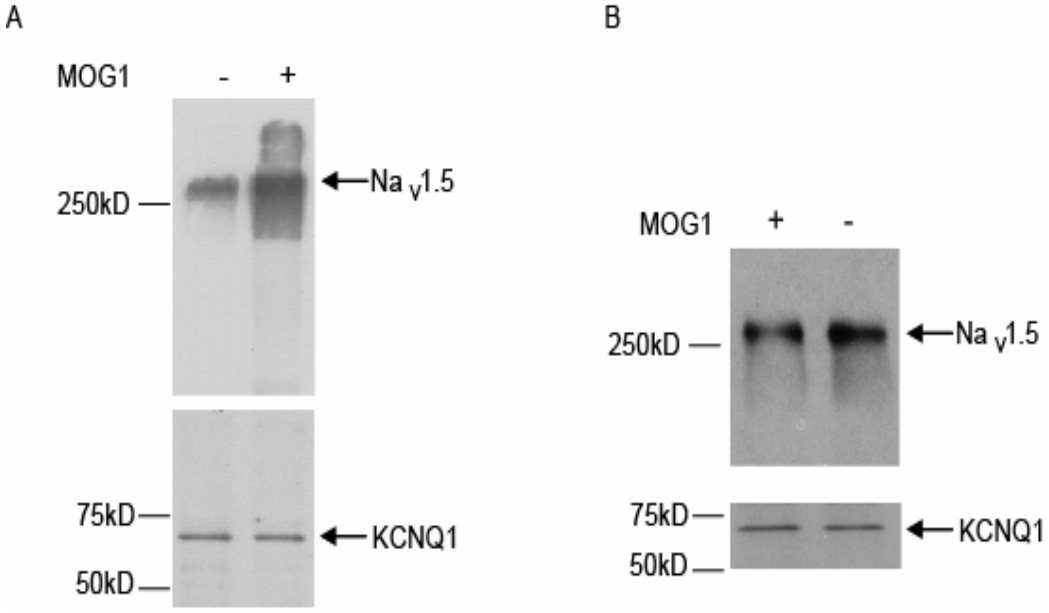

Fig. 2.9. Co-expression of MOG1 increased cell surface expression of $Na_v1.5$. A, Western blot analysis with an anti-$Na_v1.5$ antibody with the membrane fraction of protein extracts from HEK293/$Na_v1.5$ cells transfected with a MOG1 expression plasmid (+) or the empty control vector (-). The membrane filter was later immunoblotted with an anti-KCNQ1 antibody to ensure that an equal amount of proteins extracts were used in the study. Overexpression of MOG1 increased the expression of $Na_v1.5$ on cell membrane. B, Similar studies as in (A), but the cytosolic fraction of protein extracts was analyzed.

expression in the membrane fraction was increased with overexpression of MOG1 in comparison with the control. Accordingly, $Na_v1.5$ expression in the cytoplasmic fraction was reduced with overexpression of MOG1 (Fig. 2.9B). These results suggest that MOG1 increases cell surface expression of $Na_v1.5$, which is consistent with the result that co-expression of MOG 1 and $Na_v1.5$ increased sodium channel densities (Fig. 2.3 and Fig. 2.6).

2.5 DISCUSSION

Here we report a new interacting protein for the cardiac sodium channel $Na_v1.5$ and its effects on the activity of the cardiac sodium currents. Using a yeast two-hybrid screen, we identified MOG1 as a candidate protein that interacted with the cytoplasmic loop II of $Na_v1.5$. *In vitro* GST pull-down analysis showed interaction of MOG1 with loop II, but not with the loop I between domains I and II. These results suggest that the loop II of $Na_v1.5$ is the domain that interacts with MOG1. Both *in vitro* GST pull-down and *in vivo* co-immunoprecipitation analyses further demonstrated this interaction. Over-expression of MOG1 in both HEK293/$Na_v1.5$ cells and neonatal cardiomyocytes resulted in increased whole-cell sodium current density, whereas knockdown of MOG1 expression dramatically reduced or eliminated sodium currents. Our results reveal a new role for MOG1 and suggest that this small protein is a critical component in the multi-protein complex of the cardiac sodium channel with a strong modulatory effect on $Na_v1.5$.

Increased sodium current densities in HEK293/$Na_v1.5$ cells caused by the over-expression of MOG1 suggest that there is either an increase in the number of sodium

channels on the cell surface or an enhancement in single channel conductance. Kinetic analysis of the steady-state activation and inactivation kinetics of $Na_v1.5$ in HEK293/$Na_v1.5$ cells over-expressed with MOG1 revealed a small 4 mV hyperpolarizing shift in activation with little or no effects on channel inactivation. This, by itself, does not come close to accounting for the increase (~60 pF/pA) in the current density in HEK293/$Na_v1.5$ cells with overexpression of MOG1. Following examinations of excised patches from HEK293/$Na_v1.5$ cells over-expressed with MOG1, we further revealed no effect on single channel conductance (data not shown). These results prompted us to examine the possibility that an increase in the number of sodium channels on the cell surface may be the underlying mechanism for the finding of increased sodium current densities by MOG1. This hypothesis was tested by Western blot analysis, which revealed an increase of $Na_v1.5$ expression in the plasma membrane (Fig 2.9A), and a decrease of $Na_v1.5$ expression in the cytoplasm of HEK293/$Na_v1.5$ cells over-expressed with MOG1 (Fig 2.9B). Taken together, the available evidence supports a model in which MOG1 increases the number of sodium channel and/or availability on cell surface, which then results in an increase in sodium current density.

The exact physiological role of MOG1 was previously unknown. The only function of MOG1 reported to date is to form a complex with Ran (Oki et al. 1998). The hypothesized roles of hMOG1 for facilitating the release of GTP and for promoting nueclar transport of other proteins remain to be determined. Expression of MOG1 has been demonstrated in both the nucleus and cytoplasm. One function of cytoplasmic MOG1 may be to regulate the function of $Na_v1.5$. This hypothesis is further supported by the finding that MOG1 is highly expressed in intercalated disks of heart as $Na_v1.5$

does, which suggests that it plays a very important role in the cardiac cells. Northern blot analysis revealed that the heart was the tissue with the highest expression level of MOG1 (Marfatia KA et al. 2001). In this study, we studied the expression of MOG1 in the mouse heart at the protein level using two independent antibodies that were specific to MOG1. Our immunostaining results revealed that the expression of MOG1 protein was specifically high in both atrial and ventricular tissues compared to the AV node (Fig. 2.8C). Interestingly, the protein expression of MOG1 was highly localized at the intercalated discs or the cell-to-cell junctions. The expression pattern of MOG1 was similar to the pattern shown by connexin 43, the primary gap junctional protein in cardiac myocytes, whereby the expression was localized to the intercalated discs of both the atrium and ventricular sections (Fig. 2.8D). As intercalated discs are essential for regulating electrical coupling between cells in the myocardium, co-localization of MOG1 and $Na_v1.5$ in these regions suggests that MOG1 may play an important role in establishing and regulating electrical connections between cardiomyocytes.

MOG1 is highly conserved from yeast to humans, suggesting that it is an essential protein for cellular functions. However, the specific physiological function(s) of MOG1 is obscure. MOG1 was shown to interact with Ran GTPase, a protein is required for the trafficking of proteins and RNA in and out of the nucleus, and mediates the release of GTP from Ran *in vitro* (Oki et al.1998, Quimby et al. 2003). Thus, MOG1 was proposed to play a regulatory role in nuclear import and export by maintaining the Ran-GTP gradient from the nuclei to the cytoplasm (Steggerda et al. 2000). During the nucleocytoplasmic transport, MOG1 was proposed to shuttle between the cytoplasm and the nucleus (Steggerda et al. 2000). Indeed, in HEK293 cells, human MOG1 is localized

throughout the cell (Marfatia et al. 2001). Due to its cytoplasmic localization, the function of MOG1 may not be restricted to the nucleus, on the contrary, it may function outside of the nucleus. A research group showed that yeast MOG1 may interact with an osmotic stress sensor Sln1p and regulates the SLN1-SKN7 signal transduction in yeast (Lu et al. 2004). It is interesting to note that Sln1p is a plasma membrane protein, specifically a two-transmembrane domain sensor of the high-osmolarity glycerol (HOG) response pathway (Lu et al. 2003). These results suggest that MOG1 can interact with a plasma membrane protein. Thus, our finding of the interaction between MOG1 and membrane protein $Na_v1.5$ is no surprise. Oki and co-workers recently showed that yeast MOG1 can also interact with Cid13 (a poly(A) polymerase for suc22 mRNA encoding a subunit of ribonucleotide reductase) with a potential role in regulation of cell cycle S-M transition (Oki et al. 2007). In addition, genetic suppression studies in yeast implicated that MOG1 could be required for membrane localization of Opi3p, a phospholipid methyltransferase required for membrane formation, and might play a role in Ssp1-mediated stress response pathway (Oki et al. 2007). To date, all studies that explored the roles of MOG1 were either *in vitro* studies or involved yeast. The results from the present study, for the first time, reveal a novel physiological role for MOG1 in mammalian cells *in vivo* and suggest that this small protein is a critical component in the multi-protein $Na_v1.5$ complex with a modulator role in determining the amplitude of cardiac sodium currents. The function(s) of mammalian MOG1 may not overlap completely with yeast MOG1 as human MOG1 failed to fully replace the yeast MOG1 in a complementation test of growth defects of a MOG1 deletion yeast strain (Marfatia et al. 2001).

We found that in cardiomyocytes, MOG1 was mostly localized on cell membrane and outside of the nucleus (Fig. 2.8*E*). In HEK293 cells, it was reported that MOG1 was expressed throughout the cell, including the nucleus and cytoplasm (Marfatia et al. 2001), however, the study could not distinguish whether MOG1 was also localized on plasma membrane due to complication of strong signal of MOG1 in cytoplasm. The cell-specific subcellular localization of MOG1 in cardiomyocytes vs. HEK293 cells is an interesting observation, but the molecular mechanism warrants further investigations. Cell- or tissue-specific proteins that interact with MOG1 may be a rational explanation for the observation. The interaction with $Na_v1.5$ or other cardiac specific membrane proteins is expected to recruit MOG1 to the plasma membrane.

In summary, we identified MOG1 as a new interacting protein for $Na_v1.5$. We further demonstrated that MOG1 modulated the gating kinetics of $Na_v1.5$ and was required for the function of $Na_v1.5$ channels. This study may have implications in understanding of the normal physiology of the heart as well as the disease mechanism for long QT syndrome, Brugada syndrome, cardiac conduction disease, and other diseases linked to the cardiac sodium channel $Na_v1.5$. Future studies will likely offer more insights into its role and relevance in myocardial functions.

CHAPTER III

IDENTIFICATION OF GENES DIFFERENTIALLY EXPRESSED IN TRANSGENIC MICE WITH CARDIAC EXPRESSION OF LQTS MUTATION N1325S OF SCN5A BY EXPRESSION PROFILING: INDUCTION OF HIGH STAT1 EXPRESSION IN TRANSGENIC MICE WITH LQTS AND HEART FAILURE[1]

3.1. ABSTRACT

Cardiac-specific expression of the N1325S mutation of *SCN5A* in transgenic mouse hearts (TG-NS) resulted in long QT syndrome (LQTS), ventricular arrhythmias (VT), and heart failure. In this study we carried out oligonucleotide microarray analysis to identify genes that are differentially expressed in the TG-NS mouse hearts. We identified 33 genes in five different functional groups that showed differential expression. None of the 33 genes are ion channel genes. *STAT1*, which encodes a transcription factor involved in apoptosis and interferon response, showed the most significant difference of

[1]Most of the data in this chapter have been published as Wu L et al. (2007) *Biochem Biophys Res Commun* 358:449-454. However this chapter has been rewritten for the purpose of this dissertation.

expression between TG-NS and control mice (a nearly 10-fold increase in expression, $P = 4\times10^{-6}$). The results were further confirmed by quantitative real-time PCR and Western blot analyses. Accordingly, many interferon response genes also showed differential expression in TG-NS hearts. This study represents the first microarray analysis for LQTS and implicates *STAT1* in the pathogenesis and progression of LQTS and heart failure.

3.2. INTRODUCTION

The long QT syndrome (LQTS) is characterized by prolongation of the QT interval and T wave abnormalities on electrocardiograms (ECG) (Curran et al. 1995 and Wang et al. 1995). LQTS is associated with symptoms including syncope, seizures and sudden death caused by a specific ventricular arrhythmia, *torsade de pointes* (Curran et al. 1995 and Wang et al. 1995). One of the major genes identified for LQTS is the *SCN5A* gene on chromosome 3p21–23 (LQT3), which accounts for 10–20% LQTS cases (Wang et al. 1995). *SCN5A* encodes a voltage-gated sodium channel $Na_v1.5$, which is mainly expressed in the heart and responsible for the generation and rapid propagation of electrical signals (action potentials) in cardiomyocytes (Gellens et al. 1992). Besides gain-of-function mutations associated with LQTS, loss of function mutations in *SCN5A* were demonstrated to be involved in the pathogenesis of both Brugada syndrome (Chen et al. 1998) and progressive cardiac conduction defects (PCCD) (Tan et al. 2001). Mutations of *SCN5A* have also been reported to be involved in dilated cardiomyopathy/heart failure and atrial fibrillation (Olson et al. 2005 and Zicha et al. 2004).

The N1325S mutation in *SCN5A* is a substitution of an asparagine residue by a serine residue at position 1325 in the intracellular region of domain III S4–S5 of $Na_v1.5$, and is one of the earliest mutations identified in LQT3 families (Wang et al. 1995). It disrupts the Na^+ channel inactivation and generates the late persistent inward current I_{Na}. Overexpression of the N1325S mutation in *Xenopus* oocytes and HEK293 cells induced dispersed reopening in the late inactivation phase, which produced a late persistent inward sodium current (Dumaine et al. 1996 and Wang et al. 1996). We have expressed the *SCN5A* N1325S mutation in the mouse heart (TG-NS mice) (Tian et al. 2004). The TG-NS transgenic mice showed prolongation of the QT interval on ECG and high incidences of spontaneous polymorphic VT followed by sudden cardiac death (Tian et al. 2004 and Tian et al. 2007). The electrophysiological studies of cardiomyocytes from the transgenic mice showed that the N1325S mutation produced a late sodium current and prolonged the cardiac action potential duration, which is expected to prolong the QT interval on ECG (Tian et al. 2004 and Yong et al. 2007). Recent studies also detected the phenotype of dilated cardiomyopathy and heart failure in TG-NS mice (Zhang et al. 2006) as well as in a human patient with the N1325S mutation of *SCN5A* (Yong et al. 2007). Age-dependent apoptosis and abnormal calcium handling were also demonstrated in the TG-NS cardiomyocytes, and are the likely causes of dilated cardiomyopathy and heart failure (Zhang et al. 2007). However, the molecular mechanism for cardiomyocyte apoptosis in TG-NS mice is not known. In this study we found that the expression of the *STAT1* gene was highly induced in TG-NS hearts, which may be a cause or mediator of apoptosis in these mice.

STAT1 is a member of the Signal Transducers and Activators of Transcription family of transcription factors which mediate various biological responses, including cell proliferation, differentiation, survival and apoptosis. The signals are transduced from various ligands (cytokines, growth factors, stress-induced stimuli) to the nucleus through Janus tyrosine kinases (JAKs) or mitogen-activated protein (MAP) kinases (Adamkova et al. 2007). Seven different STAT family members have been identified, which are activated by different cytokines (Stephanou et al. 2003). STAT1 has two alternative RNA splicing isoforms, STAT1α (p91) and STAT1β (p84) (Schindler C et al. 1992). STAT1β lacks 38 amino acids at the C terminus. STAT1 forms homodimers or heterodimers with STAT3, which binds to the interferon-gamma activated sequence (GAS) on promoters and activates the expression of interferon stimulated genes (ISG). Upon stimulation by IFN-α or IFN-β, STAT1 forms a heterodimer with STAT2 and binds to the interferon stimulated response element (ISRE) on promoters (Katze et al. 2002). STAT1 has been shown to be involved in apoptosis during myocardial ischaemia and oncogenesis (Stephanou et al. 2000, Adamkova et al. 2007). *STAT1* mediates the response to interferon (IFN)-α and IFN-γ and has been shown to be pro-apoptotic (Stephanou et al. 2003). STAT1-deficient mice are more susceptible to development of tumors, which implicates *STAT1* in oncogenesis (Adamkova et al. 2007). No transgenic mice with over-expression of *STAT1* were developed, thus, the physiological effect for over-expression of *STAT1* is unknown.

Microarray analysis is an unbiased approach to study expression of thousands of genes simultaneously in a system. To date, no microarray analysis or other large-scale gene expression studies have been performed for LQTS, either in humans or mice. Here,

we took advantage of our mouse model for LQTS, the TG-NS mice, to explore global gene expression re-programming in these mice. We used mouse oligonucleotide microarrays with 22,690 unique genes to determine gene expression differences between TG-NS and non-transgenic control mice. A surprisingly large number of genes showed differential expression between the two types of mice, which may be partly caused by the marked up-regulation of transcription factor STAT1, as validated by RT-PCR and Western blot analyses. These results implicate *STAT1* in the pathogenesis and progression of LQTS and heart failure in this model and may offer insights into the observation of cardiomyocyte apoptosis in TG-NS mice.

3.3. MATERIALS AND METHODS

Transgenic mice

Human mutant *SCN5A* gene with the LQTS-causing mutation N1325S was expressed in the mouse heart using a cardiac specific promoter, the mouse α-myosin heavy chain (α-mMHC) promoter, and we named this line of transgenic mice as TG-NS. Transgenic mice with cardiac-specific expression of wild type *SCN5A*, TG-WT, were also created. The creation of TG-NS and TG-WT mice was reported by us previously (Tian et al. 2004 and Zhang et al. 2007), and they carry the comparable number of the transgenes and have a comparable level of *SCN5A* expression. Genotyping of the positive TG-NS mice was performed by polymerase chain reactions (PCR) using genomic DNA isolated from mouse tails/toes using the tail lysis buffer (50 mM Tris–HCl,

100 mM EDTA, 100 mM NaCl, 1% SDS). We used PCR primers 5′-TGT CCG GCG CTG TCC CTG CTG-3′ and 5′-CTC ATG CCC TCA AAT CGT GAC AGA-3′ for specific amplification of the *SCN5A* transgene and primers 5′-GGC ACC TGC TGC AAC GCT CTT T-3′ and 5′-GGT GGG CAC TGG AGT GGC AAC TT-3′ for amplification of *AGGF1* that serves as an internal control for quality of mouse genomic DNA. PCR was performed using standard procedures.

Microarray analysis

Total RNA was prepared from heart tissues of the non-transgenic control and TG-NS mice. First, heart tissues were homogenized by a polytron homogenizer (PT3100, Dispersing and Mixing Technology by Kinematica). Total RNA was then isolated using the TRIzol reagent (Invitrogen). The integrity and purity of the RNA was confirmed visually on a 1% denaturing agarose gel, and by measuring the optical density ratio (A260/A280). Double-stranded complementary DNA (ds-cDNA) was synthesized from 15 μg of total RNA using the Superscript Choice System (*Invitrogen*) with an HPLC-purified oligo-dT primer containing a T7 RNA polymerase promoter (GENSET, La Jolla, CA) as instructed by the manufacturer. The cDNA was extracted by the Phase Lock Gel (PLG) kit (Eppendorf) and purified by ethanol precipitation. *In vitro* transcription was performed with 1 μg of ds-cDNA using the ENZO BioArray RNA Transcript Labeling kit (ENZO Diagnostics). Fragmentation of biotinylated cRNA (20 μg), hybridization, washing, and staining were performed following the instructions by Affymetrix by the CWRU Gene Expression Core Facility. The Mouse Genome MOE430A arrays (Affymetrix) were used. Each array contains about 22,690 genes.

Statistical analysis

Microarray data was extracted from scanned images. GeneSpring 7.0 (Silicogenetics) was used to compare the data from three transgenic mice (6–8 months of age, male) with those from three non-transgenic control littermates. All samples were considered as one group of replicates. The algorithm to generate a list of genes that showed a statistically significant difference between the two groups was described previously (Archacki et al. 2003 and Tan FL et al. 2002). The median value for group comparisons was used. All raw data with a score less than zero were set to zero. Genes were further filtered by an absolute call: present (P) or marginally present (M) in the two groups for the up-regulated genes and down-regulated genes.

Quantitative real-time PCR (RT-PCR)

Quantitative RT-PCR was performed using an ABI Prism 7900HT Sequence Detection System (Applied Biosystems). Total RNA was extracted from hearts using TRIzol (Invitrogen). Reverse transcription was performed with 5 μg of RNA using the Superscript Choice System (Invitrogen). Primers spanning exon-intron junctions were designed to avoid amplification of genomic DNA. PCR conditions were 50°C for 2 min and 95°C for 10 min followed by 40 cycles of 95°C for 15 s and 60°C for 1 min. Fluorescence changes were monitored with SYBR Green PCR Supermix (VWR) after every cycle, and melting curve analysis was performed at the end of 40 cycles to verify PCR product (0.5°C/s increase from 55–99°C with continuous fluorescence reading). The 18S gene was used to normalize samples for comparison. To quantify changes in gene

expression, the $\Delta\Delta C_t$ method was used to calculate the relative fold changes as previously described (Livak et al. 2001).

Western blot analysis

To determine the expression level of the STAT1 protein, total proteins were extracted from hearts of transgenic and normal mice. Hearts from 7-8 months old mice were homogenized with Polytron, and lysed on ice with the lysis buffer (0.5% NP-40, 20 mM Tris–HCl, pH 8.0, 100 mM NaCl, 1 mM EDTA and proteinase inhibitor cocktail). The protein concentration was measured using the Bradford method (Bio-Rad). Western blot analysis was then performed. Briefly, equal amounts of protein extracts were separated on 10% SDS–polyacrylamide gels by electrophoresis. The blots were incubated with agitation at room temperature in the presence of a rabbit polyclonal anti–STAT1 antibody (Santa Cruz Biotechnology) (diluted in 1:500 in 0.3% BSA in PBST). The signal was detected using enhanced chemiluminescence (ECL kit, Amersham Biosciences). An anti-β-actin antibody and an anti-GAPDH antibody (Sigma–Aldrich) were used as loading controls at 1:1,000 dilution in PBST.

3.4. RESULTS

Identification of genes differentially expressed in the hearts from TG-NS mice

We investigated the gene expression profiles from three TG-NS mice and three age- and sex-matched control mice using the Affymetrix Mouse Genome MOE430A

Arrays. 2492 of 22,690 genes showed significant expression differences between the two groups if $P \leqslant 0.05$ (Welch *t*-test). Because of the large number of genes identified, filters exceeding 2- and 5-fold changes and several different *P* values were applied. The results are summarized in Table 3.1. With $P \leqslant 10^{-5}$, only two genes, *STAT1* encoding signal transduction and activator of transcription factor 1 and *DLM-1* encoding Z-DNA binding protein 1, showed an expression difference between two groups of mice. At *P* value of 10^{-4}, 11 genes showed differential expression of $\geqslant$5-fold, 9 up-regulated and 2 down-regulated (9↑, 2↓). At *P* value of 10^{-3}, 33 genes (31↑, 2↓) showed expression differences of $\geqslant$5-fold. The number of genes increased to 14 at $P \leqslant 10^{-4}$ and 65 at $P \leqslant 10^{-3}$ if the cut off expression difference was set to 2-fold (Table 3.1).

Our further analysis was focused on genes showing a large differential expression difference, i.e. those showing 5-fold expression differences and *P* value of $\leqslant$0.001. As a result, 31 genes were found to be up-regulated and 2 genes down-regulated in TG-NS mice (Table 3.1). These genes can be divided into five functional groups: 11 genes are involved in interferon-responses; 4 genes are related to apoptosis and inflammation; 4 genes may mediate other immune responses; 4 genes encode enzymes; 11 unknown genes (Table 3.2 and Supplementary Table 3.1).

Validation of microarray results by real-time PCR (RT-PCR)

To verify the results from the microarray analysis, quantitative RT-PCR was performed with 9 additional TG-NS and 7 control mice (6–8 months of age). Results from RT-PCR analysis of 6 highly significant genes, including *STAT1*, *Usp18*, *Oas1 1G*, *Helicard*, *Trim34 delta*, and *Phgdh*, are shown in Table 3.3. The real-time PCR results

Table 3.1. Summary data for the number of genes showing differential expression in TG-NS hearts

Fold difference of expression	P value			
	0.01	**0.001**	**0.0001**	**0.00001**
Up-regulated genes				
2-fold	470	54	12	2
5-fold	101	31	9	2
Down-regulated genes				
2-fold	306	11	2	0
5-fold	53	2	2	0

Table 3.2 List of genes showing differential expression in TG-NS hearts by microarray analysis[1]

Accession #	Symbol	Gene	P value	Fold of change
(A) Genes involved in interferon (IFN)-signaling pathways				
NM_008332.1	*Ifit 2*	Interferon-induced protein with tetratricopeptide repeats 2	1.3×10^{-4}	43.9
NM_011909.1	*Usp18*	Ubiquitin specific protease 18	6.5×10^{-5}	31.8
NM_010501.1	*Ifit 3*	Interferon-induced protein with tetratricopeptide repeats 3	8.3×10^{-4}	31.5
NM_008331.1	*Ifit 1*	Interferon-induced protein with tetratricopeptide repeats 1	2.2×10^{-4}	26.0
NM_016850.1	*Irf 7*	Interferon regulatory factor 7	1.3×10^{-4}	18.6
NM_018734.1	*Gbp3*	Guanylate nucleotide binding protein 3	1.8×10^{-4}	13.5
AF136520	*Dlm-1*	Tumor stroma and activated macrophage protein DLM-1	8.6×10^{-6}	12.9
NM_009283	*STAT1*[2]	Signal transducer and activator of transcription 1	4.0×10^{-6}	9.8
AB067533.1	*Oasl 9*	2,5-Oligoadenylate synthetase-like 9	9.8×10^{-4}	6.6
BC018470	Oasl 1G	2'-5' Oligoadenylate synthetase 1G	2.0×10^{-4}	6.5
AY090098.1	*Isg 12*	Interferon stimulated gene 12	2.7×10^{-4}	6.2
NM_009283	*STAT1*[2]	Signal transducer and activator of transcription 1	4.0×10^{-6}	9.8
AY075132	*Helicard*	Helicard	2.1×10^{-5}	7.9
AF220142	*Trim34 delta*	Tripartite motif protein 34 delta	8.1×10^{-5}	5.5
NM_126166	*Tlr3*	Toll-like receptor 3	2.5×10^{-4}	5.4
(B) Genes with a potential role in apoptosis and inflammation				
AY075132	*Helicard*	Helicard	2.1×10^{-5}	7.9
AF220142	*Trim34 delta*	Tripartite motif protein 34 delta	8.1×10^{-5}	5.5
NM_126166	*Tlr3*	Toll-like receptor 3	2.5×10^{-4}	5.4

[1]Additional genes showing differential expression in TG-NS hearts are listed in Appendix C. [2]*STAT1* is involved in both IFN signaling and apoptosis.

Table 3.3 Conformation of results from mircroarray analysis by RT-PCR

Gene	Microarray[1]	RT-PCR[2]
STAT1:Signal transducer and activator of transcription 1	9.8	8.4
Usp18: Ubiquitin specific protease 18	31.8	65.9
Oas1 1G: 2'-5' Oligoadenylate synthetase 1G	6.5	14.9
Helicard: Helicard	7.9	3.4
Trim34 delta: Tripartite motif protein Trim34 delta	5.5	7.9
Phgdh: 3-Phosphoglycerate dehydrogenase	53.8	66.3

[1]data of fold difference of expression between 3 TG-NS and 3 control mice. [2]data of fold difference of expression between 9 TG-NS and 7 control mice; no overlapping of samples between the microarray and RT-PCR studies.

generally confirmed the results from microarray analysis. Liner regression analysis demonstrated a strong positive correlation between the two technological platforms with R=0.93.

STAT1 showed the most significant differential expression in TG-NS mice

STAT1 is the gene showing the most significant expression difference between TG-NS and control mice with a P value of 4.0×10^{-6} and a fold difference of 9.8 (Table 3.2). In addition to the RT-PCR analysis described above (Fig. 3.1A and Table 3.3), Western blot analysis was also used to validate the finding of increased STAT1 expression in TG-NS mice compared to control littermate mice (Fig. 3.1B). Western blot analysis demonstrated that the basal expression level of the STAT1 protein in non-transgenic control mice was low, however, it dramatically increased in TG-NS hearts (Fig. 3.1B).

Recently, we created and studied transgenic mice with cardiac-specific expression of wild type *SCN5A* (TG-WT) (in contrast to TG-NS with mutant *SCN5A* containing the N1325S mutation) (Zhang T et al. 2007). TG-WT mice did not develop LQTS, VT, or heart failure (Zhang T et al. 2007), thus they could serve as an excellent control for TG-NS mice (note that the TG-WT mice were not available when the microarray project started). Western blot analysis was used to compare the expression level of the STAT1 protein between TG-NS to TG-WT mice. As shown in Fig. 3.1C, the expression level of STAT1 in TG-WT heart was comparable to that in non-transgenic control hearts, but much lower than that in TG-NS hearts. These results suggest that induction of STAT1 expression is specific to TG-NS mice with the *SCN5A* mutation N1325S.

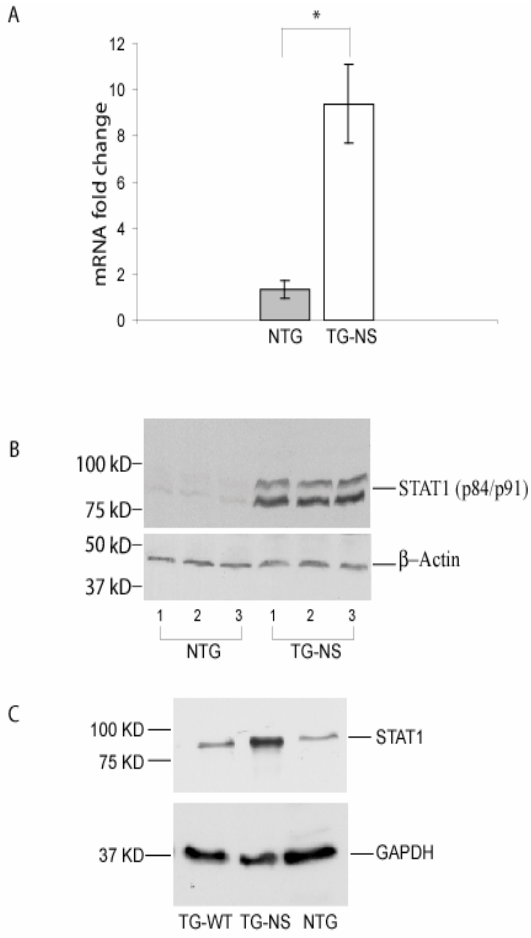

Fig. 3.1. Markedly increased expression of *STAT1* in TG-NS hearts. (A) Quantitative RT-PCR analysis with RNA isolated from 9 TG-NS and 7 NTG (non transgenic control) hearts (age = 6–8 months). Data were normalized to 18S RNA expression in the same samples and reported as fold changes (mean ± SE) from levels in control mice (**P* = 0.0016). (B) Western blot analysis of STAT1 from three NTG and three TG-NS hearts (age = 6–8 months). β-Actin was used as loading control. The experiment was repeated three times and similar results were obtained. (C) Western blot analysis of STAT1 from non-transgenic control (NTG), TG-NS, and TG-WT hearts (age = 6–8 months). The experiment was repeated twice and similar results were obtained. Note that TG-NS and TG-WT have the comparable copy number of the transgene and a similar level of expression of the cardiac sodium channel (see Reference by Zhang T et al. 2007). The only difference between these two types of mice is that TG-NS mice carry the mutant N1325S *SCN5A* and TG-WT mice carry the wild type *SCN5A*.

3.5. DISCUSSION

Microarray analysis is a large scale study that can provide unbiased assessment of expression of thousands of genes in a cell or tissue simultaneously. To date, no microarray analysis has been reported for LQTS either in the humans or mice. We performed a microarray study using a mouse model for LQTS, the TG-NS mice with cardiac expression of the *SCN5A* mutation N1325S associated with LQTS. Microarray analysis revealed 33 genes showing marked differential expression between TG-NS and wild type mice (>5-fold difference, $P \leqslant 0.001$). The results from microarray analysis were almost identical to that from the follow-up RT-PCR analysis using independent samples for all selected genes. Our results suggest the involvement of expression remodeling in the progression of LQTS. Furthermore, the results from this study suggest that in addition to its effects on basic biophysical properties of the cardiac sodium channel, the N1325S mutation has a more profound effect on cardiomyocytes *in vivo*.

The gene that showed the most significant difference between TG-NS and wild type mice is *STAT1*. Follow-up RT-PCR and Western blot analysis confirmed that expression of *STAT1* was markedly increased in TG-NS myocytes compared to non-transgenic control cells. Further analysis showed that STAT1 protein expression was also much higher in TG-NS hearts than in TG-WT hearts with cardiac expression of wild type *SCN5A* (Fig. 3.1C). STAT1 is a key signaling protein that functions as a transducer of cytokine signaling and as a sensor responding to cellular stresses, in particular, IFN response (Stephanou et al. 2003). Thus, it was interesting to note that many genes involved in the IFN response also showed increased expression in TG-NS myocytes, for

example, *Usp18*, *Ifit1*, *Ifit2*, *Ifit3*, Irf7, *Gbp3*, *Dlm-1*, *Oasl 9, Oasl 1G*, and *Isg 12* that all showed many fold increases of expression (Table 3.2). The molecular mechanism for induction of high *STAT1* expression in TG-NS hearts is not clear, however, abnormal handling of intracellular calcium transients detected in TG-NS cardiomyocytes (Yong SL et al. 2007) may be a likely cause.

STAT-1 has been shown to induce apoptosis. Human fibroblast cells deficient in *STAT1* were resistant to TNF-α-induced apoptosis (Kumar et al.1997). Neonatal rat cardiomyocytes subjected to ischemia for 4 h showed increased expression of *STAT1*, and cardiomyocytes transfected with *STAT1* showed increased apoptosis with exposure to ischemia (Stephanou et al. 2000). A trend of increased apoptosis in the absence of exposure to ischemia was also detected in cardiomyocytes transfected with a *STAT1* construct compared to control cells transfected with the vector (Fig. 3A in Stephanou et al. 2000). Because age-dependent apoptosis has been detected in TG-NS mouse hearts (Zhang T et al. 2006), we speculate that increased expression of *STAT1* may be a cause for apoptosis in these mice.

In summary, our microarray analysis of a transgenic mouse model for LQTS, TG-NS, demonstrated that gene expression remodeling existed in these mice. Of a particular interest was the finding of highly increased *STAT1* expression, which may provide insights into the findings of cardiomyocyte apoptosis in TG-NS mice and high risk of heart failure in these mice.

CHAPTER IV

INVESTIGATION OF LOCALIZATION OF $NA_V1.5$ IN NON-CARDIAC TISSUES: EVIDENCE OF Nav1.5 IN THE MOUSE BRAIN[1]

4.1 ABSTRACT

SCN5A encodes a sodium channel α-subunit $Na_v1.5$ that is predominantly expressed in the heart. Mutations in the human $Na_v1.5$ gene cause long QT syndrome and Brugada syndrome that are characterized by cardiac arrhythmias and sudden death during sleep or at rest. SCN5A mRNA was recently shown to be present in the rat and human brain. In this report, we determined the distribution of $Na_v1.5$ protein in the mouse brain. We generated a polyclonal antibody specific to $Na_v1.5$. The anti- $Na_v1.5$ antibody was used for immunohistochemical analysis of the $Na_v1.5$ distribution. We found that $Na_v1.5$ protein was present widely throughout the brain, and was found in the cerebral cortex, limbic system, basal ganglion, thalamus, hypothalamus, cerebellum, and brainstem. The distribution of $Na_v1.5$ immunoreactivity appeared to be more widespread

[1]Most of the data in this chapter have been published as Wu l et al. (2002) *Neuroreport* 13:2547-2551. However this chapter has been rewritten for the purpose of this dissertation.

than previously reported for the mRNA. Notably, $Na_v1.5$ protein was clustered at a high density in neuronal processes and nerve fiber bundles, but not in cell bodies. Further confocal microscopic analysis revealed that $Na_v1.5$ protein was localized on the surface membrane of the neuronal processes in the brain, and surrounded the neurofilaments. The wide distribution of $Na_v1.5$ protein in the brain and its distinct localization to the membrane of neuronal processes suggest that this protein may play a role in the physiology of the central nervous system. Abnormal neuronal activity associated with $Na_v1.5$ mutations might affect the coordination of cardiac rhythm by an indirect mechanism, which may trigger seizures, syncope, life-threatening arrhythmias, or sudden death in arrhythmic and epileptic patients.

4.2. INTRODUCTION

Voltage-dependent sodium channels are transmembrane proteins that are responsible for generating action potentials and for rapid conduction of electrical signals in excitable cells (Catterall et al. 2000). Sodium channels are classified into three types based on their sensitivity to blockade by tetrodotoxin (TTX): TTX-sensitive Na channels (TTXs), TTX-resistant Na channels (TTXr), and TTX-insensitive Na channels (TTXi) (Donahue et al. 2000, Fozzard et al. 1996). In the brain, six TTXs Na channels have been identified, including $Na_v1.1$, $Na_v1.2$, $Na_v1.3$, $Na_v1.6$, $Na_v1.7$. Only one TTXr channel, $Na_v1.9$, has been identified in the brain (Jeong et al. 2000). Recent studies suggested that SCN5A may be another gene that is responsible for generating TTXr Na currents in the brain (Donahue et al. 2000; Hartmann et al. 1999). TTXr Na channels generate currents that are slower, but recover from inactivation much faster than TTXs channels (Elliott et

al. 1993), suggesting a possible role of TTXr sodium channels in sustained firing of neurons or as pace-makers. In this study, we investigated the localization pattern of another TTXr sodium channel, $Na_v1.5$, in the mouse brain using immunohistochemistry.

SCN5A encodes the cardiac sodium channel with 2,016 amino acids and a calculated molecular weight of 227 kDa (Gellens et al. 1992). The putative structure of $Na_v1.5$ consists of four homologous domains (I-IV), each containing six transmembrane segments (S1-S6). $Na_v1.5$ mutations cause syncope, seizures, and sudden death triggered by lethal cardiac arrhythmias associated with long QT syndrome (LQTS), idiopathic ventricular fibrillation including Brugada syndrome and cardiac conduction disease (Wang et al. 1995a; Chen et al. 1998). $Na_v1.5$ was originally identified as a cardiac sodium channel. Subsequently, it was shown to be expressed in the brain at the mRNA level (Donahue et al. 2000; Hartmann et al. 1999). *In situ* hybridization, reverse transcription polymerase chain reaction (RT-PCR), and RNase protection assays detected the presence of transcripts of SCN5A in the human and rat brain tissues. Restricted regional expression of SCN5A mRNA involved piriform cortex and subcortical limbic nuclei (Donahue et al. 2000; Hartmann et al. 1999), and these two regions are related to epilepsy. These findings may explain why $Na_v1.5$ mutations are associated with seizures. However, the distribution of $Na_v1.5$ in the brain at the protein level has not been investigated previously. Here, we demonstrate selective expression of $Na_v1.5$ at the protein level in regions of the mouse central nervous system.

In this study, we investigated the localization pattern of $Na_v1.5$ protein in the mouse brain tissues using immunohistochemistry. We generated an antibody directed against a unique peptide region at the N-terminus of $Na_v1.5$. The antibody was used to

define the distribution of $Na_v1.5$ in mouse brain. We demonstrated that $Na_v1.5$ protein was widely localized in the cerebral cortex, thalamus, hypothalamus, basal ganglia, cerebellum and brainstem. Our studies confirmed the distribution of $Na_v1.5$ protein in some regions that were previously shown to contain the corresponding mRNA, but also revealed the presence of $Na_v1.5$ protein in new brain regions where $Na_v1.5$ gene expression has not been previously reported. Our data also indicate that $Na_v1.5$ protein is expressed and localized on the plasma membrane of the neuronal processes, but not in the cell bodies. The regional distribution of $Na_v1.5$ in the brain suggests that $Na_v1.5$ might regulate neuron excitability.

4.3 MATERIALS AND METHODS

Materials

An $Na_v1.5$-specific polyclonal antibody was developed against a synthetic polypeptide (AC-RPQLDLQASKKLPDLYC-Amide) corresponding to a unique portion of the N-terminus of the cardiac sodium channel $Na_v1.5$. The antibody was generated and purified as described (Harlow et al. 1988).

The mouse anti-neurofilament 200 antibody (clone NE14) was purchased from Sigma (St Louis, MO) and used at 1:40 dilution for immunohistochemistry. Fluorescein-conjugated secondary antibodies were from Jackson Immuno Research Laboratories (West Grove, PA), and used at 1:200 dilution. The Vectastain elite ABC kit, DAB substrate kit, and Vectashield anti-fading mounting media were from Vector Laboratories

(Burlingame, CA). The brain tissues for Western blotting and immunohistochemical analyses were from the mouse strain c57BL.

Western blot analysis

Mouse tissues from the heart, brain, kidney, liver, and skeletal muscle were homogenized with a glass tissue grinder (Wheaton, Millville, NJ) in 1X PBS buffer containing 0.1% NP-40, 0.05% sodium deoxycholate, and a protease inhibitor cocktail mix (Roche Biochemicals, Germany). The sample was centrifuged at 3,000 rpm for 10 minutes, and the supernatant was transferred to a microcentrifuge tube. The supernatant was then undergone ultracentrifugation at 40,000 rpm for 30 minutes. The pellet containing the membrane fraction of proteins was resuspended in the loading buffer containing 2% SDS, and denatured at room temperature for 30 minutes before loading onto SDS-PAGE. Western blot analysis was performed as described (Harlow et. al. 1988) with the anti- $Na_v1.5$ antiserum as the primary antibody. The secondary antibody was horseradish peroxidase-conjugated donkey anti-rabbit IgG (NA 934, Amersham Pharmacia Biotech, Inc., Piscataway, NJ). ECL Western blotting detection reagents (Amersham Pharmacia Biotech, Inc., Piscataway, NJ) were used to visualize the protein signals.

For HEK293 cells with or without expression of $Na_v1.5$, cells were lysed in the lysis buffer (1% Triton-100, 150 mM NaCl, 50 mM Tris-HCl, pH7.5, 1 mM EDTA) with a protease inhibitor cocktail mix on ice for 30 min. The sample was then centrifuged at 14,000 rpm for 25 min at 4^0C. The supernatant was used for Western blot analysis as described above.

Immunohistochemistry

Immunostaining was carried out as previously described (Nishiyama, et al. 1997) with minor modifications. Briefly, mouse brain sections fixed with 4% paraformaldehyde and embedded with paraffin or frozen sections were pretreated with hydrogen peroxide, blocked in blocking buffer (5% bovine serum albumin and 0.3% Triton X-100 in 1x PBS) for 2 hr, and then incubated with the primary antibody (1:250 dilution) at 4°C for 24 hours. The sections were then incubated with the biotin-conjugated secondary antibody and the avidin-biotin complex solution (Vectastain Elite ABC Kit). Immunoreactive signal was developed using the DAB substrate kit (Vector Laboratories, Burlingame, CA).

In control experiments, serial brain sections were stained with the primary anti-$Na_v1.5$ antibody preincubated with an excessive amount of the immunizing peptide antigen (100 μg of peptide vs. 13.7 μg of the anti- $Na_v1.5$ antibody).

Double immunofluorescence staining was carried out using the protocol similar to those reported previously (Nishiyama et al. 1999). In brief, mouse brain sections of 12 μm thickness were prepared from paraffin-embedded or frozen tissues, blocked, and incubated with the mixture of primary antibodies (the anti-$Na_v1.5$ antibody and the monoclonal anti-neurofilament 200 antibody) at 4°C for 24 hours. The sections were then incubated with a secondary antibody mixture containing the FITC-conjugated and Texas Red-conjugated secondary antibodies at room temperature for 2 hours. The immunostained slides were mounted with anti-fading media, and visualized under a confocal microscope.

Confocal microscope and image processing

Tissue sections immunostained with DAB were analyzed with transmitted light or Nomarski optics using a Zeiss Axiophot photomicroscope. Images observed were digitized using a Hamamatsu CCD camera, and transferred to a Power Macintosh G4 computer for digital image processing. Digital images were processed using software Adobe PhotoShop 5.5.

For immunocytochemical analysis, a confocal laser-scanning microscope (SP2; Leica, Heidelberg, Germany) equipped with 40x, 63x and 100x infinity-adjusted oil immersion objectives and double-channel photodetectors was used. By precisely stepping the microscope stage in the vertical z-axis, a series of optically thin, perfectly focused images were collected at identical x-y planes through the specimen. In general, each data set collected on the confocal microscope was processed with the 3D software of the Leica Scan Ware operating system, and used to construct an extended focus image, i.e., a computer-averaged assembly of some or all optical sections in the data set. These procedures resulted in a perfectly focused image through the depth of the specimen which was then saved in a TIFF file format and transferred to a Power Macintosh G4 for image processing. Digital images were colorized, and then combined and manipulated using Adobe PhotoShop 5.5.

Over-expression of $Na_V1.5$ in HEK293 and P19CL6 cells

Wild type $Na_v1.5$ cDNA was cloned into the pcDNA3 vector (Invitrogen, Carlsbad, CA) for expression in HEK293 and P19C16 cells (Wan et al. 2000; Wan et al. 2001). Approximately 1 x 10^5 P19CL6 cells were seeded on chamber coverglass (Nalge

Nunc International, Naperville, IL) a day prior to transfection. Two microliters of Lipofectamine (Invitrogene, Carlsbad, CA) was diluted in 50 μl of the serum free medium, and mixed with one microgram of $Na_v1.5$ expression plasmid DNA in 50 μl of the serum free medium. After incubation at room temperature for 20 minutes, the DNA-Lipofectamine complexes formed and were added into chamber slide wells. The serum free medium was replaced with the growth medium after 4-6 hours. After 48 hours of incubation, the cells were ready for immunostaining. The cells were fixed with 4% paraformaldehyde, blocked in the blocking buffer (5% bovine serum albumin and 0.3% Triton X-100 in 1x PBS), and incubated with the primary anti-$Na_v1.5$ antibody. The secondary antibody used was FITC-conjugated anti-rabbit IgG. The images were visualized with a confocal microscope as described above.

4.4. RESULTS

Characterization of the anti- $Na_v1.5$ polyclonal antibody

A polyclonal antibody specific to the $Na_v1.5$ channel was generated using a peptide immunogen located at the cytoplasmic N-terminus of $Na_v1.5$ protein (amino acids 53 to 68: RPQLDLQASKKLPDLY). To confirm the specificity of the anti- $Na_v1.5$ antibody, we performed Western blot analysis on the membrane fractions of protein extracts from a number of mouse organs, including heart, kidney, liver, brain, skeletal muscle, and human embryonic kidney cells (HEK293) expressing human $Na_v1.5$. The antibody detected a band approximately the expected size of 227 kDa (Wang et al. 1996) strongly in the heart, and very weakly in the brain, but not in the kidney, liver, and

skeletal muscle (Fig. 4.1A). These data are consistent with the results from Northern blot analysis (Gellens et al. 1992). The antibody also yielded the expected 227 kDa band in the lane loaded with protein extract from the transfected cells containing $Na_v1.5$ (Fig. 4.1B). No equivalent band was detected in the control non-transfected cells (Fig. 4.1B). These data suggest that our antibody is specific for $Na_v1.5$.

To further establish the specificity of this antibody, we determined whether the antibody binds to the cell membrane where $Na_v1.5$ is known to be localized. Immunofluorescence staining with HEK293 and P19C16 cells transfected with the $Na_v1.5$ expression construct DNA detected $Na_v1.5$-imunoreactivity only on the plasma membrane (Fig. 4.1C). No localization was evident when the antibody was pre-absorbed with an excessive amount of the peptide to which the antibody was prepared (Fig. 4.1C).

Together, these data suggest that our anti- $Na_v1.5$ antibody specifically recognizes $Na_v1.5$ protein and that the wild type $Na_v1.5$ protein is localized to the plasma membrane when expressed in non-neuronal cultured cells.

Regional distribution of $Na_v1.5$ protein in the brain

Immunohistochemistry using this anti-$Na_v1.5$ antibody was performed to determine the distribution of $Na_v1.5$ immunoreactivity in the normal mouse brain. Unlike the $Na_v1.5$ mRNA, which was reported to be expressed primarily in the limbic system (Donahue et al. 2000; Hartmann et al. 1999), the $Na_v1.5$ protein seemed to be more broadly expressed in various brain regions with some unique features (Fig. 4.2). In the immunohistochemistry experiments, a negative control was carried out on the adjacent brain sections with the anti-$Na_v1.5$ antibody pre-absorbed with the antigen peptide.

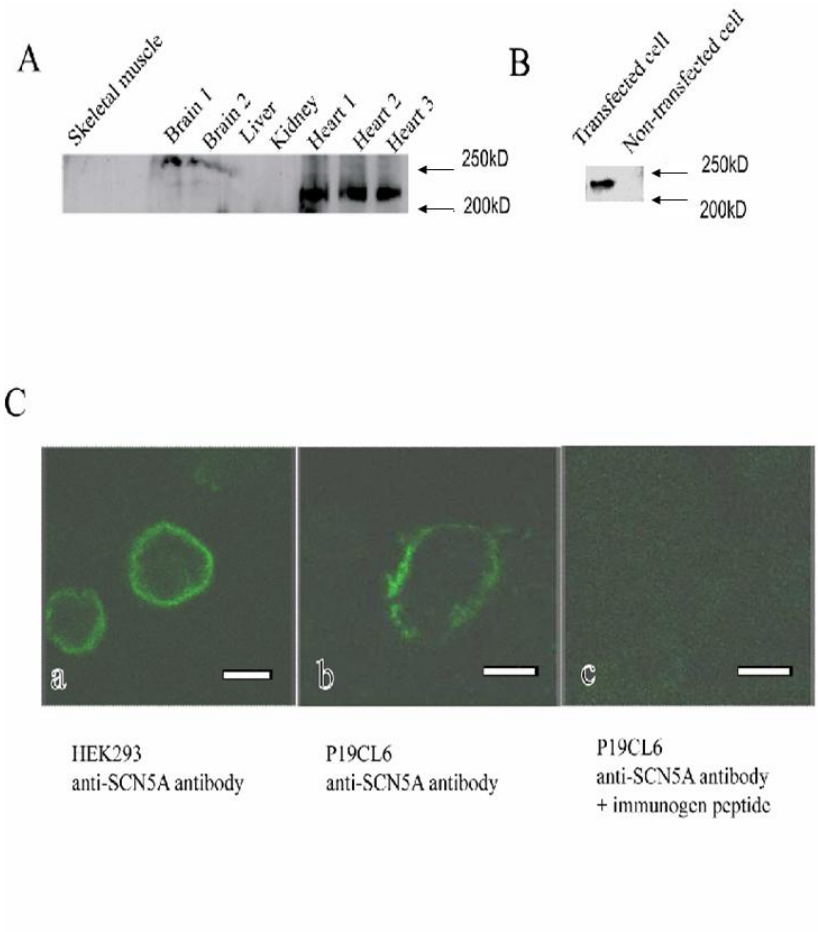

Fig. 4.1. Characterization of the anti-$Na_v1.5$ antibody. (a) Western blot analysis of mouse membrane proteins from the heart, kidney, liver, brain, and skeletal muscle tissues with the anti-$Na_v1.5$ antibody. The positions of molecular weight markers are indicated. (b) Western blot analysis with protein extracts from HEK293 cells expressing $Na_v1.5$ (transfected cell), and control cells that were not transfected with the $Na_v1.5$ expression construct (non-transfected cell). (c) Cellular localization of wild type human SCN5A protein on plasma membrane (green signal). HEK293 cells (left) and P19CL6 cells (middle) transfected with the human SCN5A expression construct were immunostained with the anti-SCN5A antibody. No detectable immunofluorescence staining was observed with the anti-SCN5A antibody pre-absorbed with the peptide antigen (right). Bar = 5 μm.

Elimination of $Na_v1.5$ immunoreactivity in the negative control experiments (compare Figs. 4.2A and 4.2B), as expected, demonstrated that positive $Na_v1.5$ staining or the $Na_v1.5$ -immunoreactivity represented the specific binding of our antibody to the immunogenic peptide sequence of $Na_v1.5$.

In the forebrain of the adult mouse, a weak, but significant, $Na_v1.5$ immunoreactivity was observed in the cerebral cortex (Fig. 4.2C). Within this region, the neuronal processes originating from cerebral cortical neurons were positively stained for $Na_v1.5$, whereas little or no immunoreactivity was detected in the neuronal cell bodies or glial components in this region (Fig. 4.2C). In contrast, none of the neurons in the dentate gyrus and hippocampus were positively stained for $Na_v1.5$, and even the neuronal processes showed little $Na_v1.5$ immunoreactivity in this area (data not shown). Interestingly, in the forebrain slides we observed intense $Na_v1.5$ signals in the olfactory tract (Fig. 4.2D), and weak staining in the olfactory tubercule (data not shown).

In the limbic system, little or no immunoreactivity for $Na_v1.5$ was detected in the cell bodies in the septal nuclei, the diagonal band of Broca, the piriform cortex, and the amygdala, where $Na_v1.5$ mRNA was reported to be expressed strongly (Donahue et al. 2000; Hartmann et al. 1999). However, moderate $Na_v1.5$ signals were detected in the nerve fibers within this region (Fig. 4.2A). The discrepancy between $Na_v1.5$ mRNA localization and $Na_v1.5$ protein distribution may be explained by our hypothesis that $Na_v1.5$ protein is transported to the nerve fibers after synthesis in the cell bodies of neurons in the limbic system.

In the basal ganglion, the anti- $Na_v1.5$ antibody showed strong positive staining in the nerve bundles, also known as the pencil fibers, whereas the cell bodies in the striatal

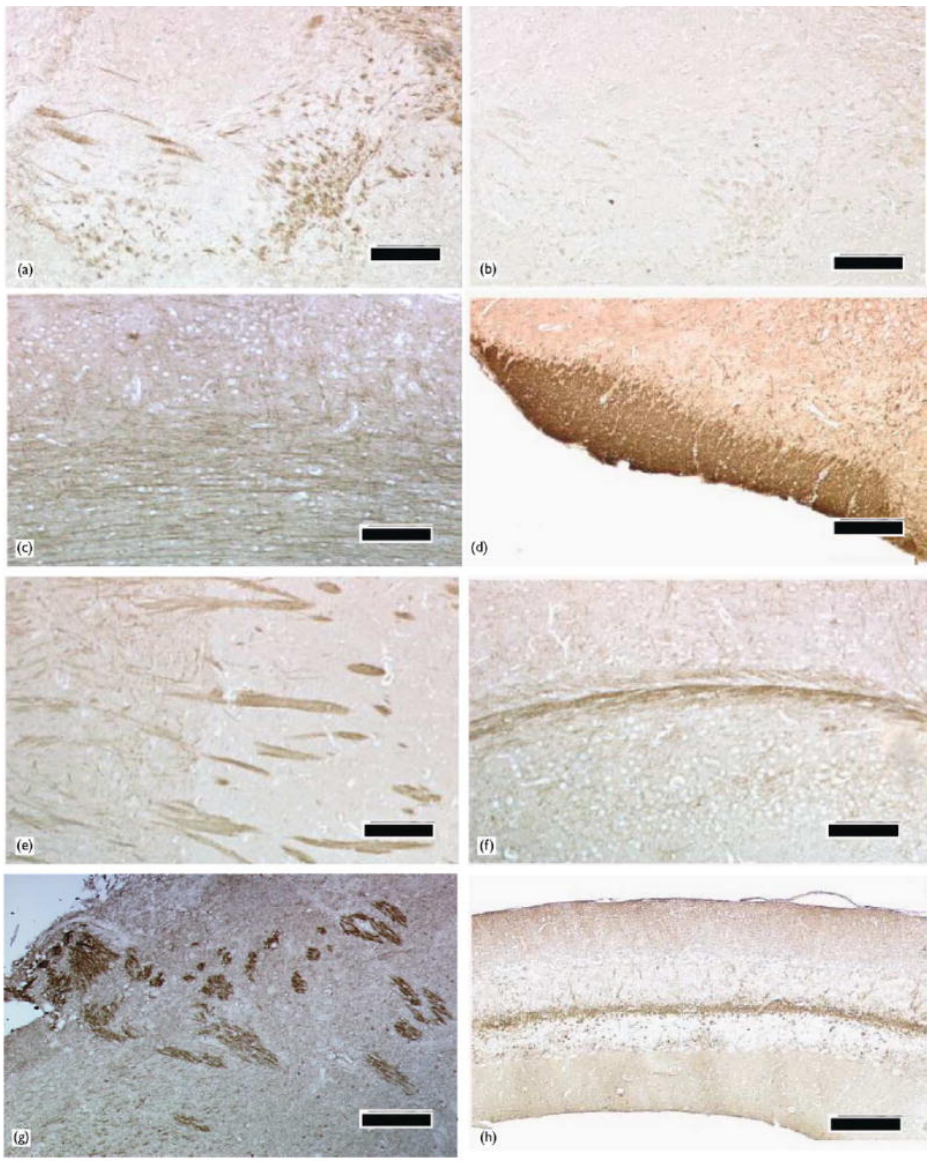

Fig. 4.2. Regional distribution of $Na_v1.5$ protein in the mouse brain. (a) Some nerve fibers in the limbic system express $Na_v1.5$ protein, whereas neuronal and glial cell bodies were not stained by the anti-$Na_v1.5$ antibody. (b) An adjacent section to the section used in (a) was stained with the anti-$Na_v1.5$ antibody pre-absorbed with the immunogenic peptide. (c) In the cerebral cortex, the neuronal processes, mainly axons, were positive for $Na_v1.5$ protein, but little or no signal was observed in the cell bodies. (d) The olfactory tract had strong $Na_v1.5$ signal. (e) In the striatum, $Na_v1.5$ protein was mainly localized to the nerve fibers (the pencil fibers). (f) The cerebral peduncle was stained by the anti- $Na_v1.5$ antibody. (g) In the brain stem, some nerve fibers in the lateral medulla were moderately positive for $Na_v1.5$. (h) In the cerebellum, the white matter consisting of nerve fibers was strongly stained for $Na_v1.5$, but there was no signal in the granular layer and the Purkinje cell layer. Bars = 100 μm.

nuclei showed little or no signal (Figs. 4.2E, 4.3A-4.3C). Interestingly, $Na_v1.5$-immunoreactivity in the pencil fibers was significantly stronger within the caudate putamen (Fig. 4.2E, right half) than within the globus pallidus (Fig. 4.2E, left half). It is important to note that not all the nerve tracts or nerve bundles through the mouse brain were positively stained for $Na_v1.5$ immunoreactivity, for example, a huge nerve tract connecting both hemispheres in the corpus callosum was not positively stained for $Na_v1.5$ (data not shown). These data suggest that the distribution of $Na_v1.5$ protein is restricted to specific nerve tracts.

In the diencephalon of the adult mouse brain, $Na_v1.5$ immunoreactivity was also localized to the nerve fiber tracts, and little or no $Na_v1.5$ signal was present in the cell bodies in the cerebral cortex. The cerebral peduncle was intensively stained for $Na_v1.5$ (Fig. 4.2F). A low level of $Na_v1.5$ immunoreactivity was localized to the hypothalamic and thalamic nuclei, but the nerve fibers in the hypothalamic and thalamic regions showed more intense $Na_v1.5$ signal than the cell bodies (data not shown).

In the brainstem, intense $Na_v1.5$ immunoreacitivy was localized to some spotty regions in the lateral medulla (Fig. 4.2G). These signals seemed to correspond to discrete nerve tracts in the medulla. Based on a report showing that $Na_v1.5$ mRNA expression is located in the lateral paragigantocellular nuclei (LPGi) (Donahue et al. 2000), some of the nerve tracts with $Na_v1.5$ immunoreactivity shown in this study may originate from LPGi.

In the cerebellum, no negligible signal was detected in the granular layer and the Purkinje cell layer. However, weak $Na_v1.5$ immunoreactivity on some fibrous structures was observed in the cerebellar molecular layer, and intense $Na_v1.5$ signals were

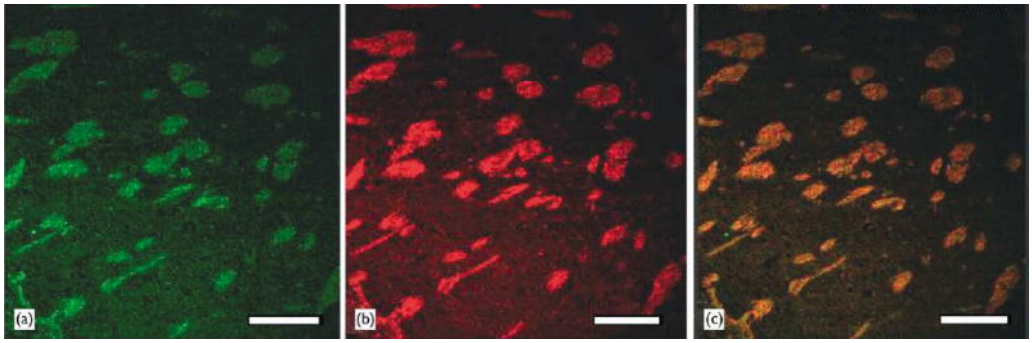

Fig. 4.3. Co-localization of $Na_v1.5$ and neurofilaments. Confocal microscopic images of caudate putamen immunostained with both the anti-$Na_v1.5$ antibody and the monoclonal anti-neurofilament 200 antibody. (a) immuno£uorescent image for $Na_v1.5$ protein, green; (b) immunofluorescent image for neurofilaments, red; (c) overlay of image A and image B. Bar = 200 μ m.

in the white matter of the cerebellum (Fig. 4.2H). $Na_v1.5$ immunoreactivity was found mostly in process-like structures, presumably neuronal processes. Neuronal cell bodies and glial cells did not label with the $Na_v1.5$ antibody.

In conclusion, $Na_v1.5$ protein is widely distributed throughout the central nervous system, and it is clustered much more densely in the neuronal processes than in the neuronal cell bodies.

Confocal microscopic analysis to define the subcellular localization of $Na_v1.5$ protein

In the central nervous system, the neuronal processes showed strong $Na_v1.5$-immunoreactivity, whereas the cell bodies showed no or very weak signal (Fig.4.2C). To further characterize the localization of $Na_v1.5$ at the subcellular level, we performed double-immunostaining with mouse brain sections using both the rabbit anti-$Na_v1.5$ antibody described above and the anti-neurofilament antibody. Fig. 3 shows confocal microscopic images of the caudate putamen of the basal ganglion. $Na_v1.5$ is clearly expressed in the nerve tracts identified by the anti-neurofilament antibody (Fig. 4.3A-C). A highly magnified image of the nerve fibers in this area showed that $Na_v1.5$ immunoreactivity (green) did not overlap with the neurofilament signals (red) (Fig. 4.3D-F). The $Na_v1.5$ signals appeared outside the neurofilament compartment, consistent with the localization of $Na_v1.5$ protein on the neuronal plasma membrane (Fig. 4.3F). These data suggest that $Na_v1.5$ protein is localized to the plasma membrane of the nerve processes and is not present in the interior.

4.5. DISCUSSION

In this report, we describe the immunohistochemical characterization of the regional and cellular distribution of the cardiac voltage-dependent sodium channel α-subunit ($Na_v1.5$) protein in the mouse brain. We found that the cell bodies of neurons did not contain $Na_v1.5$. Instead, we observed the striking and distinct subcellular localization of the $Na_v1.5$ channels on the plasma membrane of neuronal processes (Fig. 4.3) that are specialized for conducting electrical signals. This distribution is consistent with the functional role of sodium channels which are responsible for generation and propagation of the action potentials in the neurons and for conducting electrical signals throughout the nervous system.

The distribution of the cardiac sodium channel $Na_v1.5$ in the brain has not been previously characterized at the protein level. Our study represents the first detailed characterization of $Na_v1.5$ protein distribution in the mouse brain. Consistent with the distribution of $Na_v1.5$ transcripts in rat and human brain (Donahue et al. 2000; Hartmann et al. 1999), the mouse $Na_v1.5$ protein was present in the olfactory system, thalamus, and hypothalamus. However, our study revealed localization of $Na_v1.5$ protein in several brain regions that were not described or analyzed in previous studies. These regions include the cerebral cortex, basal ganglia, and the white matter of the cerebellum. Another difference between our study and the previous reports is related to the limbic system. Hartmann et al. and Donahue et al. showed strong expression of $Na_v1.5$ mRNA in the piriform cortex, septal nuclei, the diagonal band of Broca, amygdala, and habenular nuclei, whereas our study did not detect $Na_v1.5$ protein in these structures. Instead, we found weak or moderate presence of $Na_v1.5$ protein in the nerve fibrous structures in

these regions. A possible explanation for the difference between our study and the previous studies may be that $Na_v1.5$ mRNA is localized to the neuronal cell bodies, whereas the $Na_v1.5$ protein molecules are synthesized in these locations, and are transported to and accumulate in the neuronal processes.

The implications of our study are two-fold: (1) Increasing evidence suggests that the distinctive roles played by different brain Na channels are often dictated by their unique localization in excitable tissues. Our finding that $Na_v1.5$ protein is localized in the neuronal processes in certain distinct regions of the brain, as well as the fact that activation and inactivation of the $Na_v1.5$ channels are voltage-dependent, may suggest that $Na_v1.5$ could aid in efficient nerve impulse generation and propagation in these specific brain regions. Together with SCN12A, $Na_v1.5$ channels generate the TTX-resistant sodium currents in the brain, which may play a role in sustained firing of neurons or as pace-makers; (2) We and others have established that mutations in $Na_v1.5$ cause cardiac arrhythmias and sudden cardiac death associated with long QT syndrome (LQTS), idiopathic ventricular fibrillation/Brugada syndrome, and cardiac conduction disease (Chen et al. 1998; Wan et al. 2001; Wang et al. 1995b).

It has been recognized that the nervous system also plays a role in the genesis of cardiac arrhythmias. Fright, anger, depression, intense emotion, rigorous exercises, swimming, alarm clocks, ringing telephones, and other activities related to the nervous system can all trigger life-threatening arrhythmias. For LQTS, major genes have been cloned or identified as the cardiac sodium channel gene $Na_v1.5$ (LQT3) and potassium channel subunit genes *KCNQ1* (LQT1), and *KCNH2* (LQT2) (reviewed in (Wang et al. 2001). Genotype-phenotype correlation studies (Schwartz et al. 2001) found that LQT2

and LQT3 patients with mutations in $Na_v1.5$ and KCNH2 (both of them are expressed in the brain (Curran et al. 1995; Donahue et al. 2000; Emmi et al. 2000; Hartmann et al. 1999) frequently develop cardiac arrhythmias during sleep or at rest, whereas LQT1 patients with mutations in KCNQ1 (not expressed in the brain) (Wang et al. 1996) experienced cardiac events during exercise. For idiopathic ventricular fibrillation with ECG characteristics of right bundle branch block and ST segment elevation (also known as Brugada syndrome), we established that $Na_v1.5$ mutations that are functionally different from LQT mutations are the underlying causes of this disease (Chen et al. 1998). Interestingly, Brugada patients also develop life-threatening arrhythmias predominantly during sleep (Matsuo et al. 1999). Although it is speculative and remains to be investigated, it is possible that mutant $Na_v1.5$ proteins expressed in certain brain regions of LQT3 patients may play a role in generating the trigger to provoke arrhythmias during sleep or at rest. Of particular interest is the expression of $Na_v1.5$ in the brainstem which is known to be involved in regulating cardiac activities through autonomic motor neurons.

In conclusion, our results indicate that $Na_v1.5$ protein is localized to the plasma membrane of the neuronal processes within distinct regions of the brain. This study provides new insight into a possible physiological role of $Na_v1.5$ in brain function.

CHAPTER V

GENERAL DISCUSSION AND FUTURE DIRECTIONS

My thesis focuses on functional regulation of the cardiac sodium channel $Na_v1.5$. First, I identified a novel regulatory protein, MOG1, as a key component of the cardiac sodium channel $Na_v1.5$ protein complex. I demonstrated that MOG1 exerted significant effects on the function of the cardiac sodium channel (see Chapter II). The results provide insights into the structure and function of the $Na_v1.5$ protein complex in the physiology of the cardiovascular system and reveal a novel functional role for MOG1. Regulation of $Na_v1.5$ in the pathological state was studied in a mouse model for long QT syndrome, a lethal arrhythmia that causes sudden death, using genomic approaches. I found that the LQT3 mutation N1325S in $Na_v1.5$ was able to re-program the expression of many genes. Of particular interest was the highly elevated expression of STAT1, which may be related to cardiomyocyte apoptosis in transgenic N1325S hearts (see Chapter III). To explore possible novel functional roles in the brain, the expression profile of $Na_v1.5$ protein was analyzed in the mouse brain. I showed that the $Na_v1.5$ protein was localized to the plasma membrane of the neuronal processes within distinct

regions of the brain (see Chapter IV). The results provide new insights into a possible physiological role of $Na_v1.5$ in the brain. Overall, my studies contribute to the field of the functional characterization of $Na_v1.5$, and my results have also expanded current research of $Na_v1.5$ to new directions that warrant future attention as described below.

5.1. MOG1 acts as an important regulator for the function of $Na_v1.5$

MOG1 interacts with cardiac sodium channel $Na_v1.5$, and the presence/absence of MOG1 affects the sodium currents in both a heterologous transfection HEK293/$Na_v1.5$ cell line and native neonatal cadiomyocytes. MOG1 was also shown to colocalize with $Na_v1.5$ at the intercalated discs of cardiomycytes. The results suggest that MOG1 may be critical for modulating the function of cardiac sodium channel. There are several other proteins that have been identified and reported in the $Na_v1.5$ interacting protein complex (Abriel et al. 2005, Allouis et al. 2006). These proteins include structural proteins (ankyrin G, syntrophin/dystrophin), signaling proteins (FHF1B, calmodulin) and enzymes (Nedd4, Fyn, PKA, PKC, SGKs, PTPH1). However, none of these proteins have been shown to play a role in $Na_v1.5$ function in a physiological context. The functional study for these proteins were all performed in heterologous cell expression systems, but not in native cardiac cells, and the effects on $Na_v1.5$ were only evaluated by overexpressing the potential interacting protein(s). We have analyzed the effects of MOG1 on $Na_v1.5$ in cardiomyocytes and examined the sodium current by knocking down MOG1 expression in the mouse. It will be interesting to use siRNA technology to knock down expression of the other $Na_v1.5$-interacting proteins and compare their effects on sodium currents to the effects we observed for MOG1.

5.1.1. MOG1 may be involved in cell-cell communication

This thesis revealed the physiological function(s) of MOG1 in mammalian cells. A previous study with Northern blot analysis demonstrated that the heart was the tissue with the highest expression level of MOG1, suggesting that MOG1 plays an important role in cardiac function (Marfitia et al.2001). The results from the present study further define the role of MOG1 in the heart. We provide evidence that MOG1 the expression of MOG1 was highly expressed in the intercalated discs of both atrial and ventricular cells (Fig 2.8C), and colocalized with $Na_v1.5$ at the intercalated discs of cardiomyocytes (Fig 2.8E). Moreover, the expression pattern of MOG1 was similar to the pattern shown by connexin 43 (Fig 2.8C-D), the principal connexin of the working myocardium that constructs the gap junction at intercalated discs of cardiac tissue. In addition, our results are consistent with those of Malhotra research group whose work demonstrated that $Na_v1.5$ colocalizes with connexin-43 (Malhotra et al. 2004). Taken together, MOG1 and $Na_v1.5$ colocalize with connexin 43 at the intercalated disc of cardiomyocyte. The expression of $Na_v1.5$ at the intercalated disc implies that the action potential may jump in saltatory fashion from one end of the cell to the other end via $Na_v1.5$ channels (Sebastian et al. 2001). It is speculated that co-localization of MOG1 and $Na_v1.5$ at the intercalated disc may play an important role in establishing and regulating electrical connections between cardiomyocytes. Further analysis will be necessary to test this hypothesis. On the other hand, our results shown MOG1 facilitates $Na_v1.5$ expression on cell surface, which suggests that MOG1 increases the conduction velocity of electrical impulse in cardiac tissue.

5.1.2. The possible molecular mechanisms for regulating the function of $Na_v1.5$ by MOG1

As demonstrated in Chapter IV, our results revealed an increase in $Na_v1.5$ expression level in the plasma membrane and an increase in sodium currents when over-expressed with MOG1 (Fig 2.9). The detailed molecular mechanism by which MOG1 regulates the functional expression of $Na_v1.5$ on plasma membrane remains to be further defined. I showed that increased cell surface expression of $Na_v1.5$ by MOG1 may be a mechanism for increased sodium current densities by MOG1 and may potentially be achieved through increased transport of $Na_v1.5$ to cell surface and/or reduced internalization/degradation of $Na_v1.5$.

The trafficking of membrane proteins like $Na_v1.5$ is a highly regulated process. After being synthesized on ribosomes, the protein is incorporated into the endoplasmic reticulum (ER), then transported from ER to the Golgi apparatus, and subsequently trafficked to the cytoplasmic membrane. A critical step in this process is the transition from the ER to Golgi compartment, which is reported to be related to the ER retention motifs and ER export signals (Zhou et al. 2002). Little is known about regulation of sodium channel transport from *cis* face to *trans* face of the Golgi complex, and from the Golgi to the plasma membrane. There is a potential ER export signal (DXE) in the C-terminus of $Na_v1.5$ that may regulate the exit of fully folded and assembled $Na_v1.5$ out of the ER (Herfst et al. 2004). Recently, ER retention signal (RXR), which retains newly formed proteins in the ER, has been shown to play an important role in the trafficking of many membrane proteins to the cell surface including calcium channel alpha1 subunit, ATP-sensitive K^+ channel, $GABA_B$ receptor and NMDA receptor (Bichet et al. 2000,

Zerangue et al. 1999, Margeta-Mitrovic M, Scott et al. 2001). Lily Jan and colleagues first demonstrated the function of ER retention motif RXR in ATP-sensitive K^+ channel trafficking to plasma membrane, and later Bichet et al. found that this retention motif also mediated trafficking of Ca^{2+} channel α1 subunit to cell surface and proposed that binding of β subunit is a mechanism for facilitating movement of channels to plasma membrane by masking the ER retention signal in the α1 subunit (Bichet et al. 2000, Zerangue et al. 1999).

Inspection of the sequence of $Na_v1.5$ revealed a total of six ER retention motifs (RXR). Three ER retention signals are located in loop I between DI and DII which are involved in mediating the trafficking of sodium channels by PKA (Zhou et al. 2002), one at the C-terminus (at 2010-2012) next to the PDZ domain which is the interacting site for syntrophin and PTPH1, and two at the cytoplasmic loop II between DII and DIII (at 986-988 and 1193-1195) with unknown functions. Whether the two ER retention motifs in $Na_v1.5$ loop II play a similar role as those in K_{ATP} and calcium channels is an interesting question. A working model is illustrated in Fig. 5.1. It should be interesting to test whether these two ER retention motifs (RHR for 986-988 and RLR for 1193-1195) play any role in the regulation of $Na_v1.5$ trafficking to cell surface by MOG1. The two ER retention motifs can be mutated and their effects on trafficking of $Na_v1.5$ to cell membrane can be analyzed by expressing wild type and mutant channels in mammalian cell lines and comparing their differences on the expression levels on cell membrane. The effects of MOG1 on ER retention can be tested by introducing a chimeric protein CD8-loop II-Myc, in which the entire cytoplasmic sequence of CD8 is replaced by the loop II-Myc sequence. This chimeric protein is then expressed in mammalian cell lines

Sequence for $Na_v1.5$ loop II:

SSFSADNLTAPDEDREMNNLQLALARIQRGLRF
VKRTTWDFCCGLLRHRPQKPAALAAQGQLPSC
IATPYSPPPPETEKVPPTRKETQFEEGEQPGQGTP
GDPEPVCVPIAVAESDTDDQEEDEENSLGTEEES
SKQQESQPVSGWPRGPPDSRTWSQVSATASSEA
EASASQADWRQQWKAEPQAPGCGETPEDSCSE
GSTADMTNTAELLEQIPDLGQDVKDPEDCFTEG
CVRRCPCCAVDTTQAPGKVWWRLRKTCYH

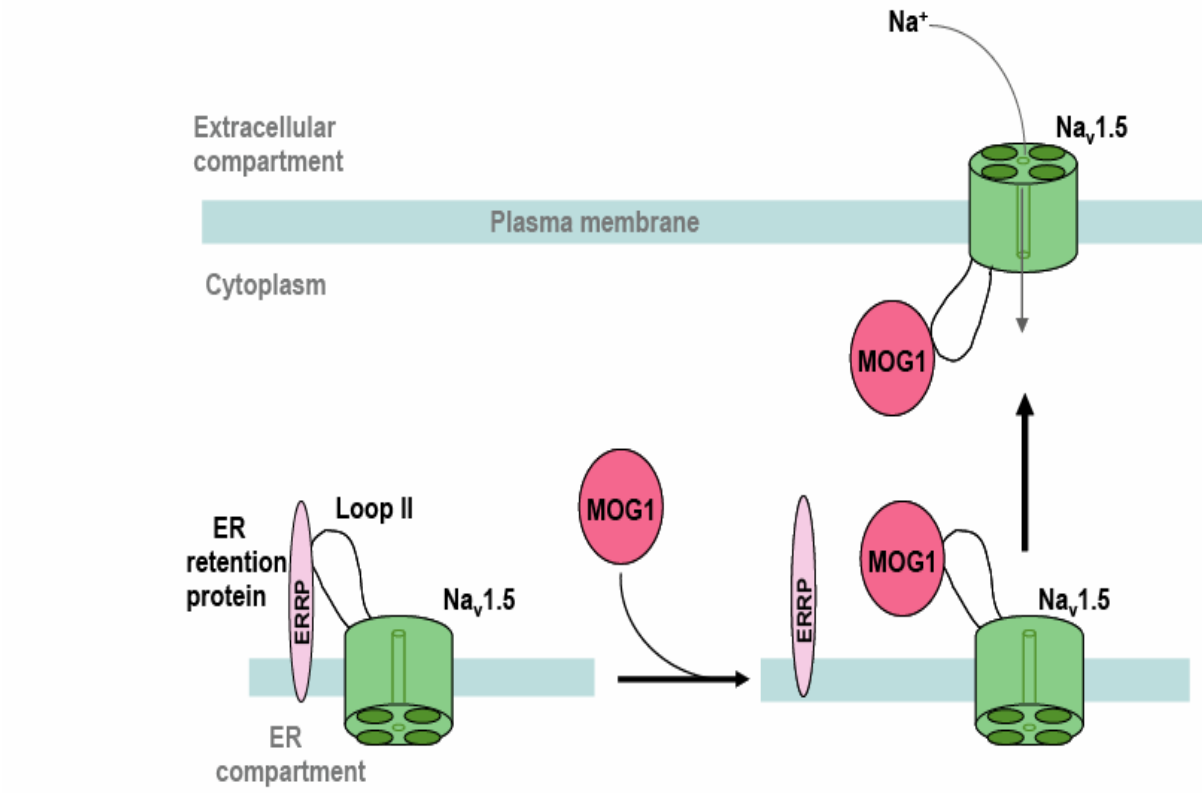

Fig. 5.1. A model for the MOG1-mediated increase in cell surface expression of sodium channel $Na_v1.5$. We have demonstrated that MOG1 is involved in the trafficking of $Na_v1.5$ to cell membrane. In the absence of MOG1, $Na_v1.5$ is trapped within the ER by binding onto an ER retention protein (ERRP) through the ER retention motif(s) in the loop II. In the presence of MOG1, binding of MOG1 to $Na_v1.5$ loop II releases the retention brake and facilitates the transport of $Na_v1.5$ to the plasma membrane. The amino acids sequence of $Na_v1.5$ loop II is shown upper left corner with the two ER retention motifs highlighted. This model was adapted from Bichet D et al. 2000. *Neuron* 25:177–190.

in the presence or absence of MOG1. The intracellular distribution of CD8-loop II-Myc can be visualized by immunostaining. In the presence of MOG1, CD8-loop II-Myc is expected to be mainly localized on cell membrane. These results will indicate that MOG1 is required for ER exit of $Na_v1.5$. To determine whether the increased cell surface expression of $Na_v1.5$ was the result of overexpression of MOG1 (by the mechanism of enhanced ER exit of $Na_v1.5$), we can compare the intracellular localization of $Na_v1.5$ in the presence or absence of MOG1. ER marker calnexin and Golgi marker GM130 can be used to visualize the position for ER and cis-Golgi separately, as described previously (Liu et al. 2007). $Na_v1.5$ signals are expected to be increased in Golgi and reduced in ER in the presence of MOG1 if MOG1 promotes trafficking of $Na_v1.5$ from the ER to Golgi complex.

5.1.3. Future Directions

Determination of the binding domains for the $Na_v1.5$-MOG interaction Eight mutations associated with Brugada syndrome, long-QT syndrome and sudden infant death have been identified in the cytoplasmic loop II of $Na_v1.5$ (Appendix A). The mutation E1053K in $Na_v1.5$ causing Brugada syndrome was shown to interrupt the localization of $Na_v1.5$ to cell surface mediated by ankyrin G (Mohler et al. 2004). In this study we showed that MOG1 is another $Na_v1.5$ cytoplasmic loop II interacting protein. However, the specific binding sites in MOG1 and loop II of $Na_v1.5$ remain to be identified. In the future, serial deletion analysis and site-directed mutagenesis in combination with protein binding assays can be employed to identify the binding site(s).

When a binding site is identified, it will reveal whether any disease-associated mutations are located within the site and affect the binding of MOG1 to $Na_v1.5$.

MOG1 may have effects on other sodium channels The sequence of $Na_v1.5$ loop II is highly homologous to two sodium channel isoforms, $Na_v1.8$ and $Na_v1.9$ which are predominantly expressed in dorsal root and trigeminal ganglia (DRG). It is reasonable to speculate that MOG1 may associate with these two sodium channels and has similar biological effects on them as it does on $Na_v1.5$. Similar experiments for studying $Na_v1.5$ and MOG1 can be performed to test this hypothesis. In addition, as shown in Chapter IV, $Na_v1.5$ was demonstrated to be distributed widely through the central nervous system and mainly localized to the axons at the cellular level. These results suggested that MOG1 may associate with $Na_v1.5$ in the brain and have effects on regulating neuronal excitability mediated by $Na_v1.5$. MOG1 can be co-expressed with expression constructs for $Na_v1.8$ and $Na_v1.9$ or other sodium channels in HEK-293 cells, and the effect of MOG1 can be determined by measuring the sodium currents. These studies should be able to determine whether the effect of MOG1 is specific for $Na_v1.5$.

Identification of MOG1 mutations in arrhythmia patients $Na_v1.5$ mutations have been associated with Brugada syndrome and other types of lethal arrhythmias. The fact that $Na_v1.5$ mutations affect the cell surface expression (trafficking) suggests that MOG1 may also be central and/or a contributor to many disease processes in the heart. Genetic mutations in MOG1 may affect the expression and function of $Na_v1.5$, leading to similar cardiac diseases. Future mutational analysis of MOG1 in patients with various arrhythmic disorders can be performed to test this hypothesis. On the other hand, identification of proteins like MOG1 that regulate expression and function of $Na_v1.5$ may

serve as interesting targets for developing interventional options to manage lethal arrhythmias associated with $Na_v1.5$ mutations or abnormalities. Furthermore, the present findings provide new insights into the physiological role of MOG1 *in vivo* in mammalian cells, and future studies of MOG1 will likely offer more insights on its role and its relevance in myocardial function.

5.2. The increased expression of STAT1 in SCN5A N1325S transgenic mouse may be involved in cardiomyocyte apoptosis

Abnormal calcium handling has been demonstrated in SCN5A N1325S transgenic mice (Yong et al. 2007). Calcium ion antagonist verapamil was shown to reduce the incidence of inhomogeneous AP in SCN5A N1325S transgenic mice (Yong et al. 2007). This finding suggests that SCN5A N1325S mutation causes the remodeling of intracellular calcium ion homeostasis in response to the $[Na^+]_i$ overload. It was reported that increased intracellular Ca^{2+} concentrations enhanced the phosphorylation of STAT1 and thus increased transcription activation of STAT1-dependent genes (Xu et al. 2005, Nair et al. 2002). Indeed, several STAT1 mediated genes were also expressed abundantly as a result of SCN5A N1325S mutation (see chapter III). There is not yet direct experimental evidence for the relationship between the expression level of STAT1 and intracellular calcium influx. In the future, TG-NS mice can be treated with calcium channel blockers (TG-WT as control), and $[Ca^{2+}]_i$ and expression of STAT1 can be measured. Decreased $[Ca^{2+}]_i$ by calcium channel blockers may correlate with reduced expression of STAT1, which will support the hypothesis that increased STAT1 expression in TG-NS mice may be related to abnormal calcium handling in these mice.

In our study, STAT1 has been shown to be highly expressed in SCN5A N1325S transgenic mice (Chapter III). STAT1 has been shown as a preapoptotic factor. Apoptosis was observed in our SCN5A N1325S transgenic mice (Zhang et al. 2007). Therefore, STAT1 may mediate apoptosis in SCN5A N1325S transgenic mice. To test this hypothesis, TG-NS mice can be breed to STAT1 knockout mice to determine whether the absence of STAT1 can prevent apoptosis induced by SCN5A mutation N1325S in TG-NS mice.

5.3. $Na_v1.5$ is a candidate gene for brain disease

Chapter IV showed that the $Na_v1.5$ protein was widely expressed in the central nervous system, including the cerebral cortex, striatum, cerebellum, and brain stem. $Na_v1.5$ was also detected on the plasma membrane of the neuronal processes within distinct regions of the brain. The implication of this finding is that $Na_v1.5$ may play a role in the physiology of the central nervous system. Interestingly, administration of propranolol, which has a potential to block sodium channels, can correct the disorder of habituation in schizophrenic patients. Recent work from Roberts et al. found that "an aboriginal genetic defect in voltage-gated Na+-channel SCN5A can give rise to susceptibility to schizophrenia" (Roberts et al. 2006). It has been known that another type of sodium channel blocker, local anesthetics, can act as an anticonvulsant by producing a conduction block in nerves and prevent a variety of seizures. On the other hand, anticonvulsants such as phenytoin have a therapeutic effect for cardiac arrhythmias by blocking sodium currents (Rogawski et al. 1990). Abnormal neuronal activity associated with $Na_v1.5$ mutations might affect both the coordination of brain function and

cardiac rhythm, which may trigger seizures, syncope, life-threatening arrhythmias, or sudden death in arrhythmic and epileptic patients. Screening $Na_v1.5$ mutations in schizophrenia and epilepsy patients may provide additional evidence to support this hypothesis.

BIBLIOGRAPHY

Abbott GW, Sesti F, Splawski I, Buck ME, Lehmann MH, Timothy KW, Keating MT, Goldstein SA. (1999). MiRP1 forms IKr potassium channels with HERG and is associated with cardiac arrhythmia. *Cell,* 97:175-87.

Abriel H, Loffing J, Rebhun JF, Pratt JH, Schild L, Horisberger JD, Rotin D, Staub O.(1999). Defective regulation of the epithelial Na+ channel by Nedd4 in Liddle's syndrome. *J Clin Invest.*, 103:667-673.

Abriel H, Kamynina E, Horisberger JD, Staub O. (2000). Regulation of the cardiac voltage-gated Na+ channel (H1) by the ubiquitin-protein ligase Nedd4. *FEBS Lett.* 466:377-80.

Abriel H, Kass RS. (2005). Regulation of the voltage-gated cardiac sodium channel Nav1.5 by interacting proteins. *Trends Cardiovasc Med*., 15:35-40.

Adamkova L, Souckova K, Kovarik J. (2007). Transcription protein STAT1: biology and relation to cancer. *Folia Biol* (Praha). 53:1-6.

Ahern CA, Zhang JF, Wookalis MJ, Horn R. (1995). Modulation of the cardiac sodium channel NaV1.5 by Fyn, a Src family tyrosine kinase. *Circ Res*., 96:991-998.

Akai J, Makita N, Sakurada H, Shirai N, Ueda K, Kitabatake A, Nakazawa K, Kimura A, Hiraoka M. (2000). A novel SCN5A mutation associated with idiopathic ventricular fibrillation without typical ECG findings of Brugada syndrome. *FEBS Lett.* 479:29-34.

Allouis M, Le Bouffant F, Wilders R, Peroz D, Schott JJ, Noireaud J, Le Marec H, Merot J, Escande D, Baro I. (2006). 14-3-3 is a regulator of the cardiac voltage-gated sodium channel Nav1.5. *Circ Res.,* 98:1538-1546.

An RH, Wang XL, Kerem B, Benhorin J, Medina A, Goldmit M, Kass RS. (1998). Novel LQT-3 mutation affects Na+ channel activity through interactions between alpha- and beta1-subunits. *Circ Res*., 83:141-146.

Antzelevitch C, Brugada P, Brugada J and Brugada R. (2005). Brugada syndrome: From cell to bedside. *Current Problems in Cardiology*. 30:9-54.

Archacki SR, Angheloiu G, Tian XL, Tan FL, DiPaola N, Shen GQ, Moravec C, Ellis S, Topol EJ and Wang Q, (2003). Identification of new genes differentially expressed in coronary artery disease by expression profiling, *Physiol*. Genomics 15:65–74.

Arnestad M, Crotti L, Rognum TO, Insolia R, Pedrazzini M, Ferrandi C, Vege A, Wang DW, Rhodes TE, George AL Jr, Schwartz PJ. (2007). Prevalence of long-QT syndrome gene variants in sudden infant death syndrome. *Circulation,* 115:361-367.

Baker RP, Harreman MT, Eccleston JF, Corbett AH, Stewart M. (2001). Interaction between Ran and Mog1 is required for efficient nuclear protein import. *J Biol Chem*., 276:41255-41262.

Balser JR, (1999). Structure and function of the cardiac sodium channels, *Cardiovasc. Res.*42:327-338.

Baroudi G, Carbonneau E, Pouliot V, Chahine M. (2000). SCN5A mutation (T1620M) causing Brugada syndrome exhibits different phenotypes when expressed in Xenopus oocytes and mammalian cells. *FEBS Lett.,* 467:12-16.

Beinder E, Grancay T, Hofbeck M. (2000). Prolongation of the QT interval and SIDS. *N Engl J Med.* 343:1896.

Bennett PB, Yazawa K, Makita N, George AL. (1995). Molecular mechanism for an inherited cardiac arrhythmia. *Nature,* 376:683-685.

Benson DW, Wang DW, Dyment M, Knilans TK, Fish FA, Strieper MJ, Rhodes TH, George AL Jr. (2003). Congenital sick sinus syndrome caused by recessive mutations in the cardiac sodium channel gene (SCN5A). *J Clin Invest*., 112:1019-1028.

Bezzina C, Veldkamp MW, van Den Berg MP, Postma AV, Rook MB, Viersma JW, van Langen IM, Tan-Sindhunata G, Bink-Boelkens MT, van Der Hout AH, Mannens MM, Wilde AA. (1999). A single Na(+) channel mutation causing both long-QT and Brugada syndromes. *Circ Res*., 85:1206-1213.

Bichet D, Cornet V, Geib S, Carlier E, Volsen S, Hoshi T, Mori Y, De Waard M. (2000). The I-II loop of the Ca2+ channel alpha1 subunit contains an endoplasmic reticulum retention signal antagonized by the beta subunit. *Neuron*. 25:177-190.

Boehmer C, Wilhelm V, Palmada M, Wallisch S, Henke G, Brinkmeier H, Cohen P, Pieske B, Lang F. (2003). Serum and glucocorticoid inducible kinases in the regulation of the cardiac sodium channel SCN5A. *Cardiovasc Res*., 57:1079-84.

Camacho JA, Hensellek S, Rougier JS, Blechschmidt S, Abriel H, Benndorf K, Zimmer T. (2006). Modulation of Nav1.5 channel function by an alternatively spliced sequence in the DII/DIII linker region. *J Biol Chem,* 281:9498-9506.

Catterall WA., (2000). From ionic currents to molecular mechanisms: the structure and function of voltage-gated sodium channels, *Neuron* 26:13-25.

Chen Q, Kirsch GE, Zhang D, Brugada R, Brugada J, Brugada P *et al.* (1998).Genetic basis and molecular mechanism for idiopathic ventricular fibrillation. *Nature* 392:293-296.

Chen LY, Ballew JD, Herron KJ, Rodeheffer RJ, Olson TM. (2007). A common polymorphism in SCN5A is associated with lone atrial fibrillation. *Clin Pharmacol Ther*., 81:35-41.

Clancy CE, Rudy Y. (1999). Linking a genetic defect to its cellular phenotype in a cardiac arrhythmia. *Nature*., 400:566-9.

Clancy CE, Rudy Y. (2002). Na(+) channel mutation that causes both Brugada and long-QT syndrome phenotypes: a simulation study of mechanism. *Circulation*, 105:1208-13.

Cronk LB, Ye B, Kaku T, Tester DJ, Vatta M, Makielski JC, Ackerman MJ. (2007). Novel mechanism for sudden infant death syndrome: persistent late sodium current secondary to mutations in caveolin-3. *Heart Rhythm*.4:161-6.

Curran ME, Splawski I, Timothy KW, Vincent GM, Green ED, Keating MT. (1995). A molecular basis for cardiac arrhythmia:HERG mutations cause long QT syndrome.*Cell*. 80:795-803.

Deschenes I, Neyroud N and DiSilvestre D *et al.* (2002). Isoform-specific modulation of voltage-gated Na(+) channels by calmodulin, *Circ Res* 90:E49–E57.

Donahue LM, Coates PW, Lee VH, Ippensen DC, Arze SE, and Poduslo SE, (2000). The cardiac sodium channel mRNA is expressed in the developing and adult rat and human brain, *Brain Res*. 887:335-343.

Dumaine R, Wang Q, Keating MT, Hartmann HA, Schwartz PJ, Brown AM, and Kirsch GE, (1996). Multiple mechanisms of Na+ channel-linked long-QT syndrome, *Circ. Res*. 78: 916-924.

Elliott AA, Elliott JR. (1993). Characterization of TTX-sensitive and TTX-resistant sodium currents in small cells from adult rat dorsal root ganglia. *J Physiol*., 463:39-56.

Emmi A, Wenzel HJ, Schwartzkroin PA, Taglialatela M, Castaldo P, Bianchi L, Nerbonne J, Robertson GA, Janigro D. (2000). Do glia have heart? Expression and functional role for ether-a-go-go currents in hippocampal astrocytes. *J Neurosci*., 20:3915-3925.

Escayg A, MacDonald BT, Meisler MH, Baulac S, Huberfeld G, An-Gourfinkel I, Brice A, LeGuern E, Moulard B, Chaigne D, Buresi C, and Malafosse A. (2000). Mutations of *SCN1A*, encoding a neuronal sodium channel, in two families with GEFS+2. *Nat Genet* 24:343–345.

Eubanks J, Srinivasan J, Dinulos MB, Disteche CM, Catterall WA. (1997). Structure and chromosomal localization of the beta2 subunit of the human brain sodium channel. *Neuroreport.,* 8:2775-9.

Fahmi AI, Patel MJ, Stevens EB, Fowden AL, James Edward John III, Lee K, Pinnock R, Morgan K, Jackson AP and Vandenberg JI. (2001). The sodium channel β-subunit SCN3b modulates the kinetics of SCN5a and is expressed heterogeneously in sheep heart. *Journal of Physiology*, 537:693-700.

Fozzard HA, Hanck DA. (1996). Structure and function of voltage-dependent sodium channels: comparison of brain II and cardiac isoforms. *Physiol Rev*., 76:887-926.

Frohnwieser B, Chen LQ, Schreibmayer W, Kallen RG. (1997). Modulation of the human cardiac sodium channel -subunit by cAMP-dependent protein kinase and the responsible sequence domain. *J Physiol* (Lond). 498:309–318.

Gavillet B, Rougier JS, Domenighetti AA, Behar R, Boixel C, Ruchat P, Lehr HA, Pedrazzini T, Abriel H. (2006). Cardiac sodium channel Nav1.5 is regulated by a multiprotein complex composed of syntrophins and dystrophin. *Circ Res*. 99:407-14.

Gellens ME, George Jr AL, Chen L, Chahine M, Horn R, Barchi RL and Kallen RG. (1992). Primary Structure and Functional Expression of the Human Cardiac Tetrodotoxin-Insensitive Voltage-Dependent Sodium Channel. Proceedings of the National Academy of *Sciences,* 89:554-558.

George AL Jr, Knittle TJ, Tamkun MM. (1992). Molecular cloning of an atypical voltage-gated sodium channel expressed in human heart and uterus: evidence for a distinct gene family. *Proc Natl Acad Sci U S A.,* 89:4893-4897.

Hamill OP, Marty A, Neher E, Sakmann B, Sigworth FJ. (1981). Improved patch-clamp techniques for high-resolution current recording from cells and cell-free membrane patches. *Pflugers Arch.*391:85-100.

Harlow E and Lane D, Antibodies: A Laboratory Manual, Cold Spring Harbor aboratory, Cold Spring Harbor, NY, 1988.

Hartmann HA, Colom LV, Sutherland ML, and Noebels JL, (1999). Selective localization of cardiac SCN5A sodium channels in limbic regions of rat brain, *Nat. Neurosci*. 2:593-595.

Hartshorne RP, Catterall WA. (1984). The sodium channel from rat brain. Purification and subunit composition. *J Biol Chem*., 259:1667-75.

Herbert E, Chahine M. (2006). Clinical aspects and physiopathology of Brugada syndrome: review of current concepts. *Can J Physiol Pharmacol*., 84:795-802.

Herzog RI, Liu C and Waxman SG *et al.* (2003). Calmodulin binds to the C terminus of sodium channels Nav1.4 and Nav1.6 and differentially modulates their functional properties, *J Neurosci* 23: 8261–8270.

Isom LL, De Jongh KS, Patton D Reber B.F.X., Offord J., Charbonneau H., Walsh K., Goldin AL and Catterall WA. (1992). Primary structure and functional expression of the β1 subunit of the rat brain sodium channel. *Science* 256:839–842.

Isom LL and Caterall WA. (1996). Na+ channel subunits and Ig domains. *Nature.* 383: 307-308.

Jacobs A, Knight BP, McDonald KT, Burke MC. (2006). Verapamil decreases ventricular tachyarrhythmias in a patient with Timothy syndrome (LQT8). *Heart Rhythm*. 3:967-70.

Jalife J. (2000). Ventricular fibrillation: mechanisms of initiation and maintenance. *Annu Rev Physiol.,* 62:25-50.

Jeong SY, Goto J, Hashida H, Suzuki T, Ogata K, Masuda N, Hirai M, Isahara K, Uchiyama Y, and Kanazawa I, (2000). Identification of a novel human voltage-gated sodium channel alpha subunit gene, SCN12A, *Biochem. Biophys. Res. Commun*. 267:262-270.

Jervell A, Lange-Nielsen F. (1957). Congenital deafmutism, functional heart disease with prolongation of the QT interval, and sudden death. *Am.Heart J.* 54:59-78.

Jespersen T, Gavillet B, van Bemmelen MX, Cordonier S, Thomas MA, Staub O, Abriel H. (2006). Cardiac sodium channel Na(v)1.5 interacts with and is regulated by the protein tyrosine phosphatase PTPH1. *Biochem Biophys Res Commun*., 348:1455-62.

Jiang C, Atkinson D, Towbin JA, Splawski I, Lehmann MH, Li H *et al.* (1994). Two long QT syndrome loci map to chromosomes 3 and 7 with evidence for further heterogeneity. *Nat.Genet*., 8:141-47.

Johnson D, Bennett ES. (2006). Isoform-specific effects of the beta2 subunit on voltage-gated sodium channel gating. *J Biol Chem*., 281:25875-81.

Katze MG, He Y & Gale M. (2002). "Viruses and interferon: a fight for supremacy.". *Nature Reviews Immunology,* 2: 675-87.

Keating M, Atkinson D, Dunn C, Timothy K, Vincent GM, Leppert M. (1991). Linkage of a cardiac arrhythmia, the long QT syndrome, and the Harvey ras-1 gene. *Science,* 252:704-6.

Keating MT, Sanguinetti MC. (2001). Molecular and cellular mechanisms of cardiac arrhythmias.*Cell.*, 104:569-80.

Kerr NC, Holmes FE, Wynick D. (2004). Novel isoforms of the sodium channels Nav1.8 and Nav1.5 are produced by a conserved mechanism in mouse and rat. *J Biol Chem*. 279:24826-24833.

Kim E, Sheng M. (2004). PDZ domain proteins of synapses. *Nat Rev Neurosci.* 5:771-781.

Kim J, Ghosh S, Liu H, Tateyama M, Kass RS, Pitt GS. (2004). Calmodulin mediates Ca^{2+} sensitivity of sodium channels, *J Biol Chem*., 279:45,004–45,012.

Kodama I, Nikmaram MR, Boyett MR, Suzuki R, Honjo H, Owen JM. (1997). Regional differences in the role of the Ca2+ and Na+ currents in pacemaker activity in the sinoatrial node. *Am J Physiol*. 272:H2793-806.

Kumar A, Commane M, Flickinger TW, Horvath CM and Stark GR, (1997). Defective TNF-alpha-induced apoptosis in STAT1-null cells due to low constitutive levels of caspases, *Science,* 278:1630–1632.

Kyndt F, Probst V, Potet F, Demolombe S, Chevallier JC, Baro I, Moisan JP, Boisseau P, Schott JJ, Escande D, Le Marec H. (2001). Novel SCN5A mutation leading either to isolated cardiac conduction defect or Brugada syndrome in a large French family.*Circulation.,* 104:3081-6.

Lemaillet G, Walker B, Lambert S. (2003). Identification of a conserved ankyrin-binding motif in the family of sodium channel alpha subunits. *J Biol Chem*. 278:27333-9.

Livak KJ and Schmittgen TD, (2001). Analysis of relative gene expression data using real-time quantitative PCR and the 2(-Delta Delta C(T)) method, *Methods* 25:402–408.

Liu Cj, Dib-Hajj SD, Waxman SG. (2001.)Fibroblast growth factor homologous factor 1B binds to the C terminus of the tetrodotoxin-resistant sodium channel rNav1.9a (NaN). *J Biol Chem.,* 276:18925-18933.

Liu CJ, Dib-Hajj SD and Renganathan M *et al.* (2003). Modulation of the cardiac sodium channel Nav1.5 by fibroblast growth factor homologous factor 1B, *J Biol Chem* 278 :1029–1036.

Liu Y, Videnskey S, Ruggiero AM, Maier S, Sitte HH, Rothstein JD. (2007) Reticulon RTN2B regulates trafficking and function of neuronal glutamate transporter EAAC1. *J Biol Chem.* Epub ahead of print

Lu T., Lee H., Kabat J.A. and Shibata E.F.. (1999). Modulation of rat cardiac sodium channel by the stimulatory G protein α subunit. *Journal of Physiology* 518.2:371-384.

Lu JM, Deschenes RJ, Fassler JS. (2004). Role for the Ran binding protein, Mog1p, in *Saccharomyces cerevisiae* SLN1-SKN7 signal transduction. Eukaryot *Cell.,* 3:1544-56.

Lu JM, Deschenes RJ, Fassler JS. (2003). Saccharomyces cerevisiae histidine phosphotransferase Ypd1p shuttles between the nucleus and cytoplasm for SLN1-dependent phosphorylation of Ssk1p and Skn7p. *Eukaryot Cell*. 2:1304-14.

Maier SK, Westenbroek RE, Schenkman KA, Feigl EO, Scheuer T, Catterall WA. (2001). An unexpected role for brain-type sodium channels in coupling of cell surface depolarization to contraction in the heart. *Proc Natl Acad Sci U S A.* 99:4073-8.

Maier SK, Westenbroek RE, McCormick KA, Curtis R, Scheuer T, Catterall WA. (2004). Distinct subcellular localization of different sodium channel alpha and beta subunits in single ventricular myocytes from mouse heart. *Circulation.,* 109:1421-7.

Makielski JC, Ye B, Valdivia CR, Pagel MD, Pu J, Tester DJ, Ackerman MJ. (2003). A ubiquitous splice variant and a common polymorphism affect heterologous expression of recombinant human SCN5A heart sodium channels. *Circ Res*., 93:821-8.

Makielski JC. (2006). SIDS: genetic and environmental influences may cause arrhythmia in this silent killer. *J Clin Invest*., 116:297-9.

Makita N, Bennett Jr PB and George Jr AL. (1994). Voltage-gated Na^+ channel beta 1 subunit mRNA expressed in adult human skeletal muscle, heart, and brain is encoded by a single gene. *Journal of Biological Chemistry,* 269: 7571-7578.

Makita N, Sasaki K, Groenewegen WA, Yokota T, Yokoshiki H, Murakami T, Tsutsui H. (2005). Congenital atrial standstill associated with coinheritance of a novel SCN5A mutation and connexin 40 polymorphisms. *Heart Rhythm*., 2:1128-34.

Malhotra JD, Chen C, Rivolta I, Abriel H, Malhotra R, Mattei LN, Brosius FC, Kass RS, and Isom LL. (2001). Characterization of Sodium Channel ⍺- and ß-Subunits in Rat and Mouse Cardiac Myocytes. *Circulation,*103: 1303-1310.

Malhotra JD, Thyagarajan V, Chen C, Isom LL. (2004). Tyrosine-phosphorylated and nonphosphorylated sodium channel beta1 subunits are differentially localized in cardiac myocytes. *J Biol Chem*. 279:40748-54.

Marfatia KA, Harreman MT, Fanara P, Vertino PM, Corbett AH. (2001). Identification and characterization of the human MOG1 gene. *Gene.* 266:45-56.

Margeta-Mitrovic M, Jan YN, Jan LY. (2000). A trafficking checkpoint controls GABAB receptor heterodimerization. *Neuron*. 27:97–106.

Maron BJ, Clark CE, Goldstein RE, Epstein SE. (1976). Potential role of QT interval prolongation in sudden infant death syndrome. *Circulation*., 54:423-430.

Matsuda JJ, Lee H, Shibata EF. (1992). Enhancement of rabbit cardiac sodium channels by beta-adrenergic stimulation. *Circ Res*., 70:199-207.

Matsuo K, Kurita T, Inagaki M, Kakishita M, Aihara N, Shimizu W, Taguchi A, Suyama K, Kamakura S, Shimomura K. (1999). The circadian pattern of the development of ventricular fibrillation in patients with Brugada syndrome.*Eur Heart J*., 20:465-70.

Medeiros-Domingo A, Kaku T, Tester DJ, Iturralde-Torres P, Itty A, Ye B, Valdivia C, Ueda K, Canizales-Quinteros S, Tusie-Luna MT, Makielski JC, Ackerman MJ. (2007). SCN4B-encoded sodium channel beta4 subunit in congenital long-QT syndrome.*Circulation.*116:134-142.

Mohler PJ, Schott JJ, Gramolini AO, Dilly KW, Guatimosim S, duBell WH, Song LS, Haurogne K, Kyndt F, Ali ME, Rogers TB, Lederer WJ, Escande D, Le Marec H, Bennett V. (2003). Ankyrin-B mutation causes type 4 long-QT cardiac arrhythmia and sudden cardiac death. *Nature*., 421:634-639.

Mohler PJ, Rivolta I, Napolitano C, LeMaillet G, Lambert S, Priori SG, Bennett V. (2004). Nav1.5 E1053K mutation causing Brugada syndrome blocks binding to ankyrin-G and expression of Nav1.5 on the surface of cardiomyocytes. *Proc Natl Acad Sci U S A.,* 101:17533-17538.

Morgan K, Stevens EB, Shah B, Cox PJ, Dixon AK, Lee K, Pinnock RD, Hughes J, Richardson PJ, Mizuguchi K, and Jackson AP. (2000). β3: An additional auxiliary subunit of the voltage-sensitive sodium channel that modulates channel gating with distinct kinetics. *PNAS.* 97:2308-2313.

Moric E, Herbert E, Trusz-Gluza M, Filipecki A, Mazurek U, Wilczok T. (2003). The implications of genetic mutations in the sodium channel gene (SCN5A). *Europace*., 5:325-34.

Murphy BJ, Rogers J, Perdichizzi AP, Colvin AA, Catterall WA. (1996). cAMP-dependent phosphorylation of two sites in the alpha subunit of the cardiac sodium channel. *J Biol Chem*. 271:28837-43.

Nair JS, DaFonseca CJ, Tjernberg A, Sun W, Darnell JE Jr, Chait BT, Zhang JJ. (2002). Requirement of Ca2+ and CaMKII for Stat1 Ser-727 phosphorylation in response to IFN-gamma. *Proc Natl Acad Sci U S A.,* 99:5971-6.

Nelson MR,Chazin WJ. (1998). An interaction-based analysis of calcium-induced conformational changes in Ca^{2+} sensor proteins. *Protein Sci.* 7:270-282.

Neyroud N, Tesson F, Denjoy I, Leibovici M, Donger C, Barhanin J, Faure S, Gary F, Coumel P, Petit C, Schwartz K, Guicheney P. (1997). A novel mutation in the potassium channel gene KVLQT1 causes the Jervell and Lange-Nielsen cardioauditory syndrome. *Nat Genet*.,15:186-9.

Nishiyama K, Trapp BD, Ikezu T, Ransohoff RM, Tomita T, Iwatsubo T, Kanazawa I, Hsiao KK, Lisanti MP, and Okamoto T, (1999). Caveolin-3 upregulation activates beta-secretase-mediated cleavage of the amyloid precursor protein in Alzheimer's disease, *J. Neurosci*. 19:6538-6548.

Niu DM, Hwang B, Hwang HW, Wang NH, Wu JY, Lee PC, Chien JC, Shieh RC, Chen YT. (2006). A common SCN5A polymorphism attenuates a severe cardiac phenotype caused by a nonsense SCN5A mutation in a Chinese family with an inherited cardiac conduction defect. *J Med Genet*., 43:817-21.

Novakovic S.D., Eglen R.M. and Hunter J.C. (2001). Regulation of Na+ channel distribution in the nervous system. *Trends in neurosciences*. 24: 473-478.

Nuss HB, Chiamvimonvat N, Perez-garcia MT, Tomaselli GF and Marban E. (1995). Functional association of the beta 1 subunit with human cardiac (hH1) and rat skeletal muscle (mu 1) sodium channel alpha subunits expressed in *Xenopus* oocytes. *Journal of General Physiology* 106:1171-1191.

Nuyens D, Stengl M, Dugarmaa S, Rossenbacker T, Compernolle V, Rudy Y, Smits JF, Flameng W, Clancy CE, Moons L, Vos MA, Dewerchin M, Benndorf K, Collen D, Carmeliet E, Carmeliet P. (2001). Abrupt rate accelerations or premature beats cause life-threatening arrhythmias in mice with long-QT3 syndrome. *Nat Med.* 7:1021-1027.

Ogata K, Jeong SY, Murakami H, Hashida H, Suzuki T, Masuda N, Hirai M, Isahara K, Uchiyama Y, Goto J, and Kanazawa I, (2000). Cloning and expression study of the mouse tetrodotoxin-resistant voltage-gated sodium channel alpha subunit NaT/Scn11a, *Biochem. Biophys. Res. Commun*. 267:271-277.

Oki M, Nishimoto T. (1998). A protein required for nuclear-protein import, Mog1p, directly interacts with GTP-Gsp1p, the Saccharomyces cerevisiae ran homologue. Proc *Natl Acad Sci U S A.,* 95:15388-93.

Oki M, Ma L, Wang Y, Hatanaka A, Miyazato C, Tatebayashi K, Nishitani H, Uchida H, Nishimoto T. (2007). Identification of novel suppressors for Mog1 implies its involvement in RNA metabolism, lipid metabolism and signal transduction. *Gene.* 400:114-21.

Olson TM, Michels VV, Ballew JD, Reyna SP, Karst ML, Herron KJ, Horton SC, Rodeheffer RJ, Anderson JL.(2005). Sodium channel mutations and susceptibility to heart failure and atrial fibrillation. *JAMA*. 293:447-454.

Ou Y, Strege P, Miller S.M., Makielski J., Ackermn M., Gibbons S.J., and Farrugia G.. (2003). Syntrophin γ2 Regulates NAV1.5 Gating by a PDZ Domain-mediated Interaction *J. Biol. Chem*. 278: 1915-1923.

Plant LD, Bowers PN, Liu Q, Morgan T, Zhang T, State MW, Chen W, Kittles RA, Goldstein SA. (2006). A common cardiac sodium channel variant associated with sudden infant death in African Americans, SCN5A S1103Y. *J Clin Invest*., 116:430-5.

Plaster NM, Tawil R, Tristani-Firouzi M, Canun S, Bendahhou S, Tsunoda A, Donaldson MR, Iannaccone ST, Brunt E, Barohn R, Clark J, Deymeer F, George AL Jr, Fish FA, Hahn A, Nitu A, Ozdemir C, Serdaroglu P, Subramony SH, Wolfe G, Fu YH, Ptacek LJ. (2001). Mutations in Kir2.1 cause the developmental and episodic electrical phenotypes of Andersen's syndrome. *Cell.*105:511–519.

Plummer NW, Meisler MH. (1999). Evolution and diversity of mammalian sodium channel genes. *Genomics.,* 57:323-331.

Probst V, Kyndt F, Potet F, Trochu JN, Mialet G, Demolombe S, Schott JJ, Baro I, Escande D, Le Marec H. (2003). Haploinsufficiency in combination with aging causes SCN5A-linked hereditary Lenegre disease. J Am Coll Cardiol. 41:643-52.

Probst V, Allouis M, Sacher F, Pattier S, Babuty D, Mabo P, Mansourati J, Victor J, Nguyen JM, Schott JJ, Boisseau P, Escande D, Le Marec H. (2006). Progressive cardiac conduction defect is the prevailing phenotype in carriers of a Brugada syndrome SCN5A mutation. *J Cardiovasc Electrophysiol*., 17:270-5.

Ptacek LJ, George AL Jr, Griggs RC, Tawil R, Kallen RG, Barchi RL, Robertson M, Leppert MF. (1991). Identification of a mutation in the gene causing hyperkalemic periodic paralysis. *Cell*. 67:1021-7.

Ptacek LJ, George AL Jr, Barchi RL, Griggs RC, Riggs JE, Robertson M, and Leppert MF, (1992). Mutations in an S4 segment of the adult skeletal muscle sodium channel cause paramyotonia congenita, *Neuron* 8:891-897.

Qu Y, Isom LL, Westenbroek RE, Rogers JC, Tanada TN, McCormick KA, Scheuer T, Catterall WA. (1995). Modulation of cardiac Na+ channel expression in Xenopus oocytes by beta 1 subunits. *J Biol Chem*., 270:25696-701.

Qu Y, Rogers JC, Tanada TN, Catterall WA, Scheuer T. (1996). Phosphorylation of S1505 in the cardiac Na+ channel inactivation gate is required for modulation by protein kinase C. *J Gen Physiol*.,108(5):375-9.

Qu Y., Rogers JC, Chen SF, McCormick KA, Scheuer T, and Catterall WA. (1999). Functional Roles of the Extracellular Segments of the Sodium Channel α Subunit in Voltage-dependent Gating and Modulation by β1 Subunits. *J Biol Chem*. 274: 32647-32654.

Qu Y, Curtis R, Lawson D, Gilbride K, Ge P, DiStefano PS, Silos-Santiago I, Catterall WA, Scheuer T. (2001). Differential modulation of sodium channel gating and persistent sodium currents by the beta1, beta2, and beta3 subunits. *Mol Cell Neurosci.*, 18:570-80.

Quimby BB, Dasso M. (2003). The small GTPase Ran: interpreting the signs. *Curr Opin Cell Biol.* 15:338-44.

Remme CA, Verkerk AO, Nuyens D, van Ginneken AC, van Brunschot S, Belterman CN, Wilders R, van Roon MA, Tan HL, Wilde AA, Carmeliet P, de Bakker JM, Veldkamp MW, Bezzina CR. (2006). Overlap syndrome of cardiac sodium channel disease in mice carrying the equivalent mutation of human SCN5A-1795insD. *Circulation,*114:2584-2594.

Rivolta I, Clancy CE, Tateyama M, Liu H, Priori SG, Kass RS. (2002). A novel SCN5A mutation associated with long QT-3: altered inactivation kinetics and channel dysfunction. Physiol *Genomics*,10:191-7.

Roberts E. (2006). GABAergic malfunction in the limbic system resulting from an aboriginal genetic defect in voltage-gated Na+-channel SCN5A is proposed to give rise to susceptibility to schizophrenia. *Adv Pharmacol*., 54:119-145.

Rogawski M.A. & Porter, R.J.(1990) *pharmacol. Rev*. 42, 223-286.

Romano C. (1965). Congenital cardiac arrhythmia. *Lancet*.1:658-659.

Rook MB, Bezzina Alshinawi C, Groenewegen WA, van Gelder IC, van Ginneken AC, Jongsma HJ, Mannens MM, Wilde AA. (1999). Human SCN5A gene mutations alter cardiac sodium channel kinetics and are associated with the Brugada syndrome. *Cardiovasc Res*., 44:507-517.

Rossenbacker T, Carroll SJ, Liu H, Kuiperi C, de Ravel TJ, Devriendt K, Carmeliet P, Kass RS, Heidbuchel H. (2004). Novel pore mutation in SCN5A manifests as a spectrum of phenotypes ranging from atrial flutter, conduction disease, and Brugada syndrome to sudden cardiac death. *Heart Rhythm*.,1:610-615.

Rossenbacker T, Schollen E, Kuiperi C, de Ravel TJ, Devriendt K, Matthijs G, Collen D, Heidbuchel H, Carmeliet P. (2005). Unconventional intronic splice site mutation in SCN5A associates with cardiac sodium channelopathy. *J Med Genet*., 42:e29.

Royer A, van Veen TA, Le Bouter S, Marionneau C, Griol-Charhbili V, Leoni AL, Steenman M, van Rijen HV, Demolombe S, Goddard CA, Richer C, Escoubet B, Jarry-Guichard T, Colledge WH, Gros D, de Bakker JM, Grace AA, Escande D, Charpentier F. (2005). Mouse model of SCN5A-linked hereditary Lenegre's disease: age-related conduction slowing and myocardial fibrosis. *Circulation*, 111:1738-46.

Rush AM, Waxman SG. (2004). PGE2 increases the tetrodotoxin-resistant $Na_v1.9$ sodium current in mouse DRG neurons via G-proteins. *Brain Res.* 1023:264-71.

Saab CY, Cummins TR, Waxman SG. (2003). GTP gamma S increases $Na_v1.8$ current in small-diameter dorsal root ganglia neurons. *Exp Brain Res.* 152:415-9.

Sandow A (1952). "Excitation-contraction coupling in muscular response.". *Yale J Biol Med* 25: 176-201.

Sanguinetti MC, Jiang C, Curran ME, Keating MT. (1995). A mechanistic link between an inherited and an acquired cardiac arrhythmia: HERG encodes the IKr potassium channel. *Cell*., 81(2:299-307.

Sanguinetti MC, Curran ME, Spector PS, Keating MT. (1996). Spectrum of HERG K+-channel dysfunction in an inherited cardiac arrhythmia. *Proc Natl Acad Sci U S A*. 93:2208-2212.

Schindler, C., X.-Y. Fu, T. Improta, R. Aebersold, J. E. Darnell, Jr. (1992). Proteins of transcription factor ISGF-3: one gene encodes the 91- and 84-kDa ISGF3 proteins that are activated by interferon . *Proc. Natl. Acad. Sci. USA 89*:*7836*.

Schott JJ, Charpentier F, Peltier S, Foley P, Drouin E, Bouhour JB, Donnelly P, Vergnaud G, Bachner L, Moisan JP, et al. (1995). Mapping of a gene for long QT syndrome to chromosome 4q25-27. *Am J Hum Genet*., 57:1114-22.

Schott JJ, Alshinawi C, Kyndt F, Probst V, Hoorntje TM, Hulsbeek M, Wilde AA, Escande D, Mannens MM, Le Marec H. (1999). Cardiac conduction defects associate with mutations in SCN5A, *Nat. Genet*. 23:20-21.

Schreibmayer W, Frohnwieser B, Dascal N, Platzer D, Spreitzer B, Zechner R, Kallen RG, Lester HA. (1994). ß-Adrenergic modulation of currents produced by rat cardiac Na^+ channels expressed in *Xenopus laevis* oocytes. *Receptors Channels.* 2:339–350.

Schulze-Bahr E, Wang Q, Wedekind H, Haverkamp W, Chen Q, Sun Y, Rubie C, Hordt M, Towbin JA, Borggrefe M, Assmann G, Qu X, Somberg JC, Breithardt G, Oberti C, Funke H. (1997). KCNE1 mutations cause jervell and Lange-Nielsen syndrome. *Nat Genet.*, 17:267-8.

Schwartz PJ, Periti M, Malliani A. (1975). The long Q-T syndrome. *Am.Heart J.* 89:378-90.

Schwartz PJ, Priori SG, Dumaine R, Napolitano C, Antzelevitch C, Stramba-Badiale M, Richard TA, Berti MR, Bloise R. (2000). A molecular link between the sudden infant death syndrome and the long-QT syndrome. *N Engl J Med*., 343:262-267.

Scott DB, Blanpied TA, Swanson GT, Zhang C, Ehlers MD. (2001). An NMDA receptor ER retention signal regulated by phosphorylation and alternative splicing. *J Neurosci*. 21:3063–3072.

Smits JP, Eckardt L, Probst V, Bezzina CR, Schott JJ, Remme CA, Haverkamp W, Breithardt G, Escande D, Schulze-Bahr E, LeMarec H, Wilde AA. (2002). Genotype-phenotype relationship in Brugada syndrome: electrocardiographic features differentiate SCN5A-related patients from non-SCN5A-related patients. *J Am Coll Cardiol*., 40(2):350-356.

Smits JP, Koopmann TT, Wilders R, Veldkamp MW, Opthof T, Bhuiyan ZA, Mannens MM, Balser JR, Tan HL, Bezzina CR, Wilde AA. (2005). A mutation in the human cardiac sodium channel (E161K) contributes to sick sinus syndrome, conduction disease and Brugada syndrome in two families. *J Mol Cell Cardiol*., 38:969-81.

Splawski I, Tristani-Firouzi M, Lehmann MH, Sanguinetti MC, Keating MT. (1997). Mutations in the hminK gene cause long QT syndrome and suppress IKs function. *Nat.Genet*., 17:338-40.

Splawski I, Timothy KW, Sharpe LM, Decher N, Kumar P, Bloise R, Napolitano C, Schwartz PJ, Joseph RM, Condouris K, Tager-Flusberg H, Priori SG, Sanguinetti MC, Keating MT. (2004). Ca(V)1.2 calcium channel dysfunction causes a multisystem disorder including arrhythmia and autism. *Cell.* 119:19-31.

Steggerda SM, Paschal BM. (2000). The mammalian Mog1 protein is a guanine nucleotide release factor for Ran. J Biol Chem., 275:23175-23180.

Stephanou A, Brar BK, Scarabelli TM, Jonassen AK, Yellon DM, Marber MS, Knight RA and Latchman DS, (2000). Ischemia-induced STAT-1 expression and activation play a critical role in cardiomyocyte apoptosis, *J. Biol. Chem.* 275:10002–10008.

Stephanou A and Latchman DS, (2003). STAT-1: a novel regulator of apoptosis, *Int. J. Exp. Pathol.* 84: 239–244.

Stevens EB, Cox PJ, Shah BS, Dixon AK, Richardson PJ, Pinnock RD, Lee K. (2001). Tissue distribution and functional expression of the human voltage-gated sodium channel beta 3 subunit. *Pflügers Archiv* 441:481-488.

Stewart M, Baker RP. (2000). 1.9 A resolution crystal structure of the Saccharomyces cerevisiae Ran-binding protein Mog1p. *J Mol Biol.*, 299:213-323.

Susanne M. Steggerda and Bryce M. Paschal. (2000). The Mammalian Mog1 Protein Is a Guanine Nucleotide Release Factor for Ran. *J. Biol. Chem.*. 275: 23175-23180.

Takehara N, Makita N, Kawabe J, Sato N, Kawamura Y, Kitabatake A, Kikuchi K. (2004). A cardiac sodium channel mutation identified in Brugada syndrome associated with atrial standstill. *J Intern Med*., 255:137-142.

Tan FL, Moravec CS, Li J, Pperson-Hansen C, McCarthy PM, Young JB and Bond M, (2002). The gene expression fingerprint of human heart failure, *Proc. Natl. Acad. Sci. USA.,* 99: 11387–11392.

Tan HL, Bink-Boelkens MT, Bezzina CR, Viswanathan PC, Beaufort-Krol GC, van Tintelen PJ, van den Berg MP, Wilde AA, Balser JR. (2001). A sodium-channel mutation causes isolated cardiac conduction disease. *Nature*. 409:1043-1047.

Tan HL, Kupershmidt S, Zhang R, Stepanovic S, Roden DM, Wilde AA, Anderson ME, Balser JR. (2002). A calcium sensor in the sodium channel modulates cardiac excitability. *Nature*., 415:442-447.

Tateyama M, Kurokawa J, Terrenoire C, Rivolta I, Kass RS. (2003). Stimulation of protein kinase C inhibits bursting in disease-linked mutant human cardiac sodium channels.*Circulation*., 107:3216-3222.

Tester DJ, Ackerman MJ. (2005). Sudden infant death syndrome: how significant are the cardiac channelopathies? *Cardiovasc Res*., 67:388-96.

Tian XL, Yong SL, Wan X, Wu L, Chung MK, Tchou PJ, Rosenbaum DS, Van Wagoner DR, Kirsch GE, Wang Q. (2004). Mechanisms by which SCN5A mutation $N_{1325}S$ causes cardiac arrhythmias and sudden death in vivo. *Cardiovascular research.,* 61:256-267.

Tian XL, Cheng Y, Zhang T, Liao MLC, Yong SL, and Wang QK. (2007). Optical mapping of ventricular arrhythmias in LQTS mice with SCN5A mutation N1325S. *Biochemical and Biophysical Research Communications.,* 352: 879-883.

Tinel N, Diochot S, Borsotto M, Lazdunski M, Barhanin J. (2000). KCNE2 confers background current characteristics to the cardiac KCNQ1 potassium channel. *EMBO J.,* 19:6326-30.

Towbin JA, Vatta M. (2001). Molecular biology and the prolonged QT syndromes. *Am J Med.* 110:385-398.

Tristani-Firouzi M, Jensen JL, Donaldson MR, Sansone V, Meola G, Hahn A, Bendahhou S, Kwiecinski H, Fidzianska A, Plaster N, Fu YH, Ptacek LJ, Tawil

R. (2002). Functional and clinical characterization of KCNJ2 mutations associated with LQT7 (Andersen syndrome). *J Clin Invest*.,110:381-388.

Eubanks J, Srinivasan J, Dinulos MB, Disteche CM, Catterall WA. (1997). Structure and chromosomal localization of the beta2 subunit of the human brain sodium channel. *Neuroreport*., 8:2775-9.

Vatta M, Ackerman MJ, Ye B, Makielski JC, Ughanze EE, Taylor EW, Tester DJ, Balijepalli RC, Foell JD, Li Z, Kamp TJ, Towbin JA. (2006). Mutant caveolin-3 induces persistent late sodium current and is associated with long-QT syndrome.*Circulation*,114:2104-21012.

Van Bemmelen MX, Rougier JS and Gavillet B *et al.* (2004). Cardiac voltage-gated sodium channel Nav1.5 is regulated by Nedd4-2 mediated ubiquitination, *Circ Res.,* 95: 284–291.

Viskin S, Belhassen B. (1990). Idiopathic ventricular fibrillation. *Am Heart J.*,120:661-71.

Viskin S, Belhassen B. (1998). Polymorphic ventricular tachyarrhythmias in the absence of organic heart disease: classification, differential diagnosis, and implications for therapy. *Prog Cardiovasc Dis*., 41(1):17-34.

Wan X, Wang Q, Kirsch GE. (2000). Functional suppression of sodium channels by beta(1)-subunits as a molecular mechanism of idiopathic ventricular fibrillation. *J Mol Cell Cardiol.* 32:1873-1884.

Wan X, Chen S, Sadeghpour A, Wang Q, Kirsch GE. (2001). Accelerated inactivation in a mutant Na(+) channel associated with idiopathic ventricular fibrillation. *Am J Physiol Heart Circ Physiol.,* 280:H354-60.

Wang DW, Yazawa K, George AL Jr, Bennett PB. (1996). Characterization of human cardiac Na^+ channel mutations in the congenital long QT syndrome. *Proc Natl Acad Sci U S A.* 93:13200-13205.

Wang DW, Makita N, Kitabatake A, Balser JR, George AL Jr. (2000). Enhanced Na(+) channel intermediate inactivation in Brugada syndrome.*Circ Res*.,13;87:E37-43.

Wang DW, Desai RR, Crotti L, Arnestad M, Insolia R, Pedrazzini M, Ferrandi C, Vege A, Rognum T, Schwartz PJ, George AL Jr. (2007). Cardiac sodium channel dysfunction in sudden infant death syndrome. *Circulation*. 115:368-376.

Wang Q, Shen J, Splawski I, Atkinson D, Li Z, Robinson JL *et al.* (1995a). SCN5A mutations associated with an inherited cardiac arrhythmia, long QT syndrome. *Cell.* 80:805-811.

Wang Q, Shen J, Li Z, Timothy K, Vincent GM, Priori SG *et al.* (1995b). Cardiac sodium channel mutations in patients with long QT syndrome, an inherited cardiac arrhythmia. *Hum.Mol.Genet*. 4:1603-1607.

Wang Q, Li Z, Shen J, and Keating MT, (1996). Genomic organization of the human SCN5A gene encoding the cardiac sodium channel, *Genomics*.; 34:9-16.

Wang Q, Curran ME, Splawski I, Burn TC, Millholland JM, VanRaay TJ, Shen J, Timothy KW, Vincent GM, de Jager T, Schwartz PJ, Toubin JA, Moss AJ, Atkinson DL, Landes GM, Connors TD, Keating MT. (1996). Positional cloning of a novel potassium channel gene: KVLQT1 mutations cause cardiac arrhythmias. *Nat Genet*., 12:17-23.

Wang Q, Chen Q, Li H, Towbin JA. (1997). Molecular genetics of long QT syndrome from genes to patients. *Curr.Opin.Cardiol*. 12:310-320.

Wang Q, Pyeritz RE, Seidman CE, and Basson CT, Genetic studies of myocardial and vascular disease. In: Topol EJ (Ed.), (2001). Textbook of Cardiovascular Medicine, Lippincott Williams & Wilkins, Philadelphia, PA, pp. in press.

Ward, O. C. (1964). A new familial cardiac syndrome in children. *J.Ir.Med.Assoc*. 54:103-106.

Wedekind H, Smits JP, Schulze-Bahr E, Arnold R, Veldkamp MW, Bajanowski T, Borggrefe M, Brinkmann B, Warnecke I, Funke H, Bhuiyan ZA, Wilde AA, Breithardt G, Haverkamp W. (2001). De novo mutation in the SCN5A gene associated with early onset of sudden infant death. *Circulation*.,104:1158-64.

Wehrens XH, Abriel H, Cabo C, Benhorin J, Kass RS. (2000). Arrhythmogenic mechanism of an LQT-3 mutation of the human heart Na(+) channel alpha-subunit: A computational analysis. *Circulation*, 102:584-90.

West JW, Patton DE, Scheuer T, Wang Y, Goldin AL, Catterall WA. (1992). A cluster of hydrophobic amino acid residues required for fast Na(+)-channel inactivation. *Proc Natl Acad Sci U S A.,* 89:10910-10914.

Wingo TL, Shah VN, Anderson ME, Lybrand TP, Chazin WJ, Balser JR. (2004). An EF-hand in the sodium channel couples intracellular calcium to cardiac excitability. *Nat Struct Mol Biol*.,11:219-25.

Wu L, Nishiyama K, Hollyfield JG, Wang Q. (2002). Localization of Nav1.5 sodium channel protein in the mouse brain. *Neuroreport.* 13:2547-2551.

Xu W, Nair JS, Malhotra A, Zhang JJ. (2005). B cell antigen receptor signaling enhances IFN-gamma-induced Stat1 target gene expression through calcium mobilization

and activation of multiple serine kinase pathways. *J Interferon Cytokine Res.*, 25:113-124.

Yagi T, Pu J, Chandra P, Hara M, Danilo P Jr, Rosen MR, Boyden PA. (2002),Density and function of inward currents in right atrial cells from chronically fibrillating canine atria. *Cardiovasc Res.*,54:405-415.

Yong SL, Ni Y, Zhang T, Tester DJ, Ackerman MJ, and Wang QK, (2007) Characterization of the cardiac sodium channel SCN5A mutation, N1325S, in single murine ventricular myocytes, *Biochem. Biophys. Res. Commun.* 352:378-383.

Yong SL, Wang QK.(2006). Animal models for cardiac arrhythmias. *Methods Mol Med*.,129:127-48.

Young KA, Caldwell JH. (2005) Modulation of Skeletal and Cardiac Voltage-gated Sodium Channels by Calmodulin. *J Physiol.,* 565:349-370.

Yu FH, Westenbroek RE, Silos-Santiago I, McCormick KA, Lawson D, Ge P, Ferriera H, Lilly J, DiStefano PS, Catterall WA, Scheuer T, and Curtis R. (2003). Sodium Channel β4, a New Disulfide-Linked Auxiliary Subunit with Similarity to β2 . *The Journal of Neuroscience*. 23:7577-7585.

Zareba W. Genotype-specific ECG patterns in long QT syndrome. (2006). *J Electrocardiol.,* 39:S101-6.

Zerangue N, Schwappach B, Jan YN, Jan LY. (1999). A new ER trafficking signal regulates the subunit stoichiometry of plasma membrane K(ATP) channels. *Neuron*. 22:537-48.

Zhang T, Yong S, Drink J, Popvic Z and Wang Q, (2006). Late sodium currents generated by mutation N1325S in sodium channel gene SCN5A cause heart failure, *Circulation* 114:II–65.

Zhang T, Yong S, Tian XL and Wang QK, (2007). Cardiac-specific overexpression of SCN5A gene leads to shorter P wave duration and PR interval in transgenic mice, *Biochem. Biophys. Res. Commun.* 355:444–450.

Zhou J,Yi J, Hu NN, George AL, Murray KT. (2000). Activation of Protein Kinase A Modulates Trafficking of the Human Cardiac Sodium Channel in *Xenopus Oocytes* Circ Res.,87:33-38.

Zhou J, Shin HG, Yi J, ShenW, Williams CP, Murray KT. (2002). Phosphorylation and Putative ER Retention Signals Are Required for Protein Kinase A-Mediated Potentiation of Cardiac Sodium Current. *Circulation Research,* 91:540-546.

Zhou R, Snyder PM. (2005). Nedd4-2 phosphorylation induces serum and glucocorticoid-regulated kinase (SGK) ubiquitination and degradation. *J Biol Chem.*,280:4518-23.

Zicha S, Maltsev VA, Nattel S, Sabbah HN, Undrovinas AI. (2004) Post-transcriptional alterations in the expression of cardiac Na+ channel subunits in chronic heart failure. *J Mol Cell Cardiol,* 37: 91-100.

APPENDICES

Appendix A. Summary of mutations associated with the $Na_v1.5$ gene

Mutation [1]	Coding effect	Region[2]	Disease[3]	Reference
G9V	Missense	N-terminal	LQT3	Millat G et al, 2006
R27H	Missense	N-terminal	BS	Priori S et al. 2002
G35S	Missense	N-terminal	BS	Nissenbaum E et al. 2001
Q55X	Nonsense	N-terminal	BS	Makita N et al. 2007
V95I	Missense	N-terminal	BS	Liang P et. Al. 2006.
R104Q	Missense	N-terminal	BS	Nissenbaum E et al. 2001
	Splicing insertion	N-terminal	BS	Sangwatanaroj S et al. 2002
K126E	Missence	DIS1	BS	Vatta M et al. 2002
E161K	Missense	DIS2	BS/SSS/ PCCD	Smits J et al. 2002; Smits JP, 2005
T187I,	Missense	DIS2-S3	BS/SSS	Makiyama T 2006
20-bp Deletion	Frame-shift and truncation	DIS2–S3	BS	Vatta M et al. 2002
L212P	Missense (Cx40)	DIS3-S4	AS	Makita N,2005
S216L	Missense	DIS4	SIDS	Wang DW et al. 2007
T220I,	Missense	DIS4	DCM/SS S	Olson TM, 2005, Benson DW 2003
R225Q	Missense	DIS4	LQT3	Millat G, 2006

A226V	Missense	DIS4	BS	Priori Set al. 2002
I230V	Missense	DIS4	BS	Priori Set al. 2002
R282H	Missense	DIS5–S6	BS	Priori Set al. 2002
G292S	Missense	DIS5 -S6	BS	Niimura H et al.2004
V294M	Missense	DIS5–S6	BS	Priori S et al. 2002
NA	Nonsense	DIS5–S6	BS	Smits J et al. 2002
R282H	Missense	DIS5-S6	BS	Poelzing S et al.2006
K317N	Missense	DIS5-S6	BS	Yi SD, et al.2003
G319S	Missence	DIS5–S6	BS	Priori S et al. 2002
P336L	Missense	DIS5-S6	BS	Cordeiro et al. 2006
G351V	Missence	DIS5–S6	BS	Vatta M et al. 2002
T353I	Missense	DI S5-S6	BS	Pfahnl AE et al. 2007
R367H	Missense	DIS5–S6	BS	Vatta M et al. 2002
R367C	Missense	DIS5–S6	BS	Smits J et al. 2002
R367H	Missense	D1S5-S6	BS/AS	Takehara N, 2004
M369K	Missense	DIS5–S6	BS	Smits J et al. 2002
R376H	Missense	DIS5-S6	BS/PCCD	Rossenbacker T, 2004
D356N	Missense	DIS5-S6	BS	Makiyama T 2006
393delF	Deletion	DIS6	BS	Priori S et al. 2002
N406S	Missense	DIS6	BS	Itoh H et al. 2005
E473X	Nonsense	DI-DII	BS	Baroudi G, 2004
K493	Deletion	DI–DII	BS	Smits J et al. 2002
G514C	Missense	DI–DII	PCCD	Tan H et al. 2001

R535X	Nonsense	DI–DII	BS	Smits J et al. 2002
			BS/SIDS	Wan X et al. 2001
A572D	Missense	DI-DII	LQT3	
A572D	Missense	DI-DII	LQT3	Paulussen A, 2003
delAL586-587	in-frame deletion	DI-DII	SIDS	Wang DW et al. 2007
G615E	Missense	DI–DII	LQT3S	Yang P et al. 2002
L618F	Missense	DI–DII	LQT3S	Yang P et al. 2002
L619F	Missense	DI-DII	LQT3	Wehrens XH, 2003
G639R	Missense	DI-DII	LQT3	Millat G, 2006
R680H	Missense	DI-DII	SIDS	Wang DW et al. 2007
H681P	Missense	DI–DII	BS	Priori S et al. 2002
A735V	Missense	DIIS1	BS	Vatta M
A735E	Missense	DIIS1	BS	Priori S et al. 2002
G752R	Missense		BS	Smits J et al. 2002
	Splice mutation	DIIS2	BS	Priori S et al. 2002
2550-2551 insTG	insertion	DIIS3-S4	DCM	Olson TM, 2005
W822X	Nonsense	DIIS4	BS	Keller DI, 2005
S835L	Missense	DIIS4 –S5	BS	
F851L	Missense	DIIS5	BS	Priori S et al. 2002
F861fs951X	Nonsense	DIIS5	BS	Schulze-Bahr E, 2003
E867X	Nonsense	DIIS5-S6	BS	Schulze-Bahr E, 2003

L867X	Missense	DIIS5-S6	BS	Smits J et al. 2002
S871fs+9X	Frame-shift	DIIS5–S6	BS	Priori S et al. 2002
F891I	Missense	DIIS5–S6	BS	Priori S et al. 2002
C896S	Missense	DIIS5–S6	BS	Priori S et al. 2002
S910L	Missense	DIIS5–S6	BS	Priori S et al. 2002
NA	Frame-shift	DII-DIII	BS	Hofman-Bang J, 2006
S941N	Missense	DII–DIII	LQT3/SIDS	Schwartz Pet al. 2000
R965C	Missense	DII–DIII	LQT3/BS	Sangwatanaroj et al. 2002, Priori S et al. 2002
A997S	Missence	DII–DIII	SIDS	Ackerman M et al. 2001
E1053K	Missence	DII–DIII	BS	Priori S et al. 2002
D1114N	Missense	DII–DIII	LQT3/BS	Sangwatanaroj S et al. 2002, Splawski I et al. 2002
W1191X	Missense	DII-DIII	BS	Shin DJ et al. 2007
R1192Q	Missense	DII-DIII	BS	Vatta M et al. 2002
E1225K	Missense	DIIIS1	BS	Smits J et al. 2002
E1225K	Missense	DIIIS1-S2	BS	Schulze-Bahr E, 2003
R1232W	Missence	DIIIS1–S2	IVF/BS	Chen Q et al. 1998
R1232W	Missense	DIIIS1–S2	IVF/BS	Chen Q et al. 1998,
R1232W+ T1620M	Missense	DIIIS1–S2	IVF/BS	Baroudi G et al. 2002

K1236N	Missense	DIIIS1–S2	BS	Priori S et al. 2002
E1240Q	Missense	DIII–S2	BS	Priori S et al. 2002
F1250L	Missense	DIII–S2	LQT3	Yang P et al. 2002
NA	Frame-shift		BS	Smits J et al. 2002
G1262S	Missense	DIII-S2	BS	Shin DJ, 2004
D1275N	Missense	DIIIS3	DCM/AF	Olson TM, 2005, Groenewegen WA, 2003
D1275N	Missense	DIIIS3	PCCD/AF	Laitinen-Forsblom PJ, 2006
F1293S	Missense	DIIIS3–S4	BS	Priori S et al. 2002
E1295K	Missense	DIIIS4	LQT3	Abriel H et al. 2001
P1298L	Missense	DIIIS4	SSS	Benson DW, 2003
T1304M	Missense	DIIIS4	LQT3/SIDS	Wattanasirichaigoon Det al. 1999 Wang DW, 2007
IVS22DS+2	Splice mutation	DIIIS4–S5	PCCD	Schott J et al. 1999
G1319V	Missense	DIIIS4-S5	BS	Smits J et al. 2002
N1325S	Missense	DIIIS4–S5	LQT3	Wang Q et al. 1995
A1330P	Missense	DIIIS4–S5	LQT3/SIDS	Wedekind H et al. 2001
A1330T	Missense	DIIIS4-S5	LQT3	Smits JP et al., 2005
S1333Y	Missense	DIII/S4-S5	SIDS	Millat G et al., 2006
F1344S	Missense	DIIIS5	BS/VF	Keller DI et al., 2006

S1382I	Missense	DIIIS5-S6	BS	Smits J et al. 2002
V1398X	Nonsense	DIIIS5–S6	BS	Chen et al. 1998, Sangwatanaroj S et al. 2002
V1405L	Missense	DIIIS5–S6	BS	Smits J et al. 2002
G1406R	Missense	DIIIS5–S6	BS/PCCD /SSS	Smits J et al. 2002, Kyndt F et al. 2001 Benson DW et al. 2003
W1421X	Missense	DIIIS5-S6	LQT3	Niu DM et al.2006
R1432G	Missence	DIIIS5–S6	BS	Deschenes I et al. 2000, Baroudi G et al. 2001
G1467fs+13X	Frame-shift	DIIIS6	BS	Priori S et al. 2002
	Splice mutation	c.4810+3_4810+6dupGGGT	BS/PCCD	Rossenbacker T et al.2005
delK1479	Missense	DIII-DIV	BS	Schulze-Bahr E et al. 2003
F1486L	Missense	DIII-DIV	SIDS	Wang DW et al. 2007
delK1500	Deletion	DIII–DIV	LQT3/BS	Priori S et al. 2002
L1501V	Missense	DIII–DIV	LQT3	Splawski I et al. 2000
G1502S	Missense	DIII–DIV	BS	Smits J et al. 2002
1503	Deletion		LQT3	Wang Q et al. 1995
delKPQ	Deletion	DIII–DIV	LQT3	Wang Q et al. 1995

1505-1507				
R1512W	Missense	DIII–DIV	BS	Rook M et al. 1999, Smits J et al. 2002
delQKP 1507-1509	Deletion	DIII-DIV	LQT3	Keller DI et al. 2003
IVS2AS-24	Splice mutation	DIVS	BS	Rook M et al. 1999
IVS21+1	Splice mutation		BS	Smits J et al. 2002
IVS24DS+28	Splice mutation	DIVS	BS	Rook M et al. 1999
K1527R	Missense	DIVS1	BS	Yokoi H et al. 2005
A1569P	Missense	DIVS2	BS	
K1578fs/52	Missense	DIVS2	BS/SSS	Makiyama T et al. 2006
26AS-5insTGGG?	Splice mutation (In-frame deletion)	DIVS2-S3	BS	Hong K et al. 2005
D1595N	Missense	DIVS3	PCCD	Wang D et al. 2002
S1609W	Missense	DIVS3	LQT3	Millat G, 2006
D1595H	Missense	DIVS3	DCM	Olson TM, 2005
delF1616	Deletion	DIVS3-S4	LQT3	Splawski I et al.2000
delF1617	Deletion	DIVS3-S4	LQT3/BS /SSS	Splawski I et al.2000/Liang P et. al. 2006, Benson DW et al. 2003
T1620M	Missense	DIVS3–S4	IVF/BS	Chen Q et al. 1998,
R1623X	Nonsense	DIVS4	SSS	Benson DW et al. 2003

R1623Q	Missense	DIVS4	LQT3	Splawski I et al. 2000
R1623L	Missense	DIVS4	LQT3	Splawski I et al. 2000
R1644H	Missense	DIVS4	LQT3	Splawski I et al. 2000
R1623X	Nonsense	DIVS4	BS/SSS	Makiyama T et al. 2006
R1623X	Nonsense	DIV-S4	BS	Todd SJ et al. 2005
R1632H	Missense	DIVS4	SSS	Benson DW et al. 2003
T1645M	Missense	DIVS4	LQT3	Wattanasirichaigoon D etla. 1999
A1649V	Missense	DIVS4-S5	BS	Liang P et. al. 2006.
I1660V	Missense	DIVS5	BS	Cordeiro JM et al. 2006
S1710L	Missense	DIVS5–S6	IVF	Shirai N et al. 2002
delS1710	Deletion		PCCD	Schott J et al. 1999
D1714G	Missense	DIVS5-S6	BS	Amin AS et al.2005
delG5130	Frame-shift	DIVS5–S6	PCCD	Schott J et al. 1999
delG5280	Frame-shift	DIVS5–S6	BS	Schott J et al. 1999
G1740R	Missense	DIVS5-S6	BS	Baroudi G et al. 2004
G1740R	Missense	DIVS5–S6	BS	Priori S et al. 2002
G1743R	Missense	DIVS5-S6	BS	Valdivia CR et al. 2004
G1743E	Missense	DIVS5-S6	BS	Smits J et al. 2002
V1763M	Missense	DIVS6	LQT3	Chang CC et al. 2004
M1766L	Missense	DIVS6	LQT3/AV block	Valdivia C et al. 2002
I1768V	Missense		LQT3	Rivolta I et al. 2002

N1774+12X?	Nonsense	C-terminal	BS	Baroudi G et al. 2004
V1777M	Missense	C-term	LQT3	Lupoglazoff J et al. 2001
E1784K	Missense	DIVS6	LQT3/BS	Deschenes I et al. 2000
S1787N	Missense	DIVS6	LQT3	Splawski I et al. 2000
D1790G	Missense	DIVS6	LQT3	An Ret al. 1998
1795insD	Insertion	DIVS6	LQT3/IVF	Bezzina C et al. 1999
Y1795C	Missense	C-terminal	LQT3	Rivolta I et al. 2001
Y1795H	Missense	C-terminal	BS	Rivolta I et al. 2001
insD1796	Insertion	C-terminal	LQT3/BS	Bezzina C et al. 1999
S1812X	Nonsense	C-terminal	BS	Schulze-Bahr E et al. 2003
D1819N	Missense	C-terminal	LQT3	Millat G, 2006
L1825P	Missense		LQT3	Makita N et al. 2002
R1826H	Missense	C-terminal	SIDS/LQT3	Ackerman M et al. 2001
D1840G	Missense	C-terminal	LQT3	Benhorin J et al.1998
L1921stop	Nonsense		BS	Cormier J et al. 2002
A1924T	Missense	C-terminal	BS/IVF	Smits J et al. 2002, Rook M et al. 1999
V1951L	Missense	C-terminal	BS/SIDS	Priori S et al. 2002,Wang DW, 2007
F2004L,	Missense	C-terminal	SIDS	Wang DW et al. 2007
P2006A	Missense	C-terminal	SIDS	Wang DW et al. 2007

[1]Standard single letter code is used for amino acids. X stands for nonsense mutation. Examples for the mutations are as the following. G9V stands for a mutant in which glycine is replaced by a valine at position 9. IVS22DS+2 stands for a mutant that insert in +2 donor splicing site of intron 22. delAL586-587 stands for a mutant where Alanine 586 and Leucine 587 are deleted. [2]Abbreviations for diseases are listed in List of Abbreviations.

Appendix B. **Positive clones obtained from a yeast two hybrid screen**. Different DNA fragment of $Na_v1.5$ as bait (upper panel) were used to screen a cardiac human cDNA library, Further protein identification using the cytoplasmic loop II of $Na_v1.5$ as a bait was shown in the bottom panel.

Baits[1]	**Number of positive clones**
N-terminus	0
DI-II Linker (Loop I)	0
DII-III Linker (Loop II)	223
DIII-IV Linker (Loop III)	29
C-terminus	Self activating

[1]The above table showed the results for yeast positive clones using baits from 5 cytoplasmic domain of $Na_v1.5$: N-terminus, loops I, II, III and C-terminus.

Hits number[2]	**Name of the protein**	**Gen bank number**
2	Cardiac Troponin I	M64247
7	MOG1A	AF265206

[2]The number of hits represents the number of positive yeast clones for the identified protein.

Appendix C. Additional genes showing differential expression in TG-NS hearts by microarray analysis[1]

(A) Genes involved in immune response

Accession #	Symbol	Gene	P value	Fold of change
NM_010395	*H2-T10*	Histocompatibility 2, T region locus 10	2.6×10^{-5}	13.3
BC027328	*Brd4*	Bone marrow stromal cell antigen 2	4.5×10^{-5}	12.0
M16120	*Tcrb-V13*	T-cell receptor insulin B-chain reactive beta chain VNDNJC	1.5×10^{-4}	9.3
L03353	*Cd3z*	CD3 theta T-cell receptor subunit	2.2×10^{-4}	-7.2

(B) Genes encoding enzymes

Accession #	Symbol	Gene	P value	Fold of change
NM_016966	*Phgdh*	3-Phosphoglycerate dehydrogenase	6.0×10^{-5}	53.8
NM_008638	*Mthfd2*	Methylenetetrahydrofolate dehydrogenase (NAD+ dependent), methenyltetrahydrofolate cyclohydrolase	3.6×10^{-4}	13.3
BC027199	Lrrk1	Leucine-rich repeat kinase 1	5.610^{-4}	-6.5
NM_080446	Helb	Helicase (DNA) B	7.1×10^{-4}	9.1

(C) Putative genes or genes with unknown functions

Accession #	Symbol	Gene	P value	Fold of change
BC020489	2310016F22Rik	RIKEN cDNA 9130022K13 gene	2.4×10^{-4}	231.3
BB741897	Vig1-pending	cDNA clone F520004L04 gene, similar to viral hemorrhagic septicemia virus(VHSV) induced gene 1	7.6×10^{-4}	25.6
AF099975	Slfn4	Clone I.M.A.G.E. consortium 638739 schlafen4	6.6×10^{-4}	17.2
AV212753	Asns	RIKEN cDNA clone 2410118F17 gene, similar to Asparagine synthetase	4.1×10^{-4}	13.4
NM_030150	D11Lgp2e	DNA segment, Chromosome 11, Lothar Hennighausen 2,expressed	2.1×10^{-4}	25.4
BB132493		cDNA clone 9830001A05 gene	5.8×10^{-4}	11.2
BB329808	AW261460	cDNA clone B630019O10	7.4×10^{-4}	10.1
BQ033138	Oasl 2	cDNA clone UI-1-CF0-axe-c-08-0-UI 3-, mRNA sequence, similar to 2-5 oligoadenylate synthetase-like 2	9.6×10^{-4}	9.8

BC023105	BC023 105	Clone:MGC:28198 IMAGE:3989161	6.7×10^{-4}	7.7
BB020681	Srr	cDNA clone UI-1-CF0-axe-c-08-0-UI 3-, mRNA sequence, similar to serine racemase	4.4×10^{-4}	5.3
BB251523	Pycs	cDNA clone A730046N23, similar to pyrroline-5-carboxylate synthetase short isoform	2.1×10^{-4}	5.2

[1]Genes involved in interferon-signaling pathways, apoptosis and inflammation are listed in Table 3.2.